



U.S. Department  
of Transportation

**Federal Highway  
Administration**

Publication No. FHWA-RD-88-269

July 1989

---

# SALT PENETRATION AND CORROSION IN PRESTRESSED CONCRETE MEMBERS

---

Research, Development, and Technology  
Turner-Fairbank Highway Research Center  
6300 Georgetown Pike  
McLean, Virginia 22101-2296

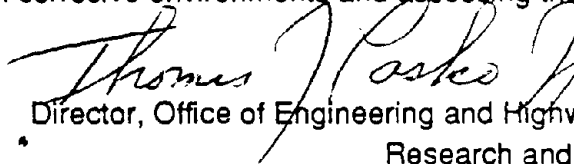
REPRODUCED BY  
U.S. DEPARTMENT OF COMMERCE  
NATIONAL TECHNICAL INFORMATION SERVICE  
SPRINGFIELD, VA. 22161

## FOREWORD

This report will be of interest to engineers who have been exposed to the basic concepts of corrosion of prestressing steel in pre-and post-tensioned bridge components caused by adverse environments.

A state-of-the-art review was conducted on failures of prestressing steel with an emphasis on the cause and mode of failure. Bridges incorporating pre-or post-tensioning systems were sampled and data analyzed to determine if active corrosion of the prestressing steel was occurring. It is established that, in northern areas, the primary cause of deterioration of PS/C members is due to penetration of solutions containing deicing salts through concrete cover and through anchorage zones. Improperly designed and maintained joints and drainage systems are the primary pathways for salt ingress. In southern areas the primary cause of deterioration is marine salts sprayed directly onto substructural elements by wave action.

The report also gives the engineer valuable insight into procedures, parameters, and threshold values for detection of corrosive environments and assessing the condition of the prestressing steel.



Director, Office of Engineering and Highway Operation  
Research and Development

## NOTICE

This document is disseminated under the sponsorship of the Department of Transportation in the interest of information exchange. The United States Government assumes no liability for its contents or use thereof.

The contents of this report reflect the views of the contractor, who is responsible for the accuracy of the data presented therein. The contents do not necessarily reflect the official policy of the Department of Transportation. This report does not constitute a standard, specification or regulation.

The United States Government does not endorse products or manufactures. Trade or manufacturers' names appear herein only because they are considered essential to the object of this document.

1. Report No. FHWA-RD-88-269	2. Government Accession No. <b>PB 90 1 155 02/AS</b>	3. Recipient's Catalog No.	
4. Title and Subtitle SALT PENETRATION AND CORROSION IN PRESTRESSED CONCRETE MEMBERS		5. Report Date July 1989	
		6. Performing Organization Code M10018	
		8. Performing Organization Report No.	
7. Author(s) V. Novokshchenov		10. Work Unit No. (TRAIS) 3 D4C0262	
9. Performing Organization Name and Address Construction Technology Laboratories, Inc. 5420 Old Orchard Road Skokie, Illinois 60077		11. Contract or Grant No. DTFH 61-87-C00031	
		13. Type of Report and Period Covered Final Report July 1987 - August 1988	
12. Sponsoring Agency Name and Address Office of Engineering and Highway Operations Research and Development Federal Highway Administration 6300 Georgetown Pike McLean, Virginia 22101-2296		14. Sponsoring Agency Code	
15. Supplementary Notes FHWA Contract Manager (COTR) : Y. P. Virmani (HNR-10)			
16. Abstract <p>A study was made of the condition of prestressed concrete PS/C bridge elements located in adverse, potentially corrosive environments. A total of five bridges were subjected to detailed surveys. Additional structures were surveyed visually and given limited investigation. Bridges were located both in northern climates subjected to application of roadway deicing salts and in southern areas subjected to marine spray.</p> <p>Results indicated that, in northern areas, primary cause of deterioration of PS/C members is due to penetration of solutions containing deicing salts through concrete cover and through anchorage zones. Improperly designed and maintained joints and drainage systems are the primary pathways for the salt ingress. In southern areas primary cause of deterioration is marine salts sprayed directly onto substructural elements by wave action.</p> <p>Recommendations concerning procedures, parameters and threshold values for detection of corrosive environments and assessing the condition of prestressing steel in bridge components are included.</p>			
17. Key Words Chlorides, Corrosion, Prestressed Concrete, Stress Corrosion		18. Distribution Statement No original distribution by the sponsoring agency. This document is available to the public through the National Technical Information Service, Springfield, Virginia 22161	
19. Security Classif. (of this report) Unclassified	20. Security Classif. (of this page) Unclassified	21. No. of Pages 212	22. Price A10

# SI\* (MODERN METRIC) CONVERSION FACTORS

## APPROXIMATE CONVERSIONS TO SI UNITS

Symbol	When You Know	Multiply By	To Find	Symbol
<b>LENGTH</b>				
in	inches	25.4	millimetres	mm
ft	feet	0.305	metres	m
yd	yards	0.914	metres	m
mi	miles	1.61	kilometres	km
<b>AREA</b>				
in <sup>2</sup>	square inches	645.2	millimetres squared	mm <sup>2</sup>
ft <sup>2</sup>	square feet	0.093	metres squared	m <sup>2</sup>
yd <sup>2</sup>	square yards	0.836	metres squared	m <sup>2</sup>
ac	acres	0.405	hectares	ha
mi <sup>2</sup>	square miles	2.59	kilometres squared	km <sup>2</sup>
<b>VOLUME</b>				
fl oz	fluid ounces	29.57	millilitres	mL
gal	gallons	3.785	litres	L
ft <sup>3</sup>	cubic feet	0.028	metres cubed	m <sup>3</sup>
yd <sup>3</sup>	cubic yards	0.765	metres cubed	m <sup>3</sup>
<b>MASS</b>				
oz	ounces	28.35	grams	g
lb	pounds	0.454	kilograms	kg
T	short tons (2000 lb)	0.907	megagrams	Mg
<b>TEMPERATURE (exact)</b>				
°F	Fahrenheit temperature	5(F-32)/9	Celsius temperature	°C

\* SI is the symbol for the International System of Measurement

## APPROXIMATE CONVERSIONS FROM SI UNITS

Symbol	When You Know	Multiply By	To Find	Symbol
<b>LENGTH</b>				
mm	millimetres	0.039	inches	in
m	metres	3.28	feet	ft
m	metres	1.09	yards	yd
km	kilometres	0.621	miles	mi
<b>AREA</b>				
mm <sup>2</sup>	millimetres squared	0.0016	square inches	in <sup>2</sup>
m <sup>2</sup>	metres squared	10.764	square feet	ft <sup>2</sup>
ha	hectares	2.47	acres	ac
km <sup>2</sup>	kilometres squared	0.386	square miles	mi <sup>2</sup>
<b>VOLUME</b>				
mL	millilitres	0.034	fluid ounces	fl oz
L	litres	0.264	gallons	gal
m <sup>3</sup>	metres cubed	35.315	cubic feet	ft <sup>3</sup>
m <sup>3</sup>	metres cubed	1.308	cubic yards	yd <sup>3</sup>
<b>MASS</b>				
g	grams	0.035	ounces	oz
kg	kilograms	2.205	pounds	lb
Mg	megagrams	1.102	short tons (2000 lb)	T
<b>TEMPERATURE (exact)</b>				
°C	Celsius temperature	1.8C + 32	Fahrenheit temperature	°F

These factors conform to the requirement of FHWA Order 5190.1A.

(Revised April 1989)

## TABLE OF CONTENTS

<u>Section</u>	<u>Page</u>
INTRODUCTION .....	1
Problem Statement .....	1
Objectives .....	1
Scope of Work and Study Approach .....	1
TYPES OF PRESTRESSING STEEL .....	3
Cold-Drawn Stress-Relieved Wire .....	3
Quenched and Tempered Wire .....	5
REPORTED FAILURES .....	6
General Survey .....	6
Bridge in the Netherlands .....	8
The Hood Canal Floating Bridge .....	8
Illinois Toll Highway Prestressed Concrete Bridges .....	8
Prestressed Panel Sub-Decks .....	9
Out-of-Service Bridge Near Ft. Morgan, Colorado .....	10
Post-Tensioned Beams in the Tidal Zone at Treat Island, Maine .....	10
Regina Pipeline .....	12
Summary of Causes of Failure .....	12
Defects of Manufacture .....	13
Improper Handling .....	14
Corrosion of Pretensioned Tendons .....	14
Corrosion of Post-Tensioned Tendons .....	15
TYPES OF CORROSION .....	17
Pitting Corrosion .....	17
Stress Corrosion .....	18
Hydrogen Embrittlement .....	18
Stress Cracking .....	20
O'HARE AIRPORT LEADS BRIDGE .....	22
Bridge Description .....	22
Visual Examination .....	26

## TABLE OF CONTENTS (continued)

<u>Section</u>	<u>Page</u>
Delamination of Concrete Cover .....	34
Petrographic Analysis .....	34
Core SP#4, G2-1 .....	34
Core SP#4, G4-3 .....	37
Chloride Concentration .....	40
Rapid Chloride Penetration .....	44
Concrete Cover Survey .....	44
Potential Survey .....	45
Metallurgical Analyses .....	50
Visual and Macroscopic Examination .....	50
Scanning Electron Microscope .....	50
Metallographic Examination .....	51
Cause of Failure .....	51
Summary .....	54
 THE ROUTE SEVEN VIADUCT .....	 56
Viaduct Description .....	56
Visual Examination .....	56
Description of Study Areas .....	67
Study Area #1 .....	67
Study Area #2 .....	68
Study Area #3 .....	68
Study Area #4 .....	68
Delamination of Concrete Cover .....	68
Petrographic Examination .....	73
Core SP#2, BB#1 .....	73
Core SP#23, BB#1 .....	74
Concentration of Chlorides .....	79
Rapid Chloride Permeability .....	79
Concrete Cover Survey .....	81
Potential Survey .....	81
Metallurgical Analyses .....	83
Visual and Macroscopic Examination .....	86
Scanning Electron Microscope Examination .....	86
Metallographic Examination .....	87
Cause of Failure .....	87
Summary .....	94

## TABLE OF CONTENTS (continued)

<u>Section</u>	<u>Page</u>
THE SIXTH SOUTH STREET VIADUCT .....	96
Bridge Description .....	96
Post-Tensioned Girders .....	96
Pretensioned Girders .....	96
Nature and Extent of the Problem .....	96
Visual Examination .....	98
Post-Tentioned Tendons .....	98
Pretentioned Strands .....	99
Anchorage Areas .....	100
External Tendons .....	100
Deck Drains .....	101
Cause of Corrosion .....	101
Petrographic Examination .....	114
Core Bent 42-G#8 .....	114
Core Bent 39-G#5 .....	114
Chunk Sample Bent 4-G#8 .....	117
Chloride Concentration .....	118
Rapid Chloride Permeability .....	119
Concrete Cover Survey .....	120
Potential Survey .....	121
Summary .....	122
THE GANDY BRIDGE .....	124
Bridge Description .....	124
Visual Examination .....	127
Corrosion Survey .....	129
Delamination Survey .....	136
Petrographic Examination .....	136
Core G-3 .....	136
Core G-4 .....	137
Concentration of Chlorides .....	138
Rapid Chloride Penetration .....	139
Concrete Cover Study .....	139
Potential Survey .....	141
Metallurgical Examination of Prestressing Steel .....	142
Visual and Macroscopic Examination .....	144

## TABLE OF CONTENTS (continued)

<u>Section</u>	<u>Page</u>
Scanning Electron Microscope Examination .....	144
Metallographic Examination .....	144
Tension Tests .....	145
Summary .....	149
 INTRACOASTAL CANAL BRIDGE .....	 152
Bridge Description .....	152
Visual Examination .....	154
Concrete Cracking .....	154
Drains .....	155
Deck Surface .....	156
Joints .....	156
Corrosion of Reinforcement .....	156
Delamination Survey .....	157
Petrographic Examination .....	164
Core Beam 1 .....	164
Core Box S9 .....	165
Concentration of Chlorides .....	165
Rapid Chloride Permeability .....	166
Concrete Cover Survey .....	167
Potential Survey .....	168
 SHIP CHANNEL BRIDGE .....	 169
Bridge Description .....	169
Visual Examination .....	169
Chloride Concentration .....	171
Concrete Cover Survey .....	171
Potential Survey .....	174
 NUECES BAY CAUSEWAY .....	 175
Bridge Description .....	175
Visual Examination .....	175
Summary .....	178



## TABLE OF CONTENTS (continued)

<u>Section</u>	<u>Page</u>
METHODS FOR DETECTING CORROSIVE ENVIRONMENTS AND ACTIVE CORROSION OF PRESTRESSING STEEL .....	181
Visual Examination .....	181
Chloride Analysis .....	183
Potential Survey .....	184
SUMMARY, CONCLUSIONS AND RECOMMENDATIONS .....	186

## LIST OF FIGURES

<u>Figure</u>	<u>Page</u>
1. Production of cold-drawn and heat-treated prestressing steel .....	4
2. O'Hare Airport Leads Bridge .....	23
3. Elevation and cross section of O'Hare Airport Leads Bridge .....	24
4. AASHTO Prestressed Concrete Girders .....	25
5. Severe cracking of concrete cover in Girder 3, Span 4 .....	28
6. Spalling of concrete cover in Girder 3, Span 4 .....	28
7. Spalling of concrete cover and exposure of prestressing strands at the end of a girder .....	29
8. Severely corroded strand on the north side of Girder 3, Span 4 .....	29
9. Fractured strand on the south side of Girder 3, Span 4 .....	30
10. Apparent stains of rust on the bottom surface of a girder .....	30
11. Wet spots under the bridge in Span 4 .....	31
12. Badly deteriorated longitudinal expansion joint .....	32
13. Badly deteriorated transverse expansion joint .....	33
14. Cracks and stains of rust in the shotcrete patch .....	35
15. Cracking and spalling of concrete cover in diaphragms adjacent to transverse leaking joints .....	35
16. Spalling of concrete cover over corroded stirrups .....	36
17. Delamination of concrete cover on internal girder surfaces .....	36
18. Typical microstructure of concrete in Core SP#4, G2-1 .....	38
19. Microstructure of concrete in core SP#4G, 2-1 .....	39
20. Typical microstructure of concrete in Core SP#G4, G-3 .....	41
21. Microstructure of concrete in Core SP#G4, G-3 .....	42
22. Potential survey of Girder 3 in Span 4 .....	47
23. Frequency distribution of potential readings in Girder 3, Span 4 .....	48
24. Cumulative frequency distribution of potential readings in Girder 3, Span 4 ...	49

## LIST OF FIGURES (continued)

<u>Figure</u>	<u>Page</u>
32. Fractured area of a wire at a magnification of 50X (left) and 500X (right) .....	52
26. The significant reduction in diameter from the bottom to top .....	53
27. The Route Seven Viaduct in Chicago Ridge .....	57
28. Bridge on Route 7, Chicago Ridge .....	58
29. Precast prestressed concrete beam .....	59
30. Signs of severe leakage of water through a joint between box girders .....	61
31. Cracking of concrete overlay in areas adjacent to expansion/contraction joints .....	61
32. Typical crack caused by corrosion of a prestressing strand .....	62
33. Moderate spalling of concrete cover over a strand .....	62
34. Very severe spalling of concrete cover over several prestressing strands .....	63
35. Concrete spall adjacent to a leaking transverse joints .....	63
36. Corrosion related spalling of concrete cover due to water running along the side of a girder .....	64
37. Corrosion related spalling of concrete cover due to water running around the malfunctioning drain .....	65
38. Failure in all six wire surrounding a central wire .....	65
39. Complete failure of a prestressing strand .....	66
40. Imprints of corroded wires on the surface of the steel-concrete interface .....	60
41. Study Area 1 .....	69
42. Study Area 2 .....	70
43. Study Area 3 .....	71
44. Study Area 4 .....	72
45. Microstructure of concrete in Core 2, Span 3 (Plane-polarized light. Magnification-100X. Length of field = 1.2 mm.) .....	75

## LIST OF FIGURES (continued)

<u>Figure</u>	<u>Page</u>
46. Microstructure of concrete in Core 2, Span 3 (Cross-polarized light. Magnification-100X. Length of field = 1.2 mm.) .....	76
47. Microstructure of concrete in Core 2, Span 23 (Plane-polarized light. Magnification-100X. Length of field = 1.2 mm.) .....	77
48. Microstructure of concrete in Core 2, Span 23 (Cross-polarized light. Magnification-100X. Length of field = 1.2 mm.) .....	78
49. Concrete cover survey .....	82
50. The test sample of the seven wire strand from Span 3, Box 2 .....	88
51. The fractured end of one of the sample wires .....	89
52. Fractured area of a wire at a magnification of 30X (left and 300X (right) .....	90
53. A typical example of the heavily cold worked microstructure exhibited near the cut end of wire .....	91
54. The microstructure of the center wire with Bakelite along the left and right edges .....	92
55. Microstructure near the fractured end of a wire .....	93
56. The Sixth South Street Viaduct, Salt Lake City, Utah .....	97
57. Exposed post-tensioned tendon in Girder 3, Span 36-37 m .....	102
58. Exposed post-tensioned tendon in Girder 10, Span 28-29 .....	102
59. Surface type corrosion on exposed surfaces of the prestressing tendon in Girder 3, Span 36-37 .....	103
60. Condition of the newly exposed surfaces of the duct and the high chair rod in girder 3 .....	103
61. Extent of corrosion on the newly exposed surface of the rod in Girder 3 .....	104
62. Condition of the tendon protected with concrete, Girder 10, Span 28-29 .....	104

## LIST OF FIGURES (continued)

<u>Figure</u>	<u>Page</u>
63. Negligible to moderate surface type corrosion on the newly exposed surface of the rod in Girder 10 .....	105
64. Corrosion protection to exposed ends of seven wire strands by means of portland cement mortar .....	105
65. Moderate corrosion of exposed strands at the end of a girder .....	106
66. Appearance of the exposed strand in Girder 5, Span 39-40 .....	106
67. Cracks in mortar and concrete in areas of anchor plates .....	107
68. Spalling of the mortar cover over anchor steel plates .....	108
69. Moderate to severe corrosion of a steel plate .....	109
70. Very severe corrosion of an anchor plate .....	109
71. Post-tensioned girders reinforced with external tendons .....	110
72. A typical external tendon .....	110
73. Accumulation of debris and deterioration of concrete in areas adjacent to the open sidewalk expansion joint.....	111
74. Deterioration of concrete in areas of expansion joints .....	111
75. Corrosion-related deterioration of concrete in a pier cap .....	112
76. Remaining short vertical portion of a drain pipe .....	112
77. Drain pipe with an increased slope .....	113
78. A lapped slice of Core Bent 42-G#8 .....	115
79. A lapped slice of Core Bent 39-G#5 .....	115
80. A lapped slice of Chunk Sample Bent 42-G#8 .....	116
81. The Gandy Bridges .....	125
82. 48 ft prestressed girder .....	126
83. Cracking of concrete cover over a top tendon.....	130
84. Cracks on the bottom side of a beam.....	130
85. Cracking through the flange of a beam .....	131

## LIST OF FIGURES (continued)

<u>Figure</u>	<u>Page</u>
86. Rust stains around cracks in the bottom surface of a girder .....	131
87. Spalling of concrete cover over a top tendon .....	132
88. Spalling of concrete cover over the bottom tendon .....	132
89. Typical cracks in a prestressed pile .....	133
90. Remains of the protection system on prestressed piles .....	133
91. Cracks in prestressed piles of out-of-service Sunshine Skyway Bridge .....	134
92. Moderate surface type corrosion .....	134
93. Very severe extent of corrosion of the prestressing rod .....	135
94. Severe corrosion of the prestressing rod in Beam 2, Span 274 .....	135
95. Sampled tendon in Beam 2, Span 130 .....	143
96. Obtaining a sample tendon using a coring machine .....	143
97. Visual appearance of the test prestressing rod .....	146
98. Extensive rust observed on the fractured surface of the rod .....	146
99. Typical EDS spectrum of rust .....	147
100. A typical example of the microstructure of perlite and ferrite observed through the metallographic section .....	148
101. Appearance of the metallographic cross section through the fractured end of the bar .....	148
102. Intracoastal Canal Bridge .....	153
103. Post-tensioned segmental box girder unit .....	153
104. Typical pretensioned beam span .....	158
105. Crack in concrete cover above a top row of prestressing strands .....	158
106. Cracking of concrete in the bottom corner of a beam .....	159
107. Severe concrete cracking inside segmental boxes .....	159
108. Crack repaired with an epoxy resin paste .....	160
109. Typical span drain .....	160

## LIST OF FIGURES (continued)

<u>Figure</u>	<u>Page</u>
110. Typical expansion/contraction joint .....	161
111. Expansion joint at the transition bent .....	161
112. Condition of the sheathing in the bottom ducts .....	162
113. Exposed seven wire strand .....	162
114. Typical prestressing anchorage system .....	163
115. Potential survey on post-tensioned box girders in Spans 19 and 21 .....	163
116. Ship Channel Bridge .....	170
117. Typical prestressed girder span .....	170
118. Spalling of concrete cover over conventional reinforcing steel bars .....	172
119. Exposed tendon in the bottom of Girder 7 .....	172
120. Heavy layer of rust on the surface of the tendon .....	173
121. Condition of prestressing wires inside the tendon .....	173
122. The Nueces Bay Causeway .....	176
123. Typical prestressed girder span .....	176
124. Strand patterns for prestressed concrete beams .....	177

## LIST OF TABLES

<u>Table</u>	<u>Page</u>
1. Corrosion protection to prestressing steel in various systems .....	13
2. Total chloride analysis for O'Hare Airport Leads Bridge .....	43
3. Permeability of the concrete to chloride ions .....	44
4. Results of concrete cover study .....	45
5. Half-potential readings in Span 4 girders .....	46
6. Total chloride analysis for The Route Seven Viaduct .....	80
7. Rapid chloride permeability .....	81
8. Potential readings in box beams of Span 3 and 22 .....	84
9. Potential readings in Study Areas 1-4 .....	85
10. Percent of potential readings in study areas .....	85
11. Concentration of chlorides in concrete at various depths .....	118
12. Permeability of concrete to chloride ions .....	119
13. Concrete cover over prestressing strands in Girder 5 .....	120
14. Concentration of chloride ions .....	138
15. Rapid chloride permeability in Core G-3 and Core G-4 .....	139
16. Concret cover (inches) over prestressing tendons.....	140
17. Potential readings in girders of Spans 2, 130, and 274 .....	141
18. Percent of potentials in girders of Spans 2, 130, and 274 .....	142
19. Concentration of chlorides .....	166
20. Rapid chloride permeability test results .....	167
21. Concrete cover (inches) over prestressing strands.....	167
22. Half-potential readings in prestressed and post-tensioned girders .....	168
23. Concentration of chlorides in Span 9 .....	171



## **INTRODUCTION**

### **Problem Statement**

In prestressed concrete (PS/C) bridges the reinforcing steel is subjected to high mechanical stresses, therefore corrosion of tendons can lead to consequences far more serious than in the case of conventionally reinforced bridges. Significant mechanical weakening may occur in prestressed reinforcement even when the same extent of corrosion in conventional reinforcement would be considered negligible. This may result in failure of the steel and consequently of a bridge structure. The failure is more likely to occur in tendons of smaller diameters. In some instances corrosion-related fracture of the steel may lead to a sudden collapse of a bridge structure without sufficient warning. Therefore, investigations to determine the causes of corrosion are essential in maintaining the required serviceability and safety of prestressed concrete bridges.

### **Objectives**

The objectives of this study were (1) to investigate the corrosion of prestressing steel in PS/C bridge components caused by the adverse environment using analytical procedures and available techniques developed for conventional reinforced concrete bridge members, (2) based on an analysis of the collected field data, to suggest a viable method of assessing the condition of prestressing steel while rehabilitation with a suitable protective system is still feasible.

### **Scope of Work and Study Approach**

A state-of-the-art review was conducted on failures of prestressing steel with an emphasis on the cause and mode of failure. Bridges which incorporate pre- or post-tensioning systems (made up of wires, strands or bars) were selectively sampled and data analyzed to determine if active corrosion of the prestressing steel was occurring.

The study included:

- Visual examination.
- Delamination survey.
- Petrographic analysis.
- Concentration of chlorides.
- Rapid chloride permeability.
- Concrete cover survey.
- Potential survey.
- Metallurgical analyses.

Bridges selected for the study were located both in northern climates subjected to application of roadway deicing salts, and in southern areas subjected to marine spray.

The following bridges were examined:

- O'Hare Airport Bridge, Des Plaines, Illinois.
- The Route Seven Viaduct, Chicago Ridge, Illinois.
- The Sixth South Street Viaduct, Salt Lake City, Utah.
- The Gandy Bridge, Tampa, Florida.
- Intracoastal Canal Bridge, Tampa, Florida.
- Ship Channel Bridge, Corpus Christi, Texas.
- Nueces Bay Causeway, Corpus Christi, Texas

The first five bridges were subjected to detailed surveys, and the remaining two were surveyed visually and given limited investigation. All bridges were examined between September 1987 and June 1988.

Based on results of the study, recommendations were made as to procedures, methods, parameters and threshold values for assessing the condition of prestressing steel in concrete bridge components.

## **TYPES OF PRESTRESSING STEEL**

In general, tendons for prestressed concrete structures are made of either (1) cold-drawn or cold-rolled steel wires manufactured by cold forming, or (2) tempered or hot-rolled steel wires and bars which obtain their mechanical properties as a result of heat treatment. Of these two types of prestressing steel cold- drawn steel, is used more extensively than heat- treated steel. <sup>(1, 2, 3)</sup>

The types of prestressing steels most commonly used in the United States are: seven-wire stress-relieved strands, cold drawn and stress-relieved wires, and cold stretched and stress-relieved bars.<sup>(4, 5, 6)</sup> Heat treated prestressing steel is not used in the United States because of its greater susceptibility to stress corrosion. Nevertheless, since this type of steel is widely used in other countries and is often referred to in the literature, some basic differences between the two types will be discussed in this report for better understanding of the mechanism of corrosion of prestressing steel. Main operations during production of both types of prestressing steel are shown in figure 1.<sup>(7)</sup>

### **Cold-Drawn Stress-Relieved Wire**

Cold drawn wire is manufactured by drawing a hot-rolled rod through a series of dies after first subjecting it to patenting and then pickling in acid.

Patenting is accomplished by heating the rod to a temperature of 1740-1830 °F (949-999 °C) in a continuous furnace with subsequent cooling in a lead bath or in air (air patenting) at a temperature of 932 °F (500 °C). The purpose of patenting is to transform the coarse austenitic structure formed after hot rolling into a more uniform fine-grained structure consisting of a mixture of sorbite and perlite. This process makes the steel more homogeneous, and more suitable for cold drawing because of increased tensile strength and ductility

After patenting and prior to drawing, the mill scale left on the surface of the rod is removed by dipping the rod into an acid bath. To prevent penetration of atomic hydrogen into the steel, the rod is washed in water and then dipped into lime to neutralize the remaining acid. After this step, the rod is phosphated and finally coated with a solution

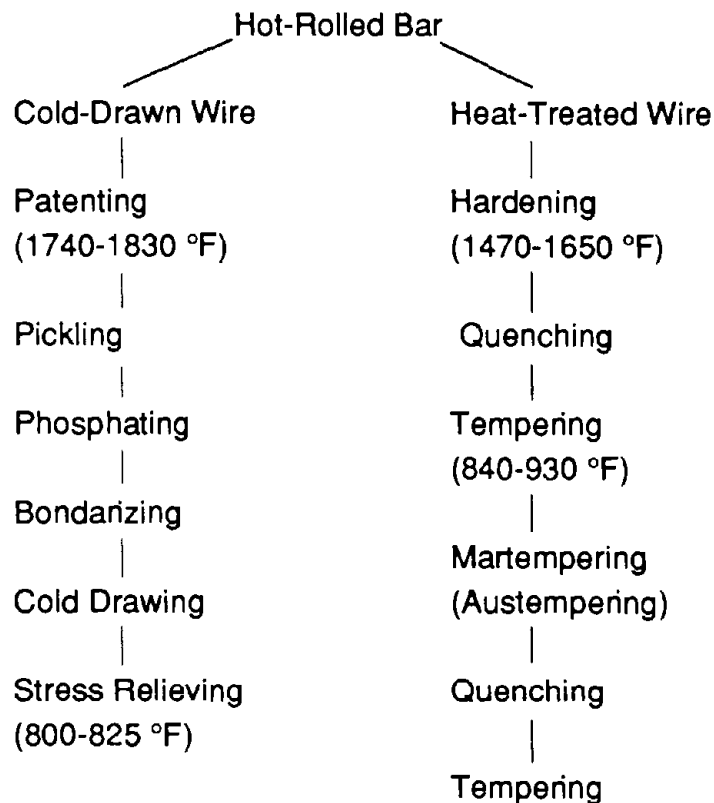


Figure 1. Production of cold-drawn and heat-treated prestressing steel.

of borax, which serves as a lubricant carrier when the rod passes through dies. Cold drawing is performed by pulling the rod through three or four tungsten carbide or alloy steel dies with approximately 20 percent reduction of the cross section at each die. During the process of drawing, the wire is subjected to both longitudinal and lateral forces which create residual nonuniform stresses in the finished product. To relieve these stresses and thus to increase the ductility and yield strength, the wire is subjected to a carefully controlled time-temperature treatment. During this treatment the wire is heated at about 800-825 °F (427-441 °C) for about 10-30 s in a bath filled with molten lead or in an air-tempering furnace. Stress relieving does not alter the sorbitic/perlitic structure of the steel formed during patenting.

Normally prior to stress relieving, the wire is straightened and then, after the treatment, is recoiled again, but to larger diameters. Small diameter wire, less than 0.12

in (3.05 mm) can be stress-relieved without recoiling. Oil and lubricant left on the surface of the wire during the process of drawing are burned off in the stress-relieving bath.

### **Quenched and Tempered Wire**

Quenched and tempered steel, as the name implies, receives its mechanical properties by applying first heat treatment, (hardening) with subsequent quenching, and later tempering. During hardening, the hot-rolled wire or bar is heated to 1470-1650 °F (799-899 °C) and then quenched in oil. As a result, the steel acquires a very hard and brittle martensitic structure. Because of internal stresses developing in the steel during hardening there is a risk that cracks will occur. For this reason, the steel is heated again, but this time to a lower temperature, usually within the range of 840 to 930 °F (449 to 499 °C). This operation is called tempering. The microstructure of quenched and tempered wire consists of round relatively fine crystallites without orientation effects. The surface of this type of wire is somewhat rougher ("more open") than that of cold-drawn wires and is sometimes blamed for low resistance of quenched and tempered steel to stress corrosion.

As a rule, quenched and tempered steel has a lower carbon content (0.5-0.7%) and a higher Mn and Si content (max. 1.25% and 1.7%, respectively) than the steel from which ordinary patented wire is made. In recent years, developments in the manufacture of quenched and tempered prestressing steel have resulted in a material of somewhat modified composition which has more favorable mechanical properties and is less susceptible to stress corrosion cracking.

## **REPORTED FAILURES**

### **General Survey**

According to the study on prestressed concrete structures built between 1950 and 1977, out of 30 million tendons installed in PS/C components only 200 tendons have been found to be affected by corrosion.<sup>(8)</sup> This amounts to 0.0007 percent, which is negligible and does not have any practical concern. Taking into consideration this fact and the fact that no catastrophic failures occurred to date (1978) it was concluded that properly detailed and constructed post-tensioned type structures will show satisfactory performance and resistance to corrosion.

This study was based on the researchers' own observations, a literature search, and information obtained from other investigators. It should be noted that this study was concerned with post-tensioned bonded and unbonded tendons, and was limited to completed structures. It did not include instances when corrosion of prestressing wires was due to improper handling of coils during shipping and storage at a project site, or due to construction and design-related deficiencies. The study also did not include cases of corrosion in tendons used temporarily to facilitate construction.

The report also describes the condition of bonded and unbonded post-tensioned tendons made of stress-relieved wires, strands, and high-strength bars in nine bridges. Most bridges were exposed to marine environments. Time of exposure varied from 2 months to 15 years. Signs of corrosion such as rust stains, cracking and spalling of concrete cover over prestressing reinforcement were observed in all examined bridges. Failure of prestressing tendons was noted in three bridges.

Another survey of failures of prestressing steel included cases which occurred in the United States between 1978 and 1982.<sup>(9)</sup> The survey was conducted based on information obtained from individuals in the prestressed concrete industry.

Summarizing results of the survey, the authors noted the described cases are mainly related to aggressive environment, poor detailing, poor construction practices, and, to a lesser extent, manufacturing defects of prestressing steel.

Out of 10 cases of brittle failures, five are related to stress corrosion. Most cases are reported to occur in post-tensioned structures. Corrosion in unbonded tendons is attributed to damage to wrapping paper or to loss of corrosion-inhibiting and corrosion-protective grease.

Improper detailing and improper protection of anchorage systems also resulted in corrosion-related damage to the prestressing systems.

Corrosion of prestressing steel in pre-tensioned structures was less prevalent. No stress corrosion was observed in pre-tensioned structures.

Most corrosion observed in post-tensioned parking garages occurred in the presence of chlorides which originated from deicing salts and penetrated into the concrete. The concentration of chlorides was as high as 0.9 percent by weight of concrete. Corrosion in all parking structures is classified as a pitting corrosion which is frequently the cause of corrosion-related deterioration of concrete in conventionally reinforced parking structures. No stress corrosion cracking was detected in any of the 15 reported cases.

Of several cases described, one is of special interest from the point of view of steel corrosion in prestressed bridges. This case involves a slab over a parking area, post-tensioned in both directions with monostrand tendons coated with a corrosion-inhibiting grease and spirally wrapped in fiber paper. Failed tendons were estimated to be about 4 percent. Most failures occurred in areas of high negative moments and sharp angles. Based on results of the investigation it appears failures occurred due to hydrogen embrittlement caused by hydrogen sulfide from lightweight aggregate (apparently furnace slag) in the concrete.

Several cases of collapse of a structure due to corrosion of the prestressing steel were also reported. In most instances a collapse occurred without warning. One of the main reasons for collapses without warning was the lack of access to prestressing tendons for inspection.

### **Bridge in the Netherlands**

Hydrogen embrittlement was identified as the cause of failure of bonded button-headed wire tendons in a bridge in The Netherlands.<sup>(10, 11)</sup> A galvanic cell was formed between the steel and aluminum parts of the sheath, facilitated by a sodium carbonate electrolyte, which was added as an accelerator in the tendon grout.

### **The Hood Canal Floating Bridge**

This bridge is located in the state of Washington in Port Gamble. The bridge consists of pontoons prestressed with 1000-ft, post-tensioning, uncovered cables. First failures of prestressing wires were observed soon after the bridge was opened to traffic in 1961. It was reported the failures were caused by pitting and stress corrosion due to inadequate protection of the prestressing cables. The tar-like coating, instead of protecting the cables from adverse effects of the marine environment, trapped moisture and sea salts creating favorable conditions for steel corrosion. It is also believed that fluctuating stresses in the tendons due to bridge movements caused fatigue of the prestressing steel thus contributing to brittle fracture of the tendons.<sup>(12)</sup>

### **Illinois Toll Highway Prestressed Concrete Bridges**

Prestressed concrete members were utilized in 224 of a total of 289 Northwest Toll Highway bridges built in 1957- 1958.<sup>(13)</sup>

A typical bridge proposed for the project incorporated I-shaped prestressed precast concrete girders with varying spans up to 107 ft (32.6 m), piers using prestressed cylindrical concrete piles 3 ft (0.91 m) in diameter with a wall thickness of 4-in (102 mm), and a prestressed precast concrete plank 2.5-in (63.5 mm) thick and 4 ft (122 mm) wide to act as deck forms and to become a part of the deck. The girders were reinforced with 40 to 73 0.44-in (11.2 mm) stress-relieved strands with an ultimate tensile strength of 255,000 psi (15 819 kg/cm<sup>2</sup>). The deck plank was centrally reinforced with 0.25-in (6.35 mm) strands. The 5-in (127 mm) cast-in-place deck slab was placed on top of prestressed planks after they were positioned on a bed of mortar to span between the girders.



Approximately 448,000 lineal ft (136 550 m) of prestressed girders, more than 19,000,000 lineal ft (5 792 683 m) of steel strand, and a little over 50,000 lineal ft (15 240 m) of 36-in (914 mm) diameter cylindrical prestressed concrete piles were used in the project.

Visual inspection of 20 bridges conducted after 25 years of exposure to freezing and thawing in the presence of moisture and deicing salts showed most girders were in an excellent condition with only slight freeze-thaw deterioration of concrete and minimal corrosion of reinforcement.<sup>(14)</sup>

In one case, severe delamination of concrete due to corrosion of prestressing strands was observed in girders in the Tri-State Tollway bridge over Harlem Avenue in Chicago. Close examination revealed some strands were fractured and the surface of the girder in this area was covered with a heavy deposit of deicing salt which presumably came through cracks and weep holes in the deck slab. The concentration of water soluble chlorides in the delaminated concrete was about 0.58 percent by weight of concrete. Stains of rust, due to corrosion of stirrups and straps around strands were observed.

### **Prestressed Panel Sub-Decks**

The function of prestressed sub-deck slabs proposed for the above project was similar to that of a steel deck in a composite floor slab, i.e. to serve as a form during placing concrete and later as the positive moment reinforcement for dead and live loads. There was some concern regarding durability of these planks due to possible noncomposite action on the deck components. Engineers were concerned that under repeated impact loads the planks would debond and cracks would develop along the strands resulting in loss of the strand bond and corrosion of the strands. Studies show that stay-in-place, precast, prestressed concrete form panels are not any more susceptible to damage than cast-in-place deck slabs.<sup>(15)</sup>

Inspection of three bridges to evaluate performance of sub-deck slabs after 7 years of service did not show any evidence of distress or noncomposite action.<sup>(16)</sup> Some transverse cracks were observed in the cast-in-place decks which extended approxi-

mately halfway through the deck. These cracks have been attributed to temperature and shrinkage.

An inspection of prestressed deck planks in Northwest Tollway bridges in 1975 found them in good condition, except for stress cracks in some negative moment regions.<sup>(17)</sup> There was no evidence of water coming through the decks. Neither concrete nor steel showed any signs of distress or deterioration.

### **Out-of-Service Bridge Near Ft. Morgan, Colorado**

This bridge was destroyed by severe floods in 1965 after 2 years in service. Following demolition of the bridge, a fragment of a prestressed girder was examined after being exposed to the same environment for an additional 1.5 years.<sup>(12)</sup> It was noticed that the strand interstices were 50 percent filled with cement paste which apparently entered the strand through separations between wires during manufacture of the girder. No evidence of corrosion was observed on surfaces of the strand in contact with concrete. There was slight corrosion on the surface of the central wire, presumably due to moisture penetrating from the damaged strand end. The depth of moisture penetration was about 2.5 in. From the above observations, it appears that 2-in. concrete cover provided good protection to the pretensioned girder strands.

### **Post-Tensioned Beams in the Tidal Zone at Treat Island, Maine**

In 1950 the U.S. Army Corps of Engineers started a study to determine the effects of severe weather exposure on the durability of prestressed concrete beams. A group of I-shaped pretensioned beams simulating bridge girders were fabricated at the Treat Island Exposure Station and subjected to cyclic wetting in seawater under an 18 ft (5.5m) tidal head and drying to a surface dry condition. During winter months the beams were exposed to cycles of freezing and thawing. The exposure period was from September 1951 to December 1975 at an average rate of 135 cycles per year.

The beams were inspected periodically to determine the degree of deterioration of the concrete, to measure crack width, to determine concentration of chlorides at the

steel level, and to evaluate the condition of the prestressing steel, conduits, end anchorages, as well as protective grease and grout.<sup>(18-26)</sup>

All beams fabricated with non-air-entrained concrete (60 out of total of 82) failed within the first 5 years of the study.

The following observations were made with remaining air-entrained concrete beams:

Concrete above reinforcing bars contained fewer voids, and was more dense than concrete beneath the bars. Most deterioration in the beams was due to corrosion of pre-tensioned steel bars.

Rust spots observed on all beams over reinforcing steel bars after 2 years of exposure indicated 0.75-in (19.1 mm) concrete cover was not sufficient to protect the reinforcement from corrosion.

Width of flexural cracks less than 0.016 in (0.4 mm) did not seem to increase the rate of steel corrosion.

No relationship was observed between the stress level and amount of corrosion in the steel.

Flush or pocket type end anchorages were better protected against corrosion than external end anchorages.

An expansive sand-cement mortar containing aluminum powder as an expansion agent and epoxy bonded concrete provided equally good protection to flush end anchorages.

Grouted tendons were found to be better protected from corrosion than paper-wrapped conduits filled with grease. Lack of wrapping paper and grease in some areas indicated the tendons might have been damaged during transporting or handling.

Chemical composition of the grout was not altered by seawater even in beams which exhibited failures of end anchorage protection.

On some occasions it was not clear if corrosion of grouted tendons was caused by excessive w/c ratio of the grout or if the tendons were corroded prior to their encapsulation with grout.

No signs of brittle fracture of the reinforcement due to hydrogen embrittlement were observed. Some wires exhibited a ductile type of failure.

Overall performance of the air-entrained prestressed concrete beams under long-term tidal exposure was rated as excellent.

### **Regina Pipeline**

Researchers described the case of a failure of a pipeline in Regina, Canada, in 1952 caused by corrosion of circumferential prestressed wires.<sup>(27-29)</sup> A metallographic examination showed all fractures were associated with longitudinal splits. The main cause of corrosion was recognized as related to the use of calcium chloride. The amount of calcium chloride in some cases was as high as 3 percent by weight of cement.

Also some shortcomings were noted in the manufacturing process of the prestressing wire and pipe section which may have contributed to the failure. It was noticed, for example, that the wire was drawn without using either water or a lubricant, which are normally used to cool the wire. Heat developed during the drawing process presumably decreased ductility of the surface steel and thus increased stresses developed in the top layer.

Corrosion of the wires was associated with the presence of relatively large voids in the steel/concrete interface, which originated during manufacturing of the pipe. The normal procedure involves winding of the circumferential wire after the core hardens, to the rough surface of the hardened core prior to application of a shotcrete mortar cover. Water penetrated to the wire through the delaminations in the wire zone and through a shotcrete cover which in many cases was found not to exceed 0.125 in (3.2 mm).

### **Summary of Causes of Failure**

In general, failure of prestressing steel in bridges may occur due to corrosion of steel tendons, deterioration of protecting sheaths, or failure of end anchorages. Different prestressing systems provide different degrees of protection to prestressing steel (table 1). Normally, pretensioned tendons are less susceptible to corrosion than post-tensioned bonded tendons. Post-tensioned unbonded tendons appear to be more susceptible to corrosion than any other prestressing tendons except for external, uncoated tendons.

Table 1. Corrosion protection to prestressing steel in various systems.

Type of Tendon	Concrete	Grout	Sheath	Grease Cover
Pretensioned	+	—	—	—
Post-tensioned bonded	+	+	+	—
Post-tensioned unbonded	+	—	+	+

Failure of prestressing steel may occur at some stage before or during service life of the ps/c bridges and related structures. Corrosion of prestressing steel prior to placing in concrete may occur mainly due to defects in steel or improper handling, or a combination of both. Causes of failures after placing in concrete and during service life are more numerous.

**Defects of Manufacture.** Failures of prestressing wires caused by defects in the steel during manufacture are not common. According to Netherlands Committee for Concrete Research, this cause of fracture was observed in only 3 out of 63 cases.<sup>(30)</sup> The defects mentioned include the presence of slag contaminants, overlapping (folding of the steel over itself during hot rolling), overdrawing of the wire, inadequate lubrication during drawing, and the presence of copper on the wire. These deficiencies can, under certain conditions, serve as points of concentration of stress and initiation of stress corrosion cracking.

As mentioned previously, lack of cooling of cold-drawn wire may have been one of the potential reasons for failure of a pipeline in Saskatchewan, Canada. Apparently, improper cooling of the wire resulted in formation of so-called martensitic zones which are known for being very brittle, and which tend to develop microcracks when stressed in tension.

Failure caused by defects of manufacture may also occur due to mechanical damage to wire, such as a notch effect, and due to additional stresses introduced by bending in small diameter coils, straightening, shaping, and winding.

**Improper Handling.** Several cases have been reported when prestressing steel failed because of improper handling during transporting and storage at the project site. In some instances failures occurred before tendons were placed in concrete or soon after the tendons were prestressed. This may happen if prestressing steel is stored in the open without protection from the weather, industrial pollution, or the splash and spray of sea water. The wire becomes particularly susceptible to fracture when tensioned if it was stored in small diameter coils.

Corrosion of prestressing steel is among early problems that California Department of Transportation was facing in the 1960's.<sup>(31)</sup> A disagreement arose between contractors and inspectors as to how much rust was allowed on prestressing steel before it was placed in a structure. Finally, the decision was made to eliminate rust completely. This was accomplished by using specially developed corrosion inhibitors and packaging forms.

**Corrosion of Pretensioned Tendons.** Corrosion of pretensioned reinforcement may occur due to one or a combination of several of the following causes:

- Presence of voids underneath high-strength bars in prestressed concrete structures.
- Lack of passivation provided by concrete surrounding prestressing steel due to decrease of alkalinity caused by carbonation.
- Presence of corrosion-inducing agents, mainly chlorides, moisture, and oxygen in contact with prestressing steel.
- Leaking joints between I-shaped girders or box girders allowing the chloride-laden water to have access to the prestressing tendons.
- Presence of chlorides in concrete surrounding prestressing tendons resulting from the use of sea water or sea aggregates.
- Inadequate concrete cover over prestressing tendons. This often results from improper construction practices.

- Permeable concrete surrounding the prestressing steel due to poor consolidation, high water/cement ratio, and incomplete hydration of portland cement.
- Presence of atomic hydrogen in contact with prestressing tendons. Possible sources of atomic hydrogen are discharge of hydrogen ions on the cathodic surface of a corrosion galvanic cell, hydrogen sulfide from polluted atmosphere, high-alumina cement and some lightweight aggregates, mainly furnace slag.
- Cracks in concrete cover promoting penetration of corrosion-inducing agents.

**Corrosion of Post-Tensioned Tendons.** Corrosion in post-tensioned tendons may arise from several sources:

- Lack of protection against pitting corrosion between prestressing and grouting operations.
- After grouting, due to incorrect concrete quality or construction procedures.
- Presence of corrosion-inducing agents, mainly chlorides, moisture, and oxygen in contact with prestressing steel. These agents can be found in contact with prestressing steel in post-tensioned bonded and unbonded tendons.
- Lack of protection to prestressing tendons in temporary and external tendons.
- Excessive local bending of the tendon.
- Faulty design of a structure allowing water or salt- laden water to collect in areas of prestressing steel and to penetrate to the steel.
- Presence of chlorides in grout.
- Presence of dissimilar metals, such as an aluminum casing at end anchorages.
- Poor grouting of post-tensioned unbonded tendons. Air pockets formed by evaporated bleed water, poor adherence of grout to prestressing tendons, inadequate filling of a sheath.
- Due to inadequate sheathing. Sheaths could have been damaged during transporting and handling at the project site. This may happen if plastic or paper sheaths are used. Sheath itself may be susceptible to corrosion, such as steel sheath, and may gradually deteriorate in concrete exposing the prestressing steel to corrosion-inducing agents.

- Accumulation of water inside a sheath.
- Concrete surrounding prestressing tendons contaminated with corrosion-inducing agents originated from external sources.
- Use of corrosion-promoting additives in concrete or in grout, or both in contact with prestressing wires.
- Use of grease which is permeable to moisture.
- Lack of grease.
- Access of water into sheathing through anchorages.



## **TYPES OF CORROSION**

As seen from the cited case histories, there are basically two major causes of brittle fracture of prestressing steel: pitting corrosion and stress corrosion cracking (SCC), sometimes referred to as stress corrosion. For some time, hydrogen embrittlement was considered a separate type of corrosion, but later it was suggested that it be treated as a variation of stress corrosion cracking.

### **Pitting Corrosion**

Unlike uniform corrosion, pitting corrosion is a localized form of galvanic corrosion. Typically galvanic corrosion occurs in metals having a passivating surface film. Corrosion starts at weak points or at points of rupture of this film and proceeds until the cross-sectional area of the wire is reduced to such an extent that tensile stresses exceed its ultimate tensile strength, and as a result, the wire fails. This type of corrosion is more harmful than the uniform type since it is difficult to predict or detect. This makes it difficult to predict the service life of a structure, besides, it may result in a sudden fracture of the wire. Since the rate of pitting corrosion is usually relatively high, time from construction to failure of the structure may be short.

Mechanism of pitting corrosion of prestressing steel is basically the same as in conventional reinforcing steel. Pitting corrosion has been thoroughly studied and well described in numerous publications and reports.<sup>(32-35)</sup> In this report pitting corrosion is discussed only as is necessary to understand brittle failure of prestressing steel.

Pitting corrosion serves as points of stress concentration which localize plastic strain in a small volume of metal. In conventional reinforcement, stresses are uniformly distributed around pitting corrosion. Therefore this steel is less susceptible to failure than high-strength steels of low ductility which do not redistribute the stresses readily, thus increasing considerably the magnitude of stresses in the areas affected by pitting corrosion.

According to Roberts, a 10-mil deep pit on the surface of an 80-mil diameter high strength wire decreases its tensile strength by approximately 15 percent.<sup>(36)</sup> Further in-

creases in depth of the pit result in a reduction of tensile strength of approximately 15 percent for each 10 mil of pit depth.

In addition to the mechanical effect, pitting corrosion serves as a source of atomic hydrogen, thus creating conditions favorable for hydrogen embrittlement.

In pretensioned tendons pitting corrosion occurs as a result of insufficient concrete cover over tendons and is commonly observed on the underside of tendons, where concrete mixing water accumulates during settlement of freshly placed concrete. In post-tensioned tendons this type of corrosion may be caused by poor grouting operations.

### **Stress Corrosion**

In the field of corrosion engineering, the term stress corrosion cracking (SCC), sometimes simply referred to as stress corrosion, is used to describe brittle fracture of prestressing steel due to intercrystalline and/or transcrystalline cracking in the presence of tensile stress and a specific active agent. Stress corrosion is defined as “chemical attack in the presence of high stress leading to intercrystalline cracking in a direction normal to the stress.”<sup>(37)</sup> Several types of stress corrosion occurring in prestressing steel have been identified to-date: stress corrosion due to hydrogen embrittlement, intercrystalline stress corrosion in nitrate (or other solutions), and fatigue corrosion.<sup>(38-39)</sup>

**Hydrogen Embrittlement.** It is believed hydrogen embrittlement occurs as follows: Atomic hydrogen diffuses into the steel, where it exists interstitially. At interior cavities, such as the interfaces produced when sulfide inclusions contract on cooling from the melt, or decohere during rolling, the hydrogen atoms can recombine to form gas. Hydrogen gas atoms in the grain boundaries are at high pressure and exert a significant tensile force tending to separate the iron atoms. The equilibrium partial pressure of hydrogen in a chloride-contaminated pit in a steel surface can be as high as 1,000 atm.<sup>(40)</sup> Embrittlement occurs when the pressure created by hydrogen gas atoms in a combination with a high tensile stress in prestressing steel exceeds the yield strength of steel, some 3 to 20,000 atm. In addition to creating an internal pressure, hydrogen gas atoms also lower the cohesive forces between adjacent grains. The danger of embrittlement increases at a higher external hydrogen activity.

For hydrogen embrittlement to occur there must be present a source of atomic hydrogen such as steel itself, hydrogen sulfide (H<sub>2</sub>S), galvanic cells, and some special solutions used in the laboratory to evaluate susceptibility of steel to stress corrosion.

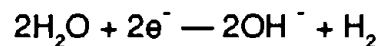
Atomic hydrogen may be present in the prestressing steel from the time when it was manufactured. Hydrogen can originate from the molten state, for example from steel refining. It also may originate during pickling of hot-rolled rods in a solution of sulfuric acid prior to cold drawing. Some impurities which may be present in sulfuric acid, such as sulfur compounds, do not allow atomic hydrogen evolving during pickling to combine into molecules.

Atomic hydrogen may also be produced by gas dissociation from hydrogen sulfide present in the atmosphere in industrial and farming regions, in high-alumina cement concrete, and in concrete made with blast furnace slag as follows:



It is believed that in hardened high-alumina cement concrete, hydrogen sulfide is formed as a result of reaction between sulfide compounds and carbon dioxide from the atmosphere.<sup>(41, 42)</sup>

A common internal source of atomic hydrogen is a galvanic cell developed in a reinforced concrete structure. In a corrosion cell hydrogen evolves as a result of water dissociation at cathodic sites:



Studies showed this reaction can occur when moisture is present, when the pH of the electrolyte does not exceed 8.3, and when the metal-solution potential is in the range of -0.6 to +0.3 V. These conditions may exist in concrete under field conditions, especially in the presence of chlorides.<sup>(43)</sup> The potentials measured in their experiments were in the range of -0.4 to +0.05 V. The pH in the corrosion pit was as low as 5. In

other words, hydrogen embrittlement may occur even when hydrogen sulfide is not present. This is in agreement with results of field observations of prestressing steel showing occurrence of hydrogen embrittlement is quite common in normal atmosphere, not polluted with  $H_2S$ , especially in the presence of chloride ions.

**Stress Cracking.** Sometimes stress cracking is mentioned as the third cause of brittle fracture of prestressing steel. It would probably be more correct to define this cause as the same hydrogen embrittlement which occurs in some strongly embrittling solutions, such as solutions of sulfuric acid, hydrogen sulfide ( $H_2S$ ), and 20 percent solutions of ammonium rhodanid ( $NH_4NCS$ ). These solutions are used in laboratories in accelerated tests to determine susceptibility of particular prestressing steel to brittle fracture. For some time nitrate solutions were used to initiate hydrogen embrittlement until doubt developed regarding validity of this test. Until recently it was believed that stress cracking could occur also in the presence of chloride ions. Researchers evaluated the effect of chlorides using cold-drawn as well as tempered steel wires which are known to be more susceptible to brittle fracture.<sup>(44-46)</sup> The steel specimens, stressed to levels 175, 200, and 225 ksi (12 304, 14 061, and 15 819 kg/cm<sup>2</sup>), were stored in a 3.5 percent solution of NaCl for up to 800 hr. The tests were conducted at room and at elevated temperatures. Despite the presence of pitting type corrosion no brittle fractures were observed in any of the test samples. Based on results of this study, it appears prestressing tendons in bridges exposed to marine and deicer environments are not likely to experience a brittle failure due to this type of corrosion.

Summarizing, it can be postulated that brittle fracture of prestressing steel can occur due to pitting corrosion as a result of decrease in the cross-sectional area and an increase of stresses and/or due to stress corrosion cracking.

Two types of SCC have been identified to occur in prestressing steel in bridges: hydrogen embrittlement and fatigue corrosion.

For hydrogen, embrittlement to occur there must be present a source of atomic hydrogen, such as steel itself, galvanic cell, or  $H_2S$  from one or several of the following sources: industrial polluted atmosphere, high-alumina cement, slag cement, slag aggre-

gate and some special solutions used in the laboratory to evaluate susceptibility of steel to stress corrosion.

For galvanic cells to evolve hydrogen there must be present potentials in the range of -0.6 to +0.3 V, and a pH lower than 8.3. If these conditions do not exist no stress corrosion will take place.

## **O'HARE AIRPORT LEADS BRIDGE**

### **Bridge Description**

O'Hare Airport Leads Bridge is located on Highway 190, East of O'Hare airport over Des Plaines River Road in Des Plaines, IL (figure 2). It consists of two bridges, one carrying westbound and the other carrying eastbound traffic. Both bridges were constructed in 1959.

The investigation was concerned only with the bridge carrying westbound traffic. This bridge has 4 spans supported by two abutments and three piers consisting of precast concrete piles with cast-in-place caps. Overall length of the bridge is 173 ft (52.73 m). The spans are comprised of I-shaped precast pretensioned concrete girders and a 7-in (177.8 mm) cast-in-place concrete deck slab (figure 3) treated with a sealing compound to a depth of 1 in (25.4 mm) prior to placing a 2.25-in (57.15 mm) bitumen wearing surface.

Precast prestressed girders were designed in accordance with American Association of State Highway Officials (AASHTO) Standard Specifications for Highway Bridges, 1957, and the criteria for prestressed concrete bridges of the Bureau of Public Roads, 1954. The girders are reinforced with Grade 250 seven wire, stress relieved strands with a nominal diameter of 7/16 in (11.11 mm), and a cross-sectional area of 0.108 in<sup>2</sup> (69.68 mm<sup>2</sup>). The end span girders have a total of 22 straight strands including 6 top and 16 bottom strands. Details of prestressing steel for a typical end span girder are shown in figure 4. The girders in the middle 2 spans contain 22 strands consisting of 16 straight and 6 bent strands. The strands are bent at a distance of 4.75 ft (1.48 m) from the center line of the girder. Initial stress in each strand was in the range of 160,185 to 175,000 psi (11 262 to 12 304 kg/cm<sup>2</sup>). Specified strength of concrete in the girders was 5,000 psi (352 kg/cm<sup>2</sup>). The stress in the strands was released when concrete gained minimum 4,000 psi (281 kg/cm<sup>2</sup>).

Three types of joints were placed throughout the deck slab of the bridge: expansion joints located over shoulder piers, transverse joints adjacent to fixed ends of beams over abutments and a center pier, and a longitudinal expansion joint located between

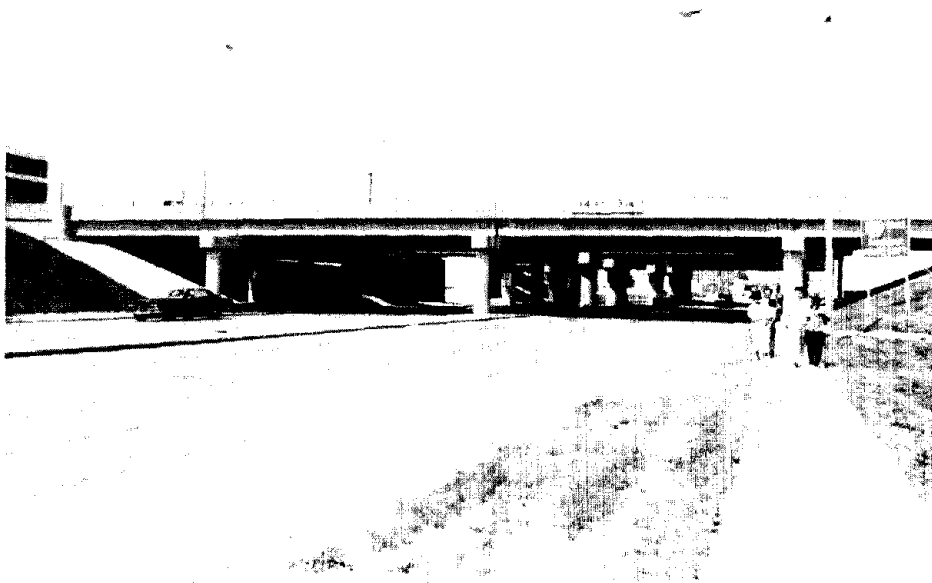


Figure 2. O'Hare Airport Leads Bridge.

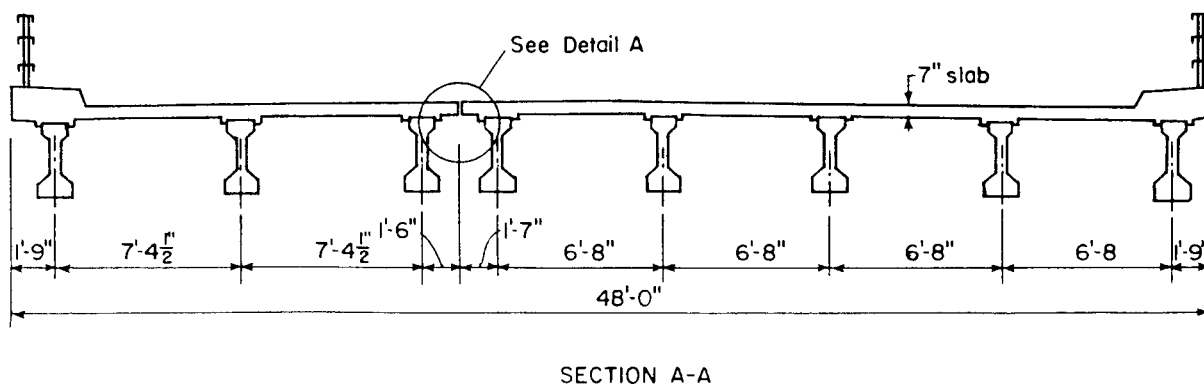
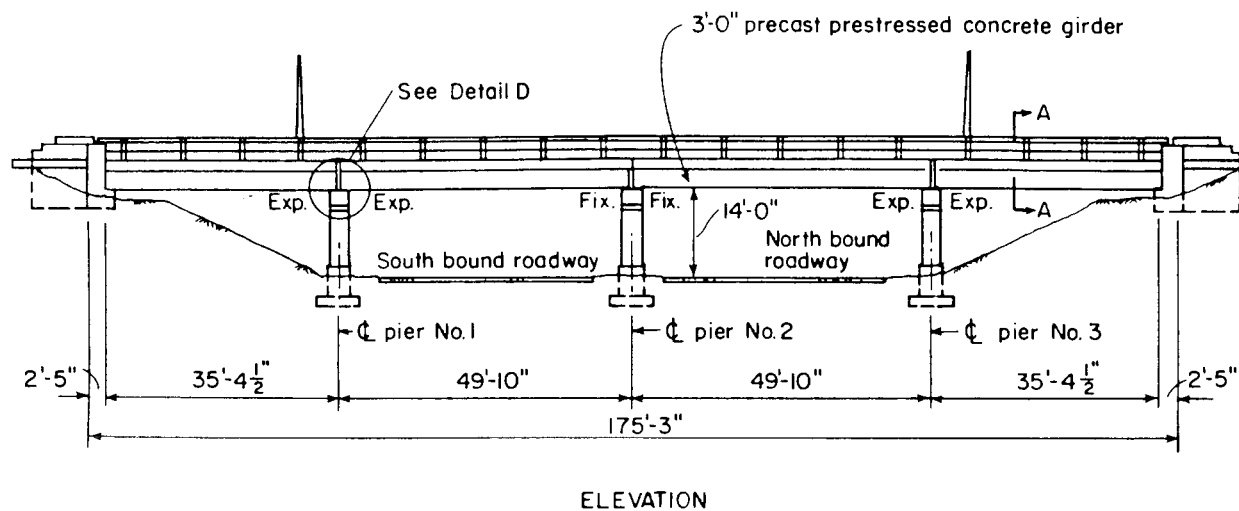
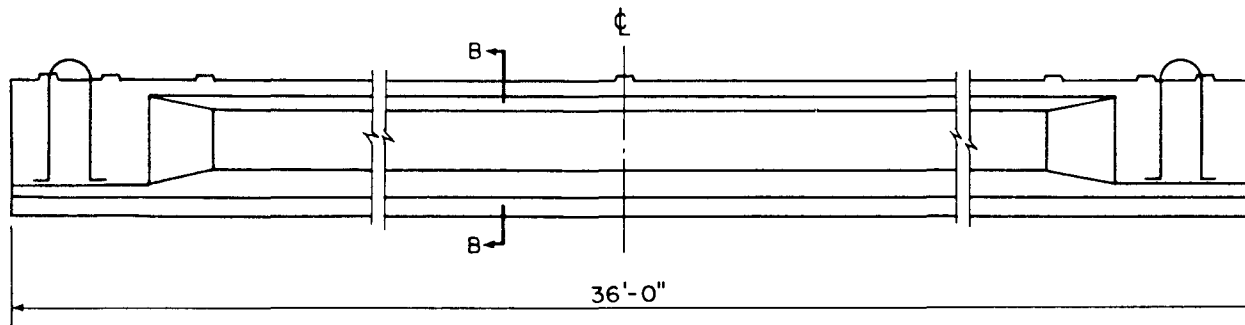
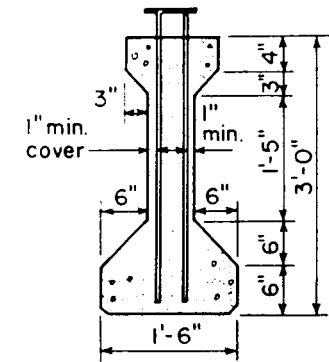


Figure 3. Elevation and cross section of O'Hare Airport Leads Bridge.

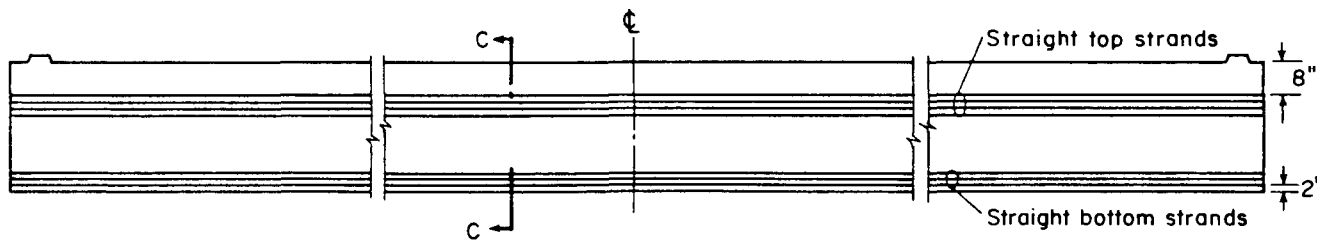




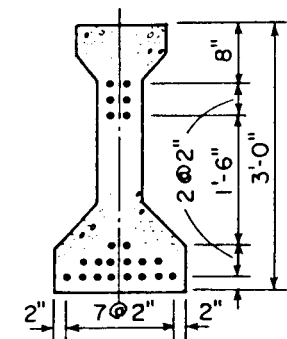
ELEVATION OF 36-IN. CONCRETE GIRDER



SECTION B-B



DETAILS OF PRESTRESSING STEEL



SECTION C-C

Notes: Prestressing Steel: Uncoated Seven  
Wire Stress-Relieved Strands  
Nominal Diameter = 9/16 in  
Cross Section Area = 0.1089 in<sup>2</sup>  
Number of Strands = 22

Figure 4. AASHTO prestressed concrete girders.

Girders 3 and 4 from the north side of the bridge. The longitudinal joint is 0.5 in (12.7 mm) wide and is filled with copper sealer and a bitumen fiber joint filler (figure 3, Detail A). A typical transverse expansion joint is shown in figure 3, Detail D. Joints at fixed ends of girders are sealed with 1-in (125.4 mm) bitumen fiber joint filler.

### **Visual Examination**

The purpose of the visual examination was to assess the extent and to determine the cause of deterioration in prestressed girders of the bridge. To aid the evaluation, some conventionally reinforced concrete structures were also examined. Among most common signs of distress were: traces of evaporated water, wet spots, discolorations, cracks and spalls in concrete cover, rust stains, delamination of concrete cover over stirrups in girder webs, as well as exposed and in some areas fractured prestressing strands.

Distress had occurred mainly in the girders adjacent to the longitudinal expansion joint in all four spans of the bridge. There was more deterioration in the end spans, especially in Span 4, than in the middle spans. Of the two girders adjacent to the leaking longitudinal joint Span 4, the girder on the north side (Girder 3) deteriorated more extensively than the girder on the south side of this joint (Girder 4). Girder 4 was used later as a reference for Girder 3.

Cracking and spalling of concrete cover in Girder 3 was due to corrosion of prestressing strands (figures 5 and 6 ). The length of cracks was up to 10 ft (3.05 m). The total area of spalls was about 0.7 ft<sup>2</sup> (0.065 m<sup>2</sup>). Neither cracks nor spalls penetrated beyond the prestressing strands.

This type of cracking was also noticed in end areas of almost all girders adjacent to transverse expansion and fixed joints over bridge piers and abutments. Normally, cracks originated at the end of a girder and penetrated towards the support steel plates at a height of about 2 to 10 in (50.8 to 254 mm), reaching occasionally in length 3 ft (0.91 m). The width of these cracks ranged from 0.06 to 0.12 in (1.52 to 3.05 mm). Commonly, cracking was accompanied by spalling of concrete cover and exposure of prestressing strands (figure 7). The length of exposed strands was 4 to 6 in (101.6 to

152.4 mm). Discolorations from evaporated water as well as wet spots were traced as far as up to 20 in. (0.51 m) in both directions from a leaking joint. Because of the better design and subsequently less leakage, corrosion-related deterioration of concrete cover was less pronounced in areas of fixed joints as compared with expansion joints.

There was not much distress observed in Spans 1, 2, and 3, except for some spalling of concrete cover over stirrups and minor discolorations on the web and the bottom surfaces of the girders adjacent to the longitudinal joint. In general, discoloration of concrete in the presence of chlorides can be used as one of the signs for possible corrosion of the reinforcement with subsequent cracking and spalling of concrete cover.

Corrosion of prestressing strands was observed in two major areas, in the bottom portion of Girder 3, Span 4 and at both ends of most bridge girders. In Girder 3 a total of two exposed strands were found on north and south sides of the bottom surface. Both strands were completely corroded and each had at least one fracture (figures 8 and 9). The strand on the bottom south side of Girder 3 was sampled to determine the mode of failure.

Unusual stains running longitudinally along the girder that looked like rust stains were observed on the bottom surface of several girders (figure 10). They were well visible along the full length of a girder. The first impression given by these stains was that they were caused by corrosion of prestressing strands. However, a more detailed study did not indicate the presence of active corrosion in these areas. These stains were noticed in girders where corrosion of strands was not expected, such as, for example, Girder 1 in Span 1.

Observing corrosion-related deterioration of concrete cover and wet spots on the surface of bridge structures (figure 11), it was noted that almost all expansion and some fixed joints were leaking to some extent. Visual examination of the deck top surface revealed that both longitudinal and transverse joints were in rather poor condition (figures 12 and 13).

One repair was observed in the bridge carrying eastbound traffic. The repair was on the bottom side of the girder adjacent to the longitudinal expansion joint. The repair appeared to be of portland cement shotcrete. Visual examination of the patch revealed



Figure 5. Severe cracking of concrete cover in Girder 3, Span 4.



Figure 6. Spalling of concrete cover in Girder 3, Span 4.

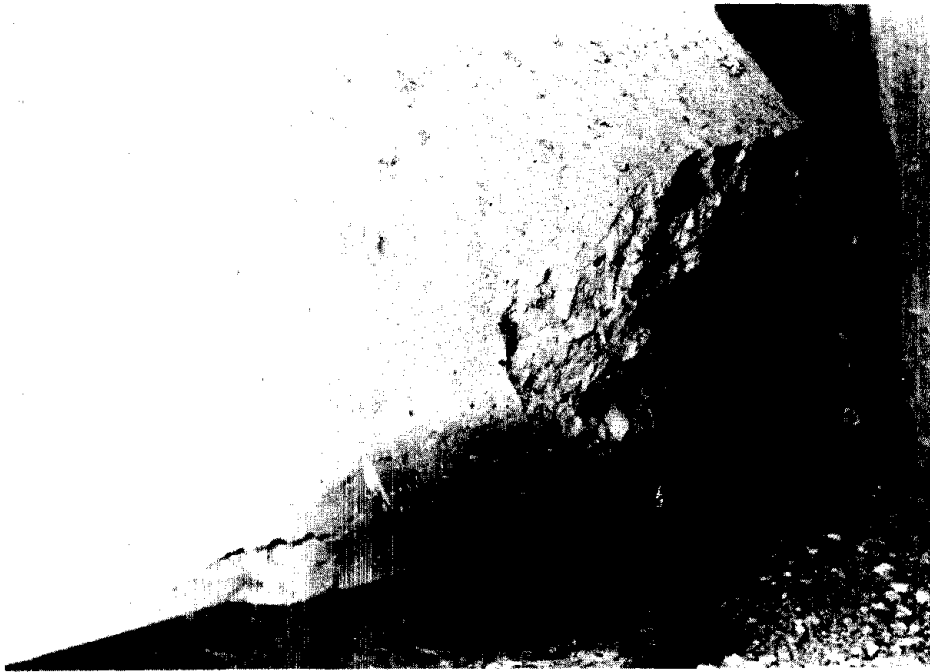


Figure 7. Spalling of concrete cover and exposure of prestressing strands at the end of a girder.

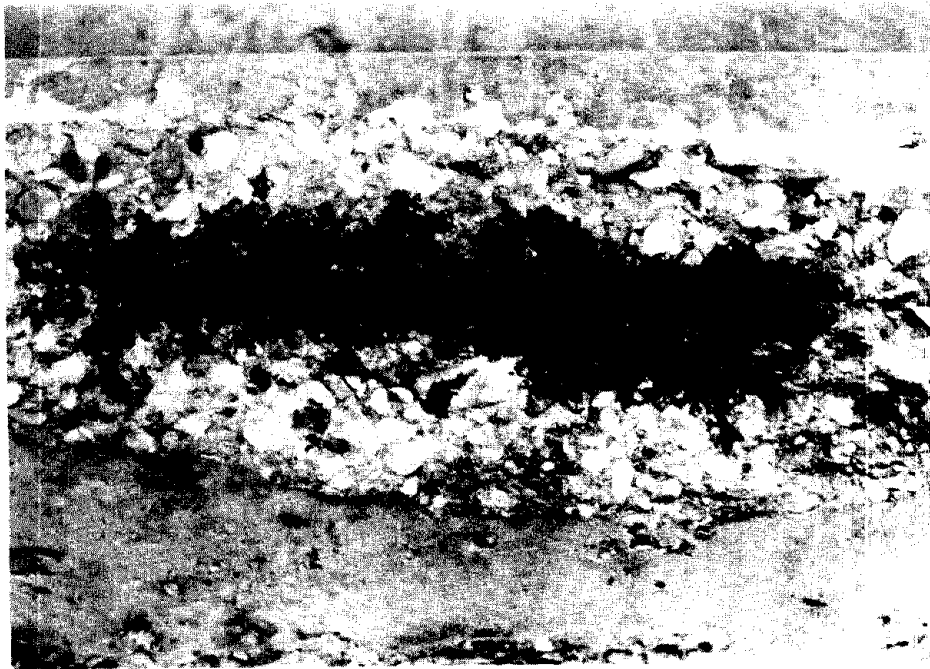


Figure 8. Severely corroded strand on the north side of Girder 3, Span 4.

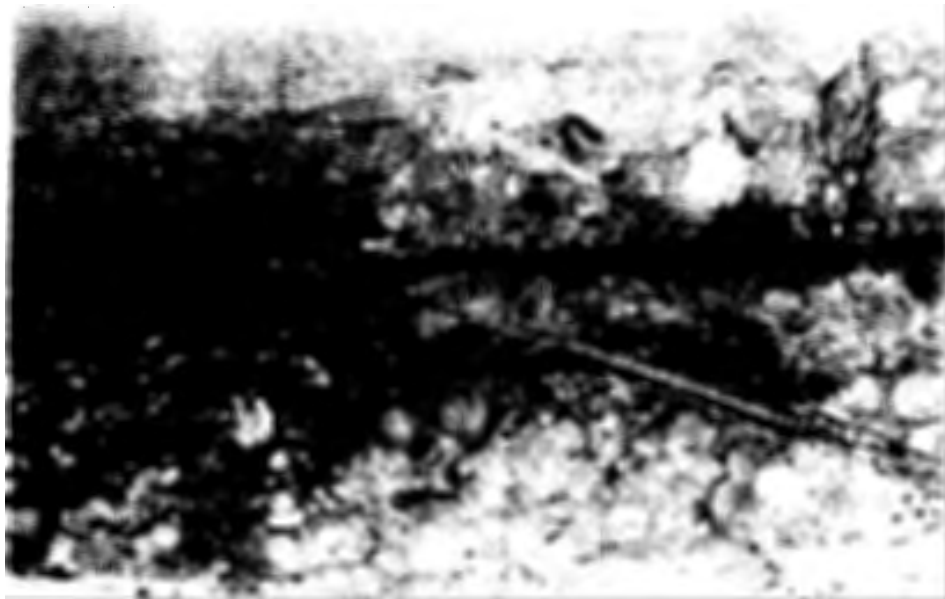


Figure 9. Fractured strand on the south side of Girder 3, Span 4.

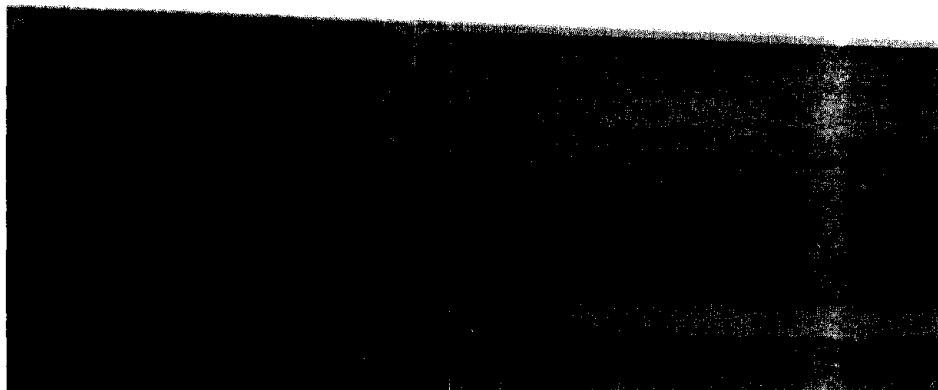
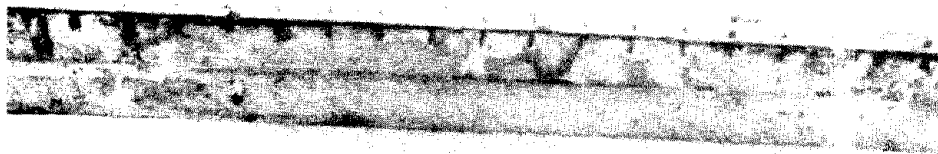


Figure 10. Apparant stains of rust on the bottom surface of a girder.

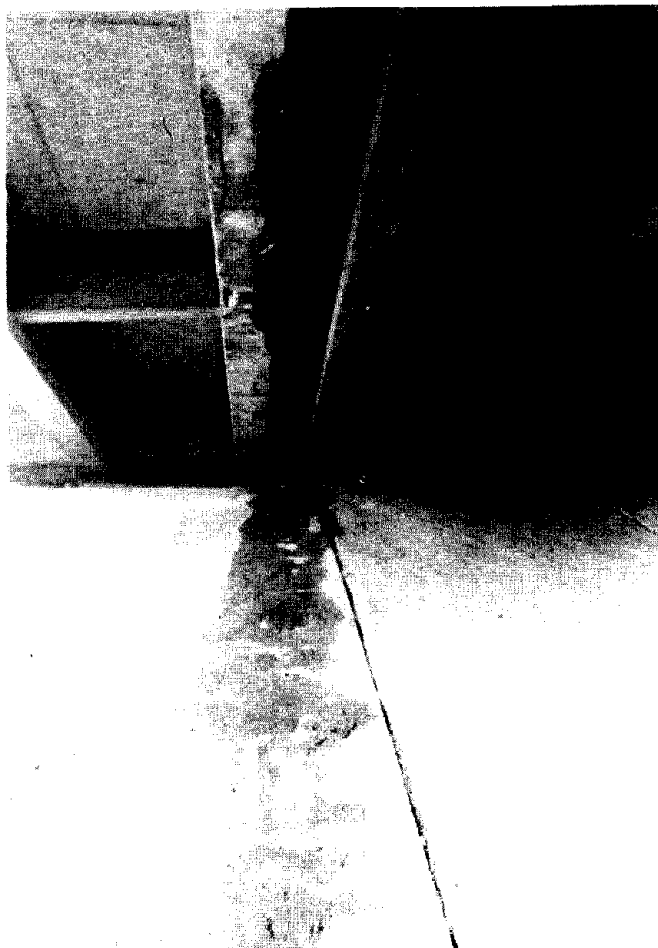


Figure 11. Wet spots under  
the bridge in Span 4.

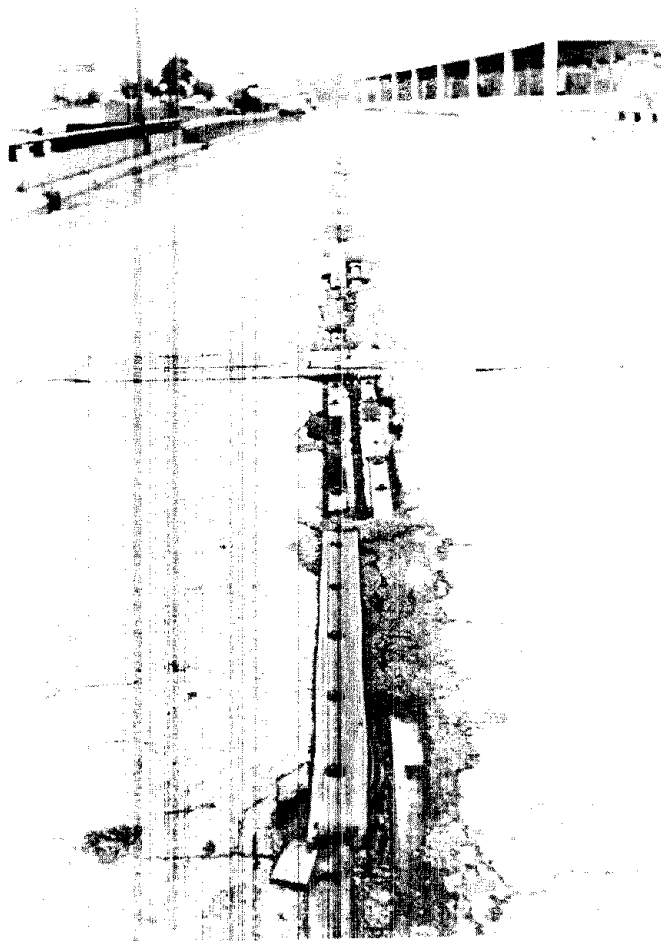


Figure 12. Badly deteriorated longitudinal expansion joint.



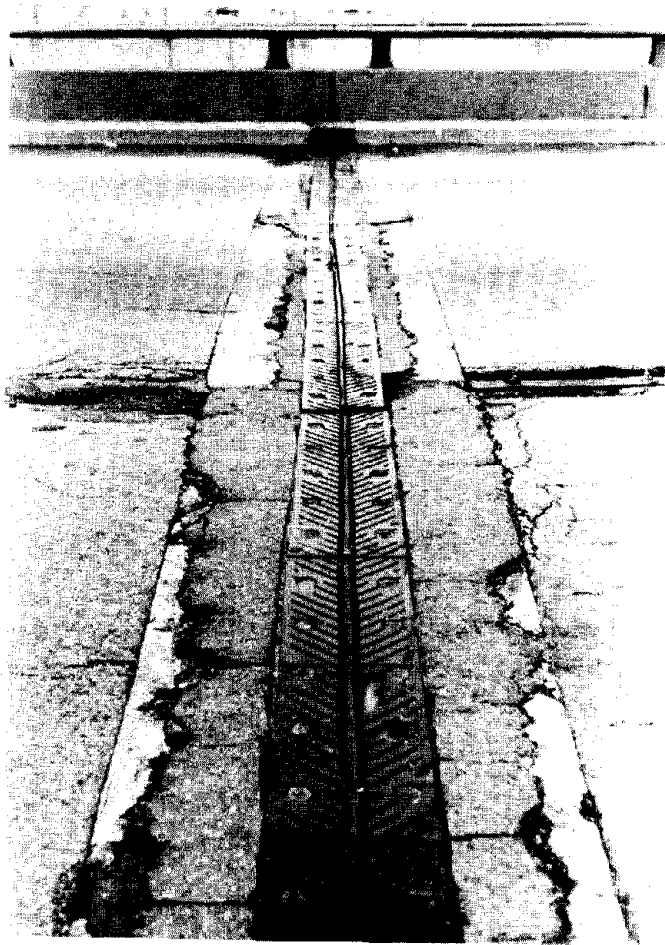


Figure 13. Badly deteriorated  
transverse expansion joint.

the presence of cracks, and rust stains of rust (figure 14), apparently caused by corrosion of prestressing strands due to chloride-laden water penetrating through the loose bond between the patch and the beam and also through the shotcrete. The patterns of deterioration in this girder resembled those in Girder 3 of Span 4, in the bridge carrying westbound traffic. It is believed that the cause of deteriorations in both cases was the same.

Corrosion of conventional reinforcement with subsequent cracking and spalling of concrete cover had occurred in diaphragms adjacent to transverse leaking joints (figure 15) and in outside prestressed girders above pier caps (figure 16). Since the bridge deck was recently repaired, there was not much deterioration of concrete on the bottom surface of the deck. Medium to severe scaling, and white deposits were noticed in areas next to the leaking longitudinal joint.

#### **Delamination of Concrete Cover**

No delamination of concrete cover was observed over prestressing strands. There was some delamination over stirrups on vertical internal surfaces in girders adjacent to the longitudinal expansion joint (figure 17). It had occurred mainly in Spans 1 and 4. The thickness of concrete cover in these areas varied from 0 to 1 in. (0 to 25.4 mm). In general, this type of concrete delamination can be used as an indication of the presence of a corrosive environment close to prestressing strands. It suggests corrosion of strands below delaminated areas is likely to occur.

#### **Petrographic Analysis**

Two cores labeled SP#4,G2-1 and SP#4,G4-3 were examined. Petrographic analysis on cores from all examined bridges was in accordance with ASTM C856-83. Cores SP#4,G2-1 and SP#4,G4-3 were obtained from Span 4, Girders 2 and 4, respectively.

**Core SP#4, G2-1.** Both ends of the core have smooth imprints of formed surfaces. Steel reinforcement is not present in the core. Fairly infrequent voids, some of which are continuous, are seen in paste and at the periphery of aggregate particles. These voids are judged to be bleed water channels. Coarse aggregate is natural calcereous-



Figure 14. Cracks and stains of rust in the shotcrete patch.



Figure 15. Cracking and spalling of concrete cover in diaphragms adjacent to transverse leaking joints.

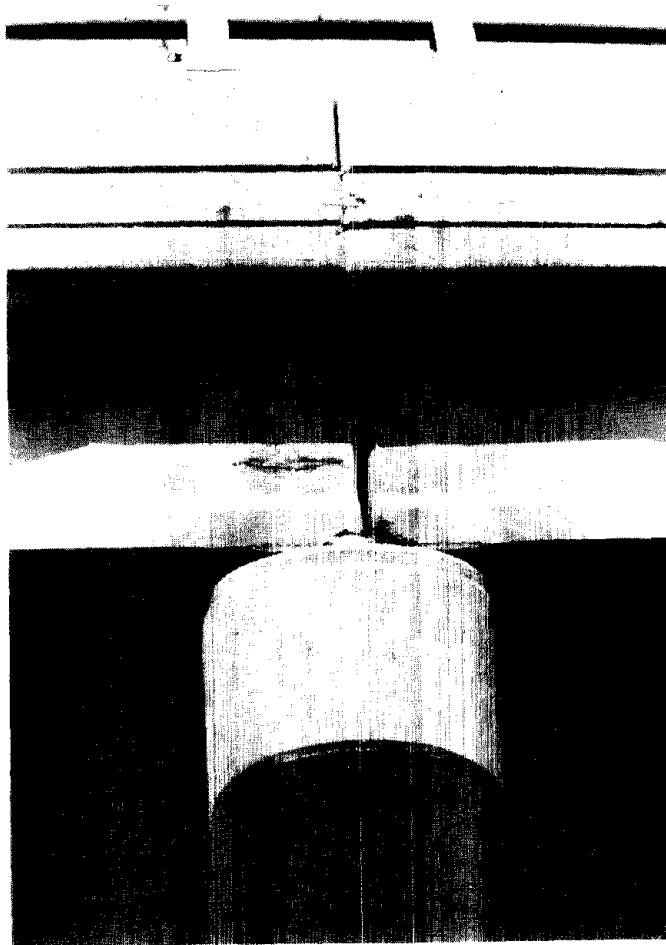


Figure 16. Spalling of concrete cover over corroded stirrups.



Figure 17. Delamination of concrete cover on internal girder surfaces.

siliceous gravel containing dolomite, limestone, granite, sandstone, siltstone, chert, diorite, ironstone, and other rock/mineral types. Due to the mixed lithology coarse aggregate particles are variously colored, hard, dense, subrounded to well-rounded, and spherical to subprismatic. Maximum measured aggregate size is 0.75 in (19.1 mm).

Fine aggregate is a natural calcareous-siliceous sand containing rock/mineral types similar to the coarse aggregate plus major amounts of quartz, moderate amount of feldspar, and minor amounts of ferromagnesian minerals. Calcareous fines are moderately abundant. Fine aggregate particles are variously colored, moderately hard to hard, somewhat porous to dense, subrounded to well-rounded, and spherical to subspherical. The aggregates are well graded and uniformly dispersed. There are no indications the aggregates performed poorly in the concrete.

Cement paste is medium brownish gray, hard, slightly porous, and fairly well-bonded to aggregate particles. Paste along freshly broken surfaces exhibits a vitreous luster, microgranular texture, and irregular fracture. Paste carbonation extends to a depth of 0.25 to 0.5 in (6.4 to 12.7 mm) from each of the formed surfaces. Residual cement particles and calcium hydroxide are moderately abundant. Based on condition of the paste, water-cement ratio of concrete is estimated to be 0.40 to 0.45. Typical microstructure of the concrete is shown in figures 18 and 19.

The concrete is air-entrained. Air content is visually estimated to be 3.5 to 4.5 percent. Most of the voids are extremely fine and spherical. Large, nonspherical voids are somewhat uncommon, suggesting the concrete was adequately consolidated. Void distribution is somewhat nonuniform with some areas containing fewer voids.

Secondary deposits are not detected in voids or aggregate sockets. There is no evidence of deterioration in concrete represented by this core.

**Core SP#4, G4-3.** Both ends of the core have smooth imprints of formed surfaces. Steel reinforcement is not present in the core. Bleed channels or water gaps are not detected.

Coarse aggregate is a natural calcareous-siliceous gravel similar to that described for Core SP#4,G2-1. Fine aggregate is natural calcareous siliceous sand similar to that in Core SP#4,G2- 1. Maximum measured aggregate size is 0.75 in (19.1 mm). The

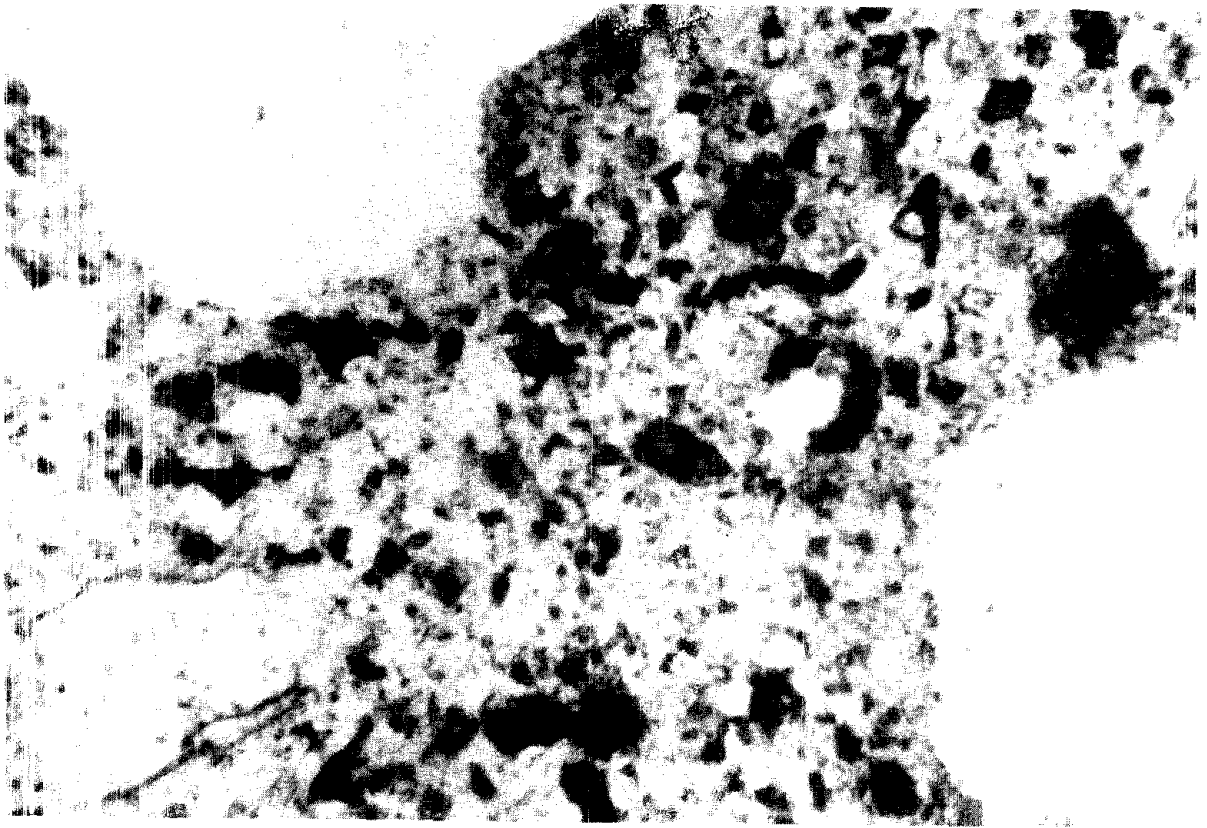


Figure 18. Typical microstructure of concrete in  
Core SP#4, G2-1. (Plane-polarized light.  
Magnification = 80X. Length of  
field = 1.2 mm.)

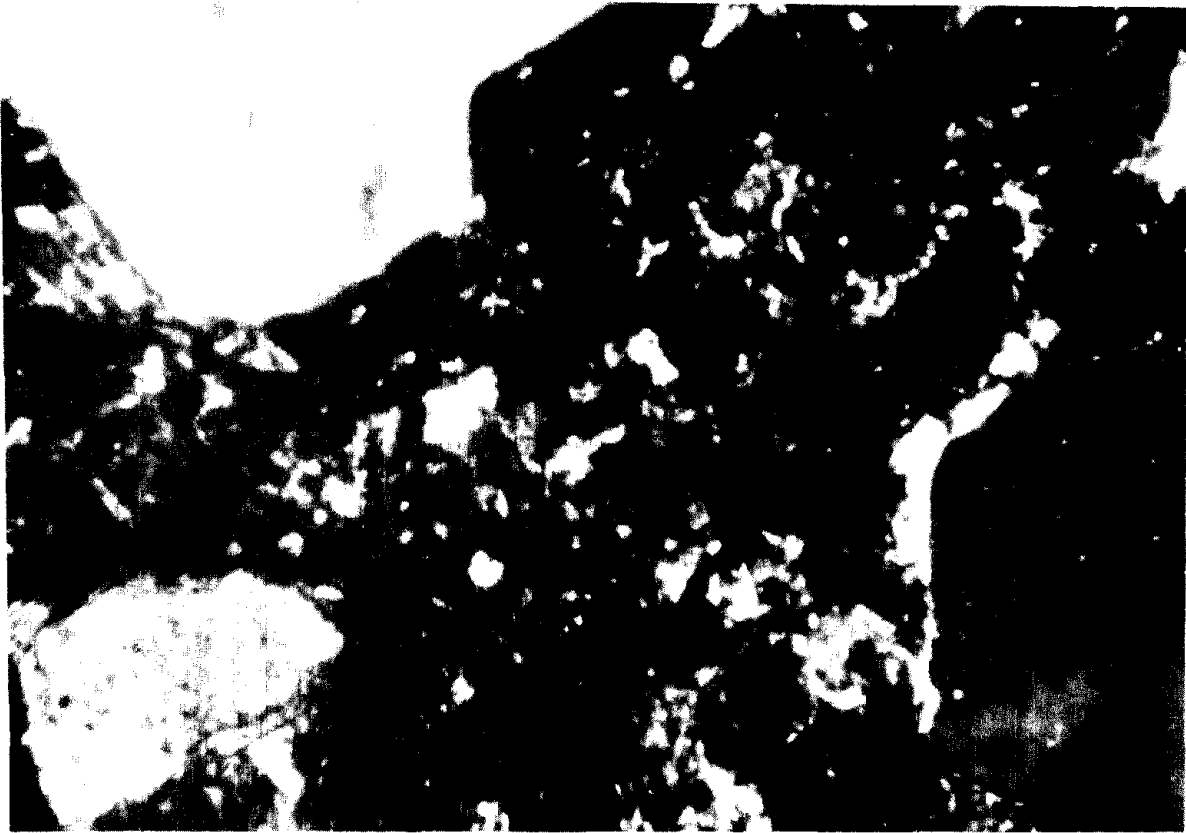


Figure 19. Microstructure of concrete in  
Core SP#4G, 2-1. (Crossed-polarized  
light. Magnification = 100X.  
Length of field = 1.2 mm.)

aggregates are well-graded and uniformly dispersed. There are no indications that the aggregates have performed poorly in service.

Cement paste is medium brownish gray, hard, slightly porous, and moderately well-bonded to aggregate particles. Paste along freshly broken surfaces exhibits a vitreous luster, microgranular texture, and irregular fracture. Paste carbonation extends 0.25 to 0.38 in (6.4 to 9.7 mm) from each of the formed surfaces. Residual cement particles and calcium hydroxide are moderately abundant. Based on interpretation of previously described paste properties, water-cement ratio of concrete is estimated to be 0.40 to 0.45. Typical microstructure of the concrete is shown in figures 20 and 21.

The concrete is air-entrained. Air content is visually estimated to be 3 to 4 percent. Many of the voids are extremely fine and spherical. Large, nonspherical voids are somewhat uncommon. The concrete appears adequately consolidated. Void distribution is somewhat nonuniform with some areas containing fewer voids than others.

Secondary deposits are not detected in voids or aggregate sockets. There is no evidence of deterioration in concrete represented by this core.

Based on results of petrographic analysis it can be concluded that concrete represented by these cores is of good quality and generally low permeability. Concrete represented by Core SP#4G2-1 is judged to be of higher permeability than that represented by Core SP#4,G4-3. None of these concretes exhibit major signs of distress.

### **Chloride Concentration**

A total of 18 samples was obtained from girders of the bridge to determine concentration of chlorides in concrete at various depths. Description of test samples and test results are shown in table 2.

Of all girders sampled the highest concentration of chlorides was found in Girder 3 where most corrosion-related deterioration of concrete had occurred. The surface concentration of chlorides was higher on the vertical side adjacent to the leaking joint than on the bottom side of the girder, being 0.742 and 0.620 percent, respectively. Concentration of chlorides at the level of the reinforcement, on the contrary, was higher on the bottom side being 0.550 as compared with 0.355 percent on the south side of the girder.



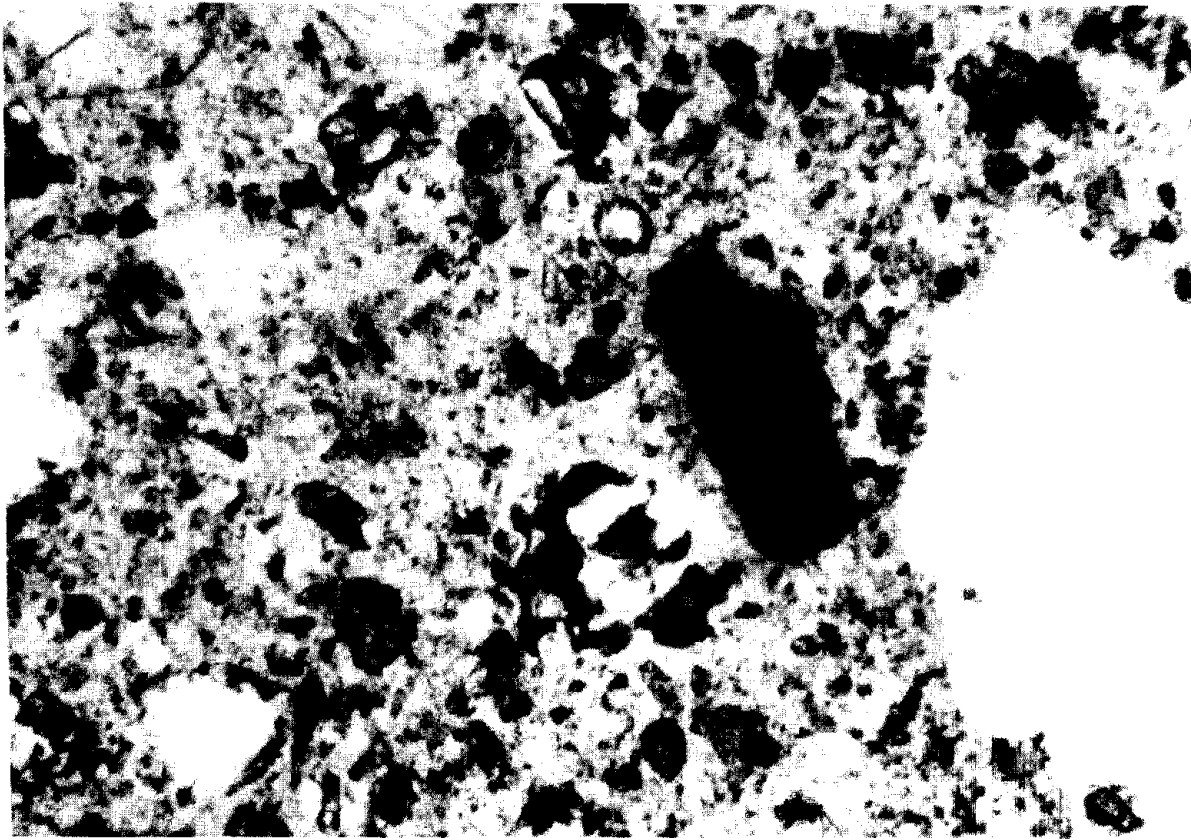


Figure 20. Typical microstructure of concrete in  
Core SP#G4, G-3. (Plane-polarized light.  
Magnification = 100X. Length of  
field = 1.2 mm.)

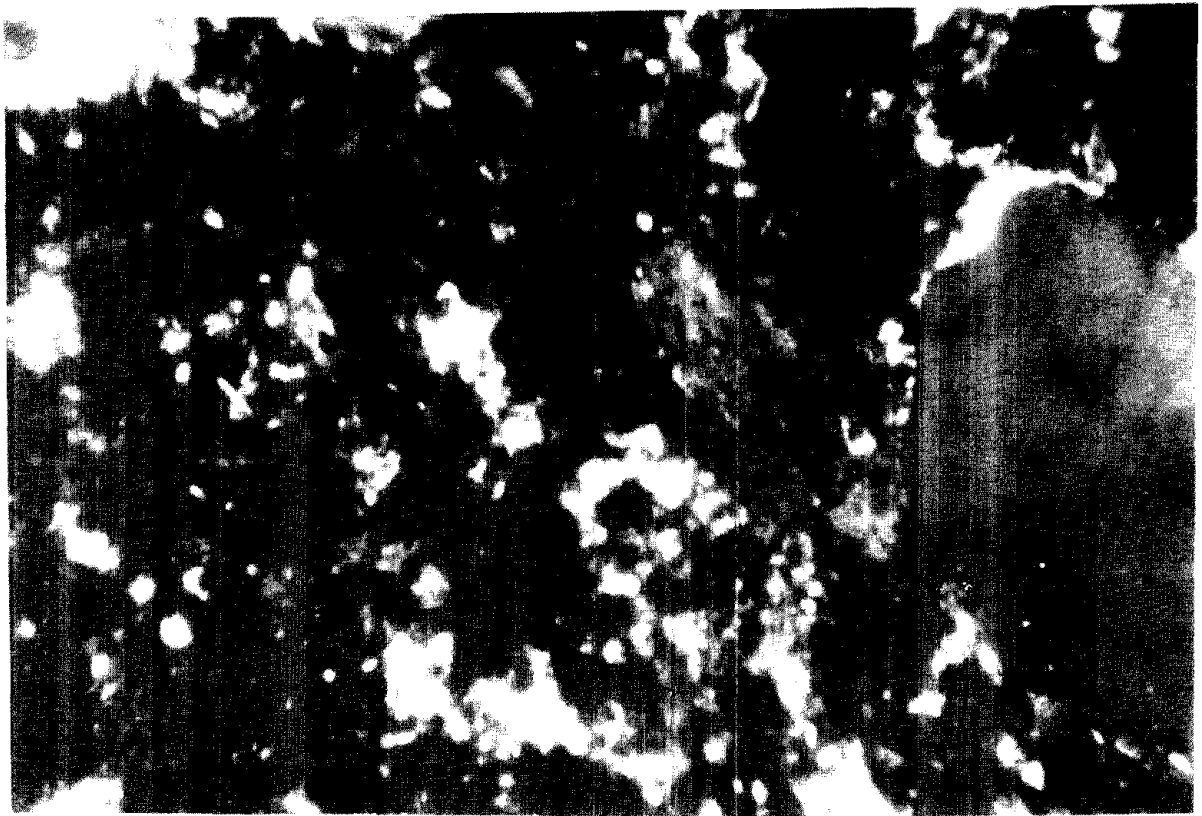


Figure 21. Microstructure of concrete in Core  
SP#G4, G-3. (Magnification = 100X.  
Length of field = 1.2 mm.)

Table 2. Total chloride analysis for O'Hare Airport Leads Bridge.

Sample No.	Location	Depth in.	Cl ions %
1	SP#1,G#2	0.5	0.092
2	Bottom surface	1.0	0.069
3		1.5	0.044
4	SP#1,G#4	0.5	0.659
5	North side	1.0	0.373
6		1.5	0.092
7	SP#4,G#4	0.5	0.078
8	Bottom surface	1.0	0.052
9		1.5	0.044
10	SP#4,G#3	0.5	0.742
11	South side	1.0	0.641
12		1.5	0.355
13	SP#4,G#3	0.5	0.620
14	Bottom surface	1.0	0.649
15		1.5	0.550
16	SP#4,G#1	0.5	0.187
17	South side	1.0	0.057
18		1.5	0.043

It is interesting to note that the reinforcement level concentration of chlorides in Girder 4, which is adjacent to the same leaking joint on the south side, was only 0.044 percent. This is comparable with the concentration of chlorides at the same level in Girder 1, Span 4, (Sample 18); and Girder 2, Span 1, (Sample 3). In other words, even

though Girder 4 is adjacent to the leaking joint, the concentration of chlorides in this girder is much lower than that in Girder 3, and is as low as in any girder remote from the leaking joint. This can be explained by the fact the bridge is sloped towards Girder 3 and therefore, chloride-laden water from the deck surface runs down the south side of Girder 3 without affecting Girder 4.

### **Rapid Chloride Penetration**

Determination of the chloride permeability was carried out on the same specimens used for petrographic analysis. Test results shown in table 3, below indicate that the permeability of the concrete to chloride ions is low.

Table 3. Permeability of the concrete to chloride ions.

Sample	Charge Passed (coulombs)	Penetration (per AASHTO T277)
SP#4,G2-1	1178	Low
SP#4,G4-3	1858	Low

These results are in agreement with findings of the petrographic analysis.

### **Concrete Cover Survey**

Survey of concrete cover was conducted on all girders in Span 4. In areas of exposed prestressing strands, the thickness of concrete cover was measured directly and then compared with R- Meter readings. Readings were taken on all sides of girders around prestressing strands at a distance of 8 ft (2.44m) (Location A) and 13 ft (3.96 m) (Location B) from the east end of the span. Test results shown in table 4 indicate the average thickness of concrete cover on the bottom side of girders is in the range of 1.74 to 1.77 in (44.2 to 45.0 mm), as compared with 1.72 to 1.98 in (43.7 to 50.3 mm) on the south and north sides of beams over the bottom prestressing strands. The average specified concrete cover around the steel strands is 2 in (50.8 mm).

Table 4. Results of concrete cover survey.

Girder No.	Thickness of concrete cover, in					
	Location A			Location B		
	North side	Bottom surface	South side	North side	Bottom surface	South side
1	2.20	1.75	1.76	2.20	1.75	1.76
2	1.88	1.85	2.10	1.88	1.75	1.70
3	1.88	1.67	1.88	1.76	1.65	1.94
4	1.76	1.80	2.10	1.76	2.18	1.76
5	2.29	1.85	1.58	1.95	1.78	1.51
6	1.70	1.65	1.70	1.88	1.68	1.60
7	1.94	1.68	1.88	1.82	1.70	1.94
8	2.20	1.65	1.82	1.60	1.65	1.54
Minimum	1.70	1.65	1.70	1.60	1.65	1.54
Maximum	2.29	1.85	2.10	2.20	2.18	1.94
Average	1.98	1.74	1.85	1.83	1.77	1.72

### **Potential Survey**

Surveys of electrical potentials in prestressed girders were conducted in Spans 1 and 4 (figure 22). A total of 16 girders were examined. Measurements were taken in a grid pattern at a spacing of 1 ft (0.3 m).

After tabulating potential readings the essential information, consisting of the minimum, maximum, average, population standard deviation, and number of observations were derived for each set of observations (table 5).

Table 5. Half-potential readings in Span 4 girders.

Statistics	Girder No.							
	G#1	G#2	G#3	G#4	G#5	G#6	G#7	G#8
MIN	0.00	0.00	0.05	0.00	0.00	0.00	0.00	0.00
MAX	0.27	0.13	0.53	0.45	0.21	0.21	0.22	0.50
AVG	0.05	0.03	0.25	0.06	0.08	0.04	0.06	0.07
STD	0.03	0.02	0.10	0.07	0.05	0.04	0.04	0.07
n	92	87	156	168	155	91	154	172

Note: Results in the above table are negative values expressed in volts (V) with reference to copper/copper sulfate electrode (CSE).

Analysis of test results show the highest negative values of half-potential readings are in Girder 3, where most deterioration had occurred. The frequency distribution chart in figure 23 shows the most frequently obtained readings are in the range of -0.20 to -0.35 V CSE. The cumulative frequency distribution chart in figure 24 indicates about 33 percent of total readings are less negative than -0.20, about 53 percent are in the range of -0.20 to -0.35, and about 14 percent are more negative than -0.35 V CSE. In other words, the corrosion activity in this girder varies from none or negligible (33%), to uncertain (53%), and to very probable (14%).

The amount of readings more negative than -0.35 V in Girder 4 is very low, only about 3 percent. The presence of these readings in Girder 4 is not unusual, since it is also adjacent to the leaking longitudinal joint. Therefore, there may be a 90 percent probability that corrosion activity had occurred in this Girder, but on a very limited scale. The approximate location of corrosion activity is on the north side of the girder (adjacent to the leaking joint) at about 27 to 29 ft (8.2 to 8.8 m) from the east end of the girder, where some delamination of concrete cover due to corrosion of stirrups was reported.

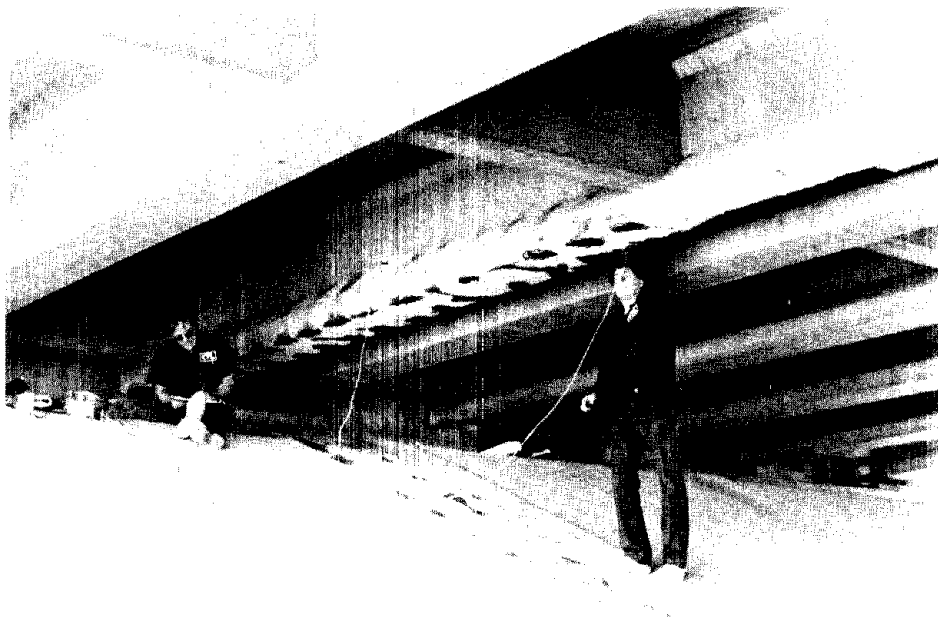


Figure 22. Potential survey of  
Girder 3 in Span 4.

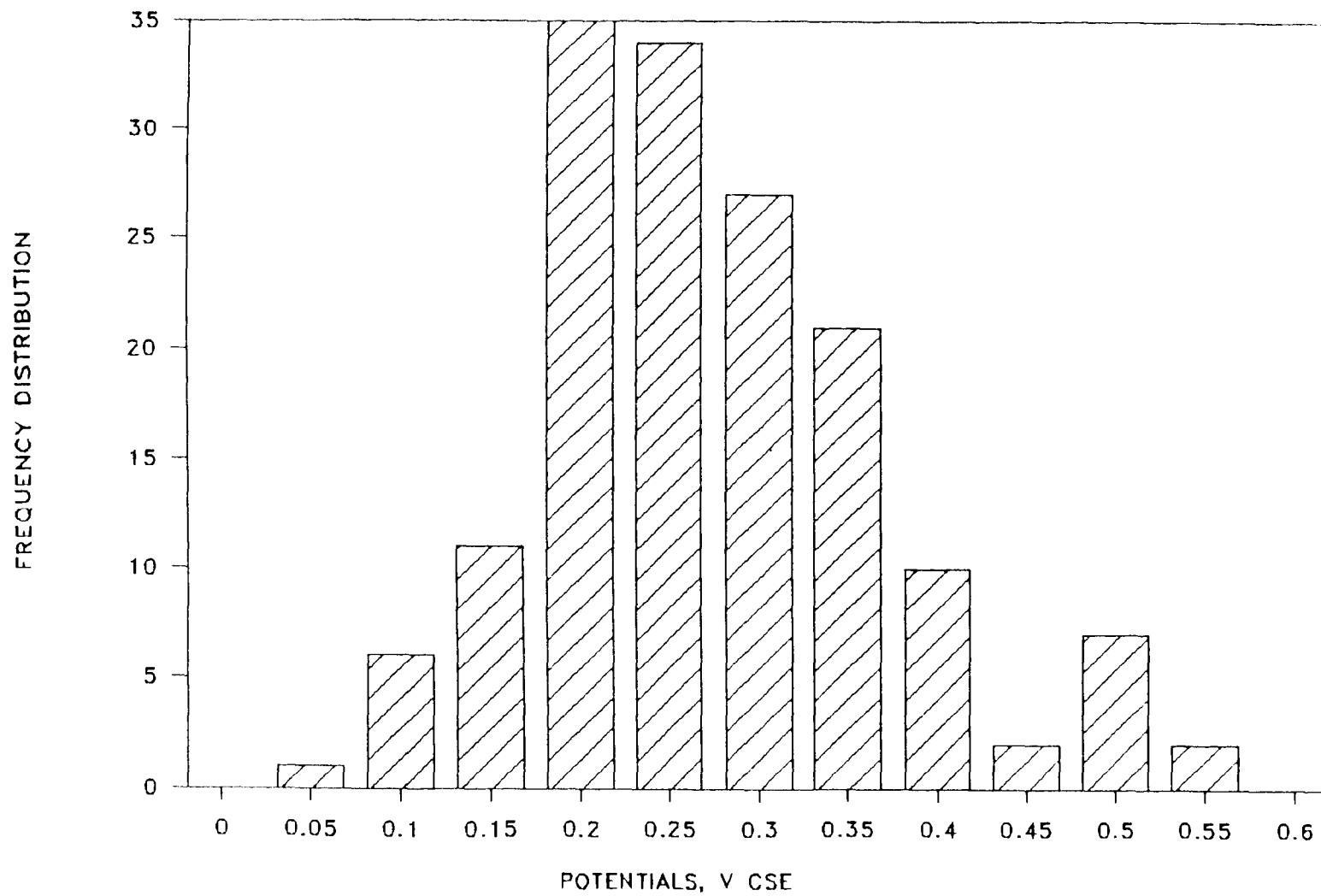


Figure 23. Frequency distribution of potential readings in Girder 3, Span 4.



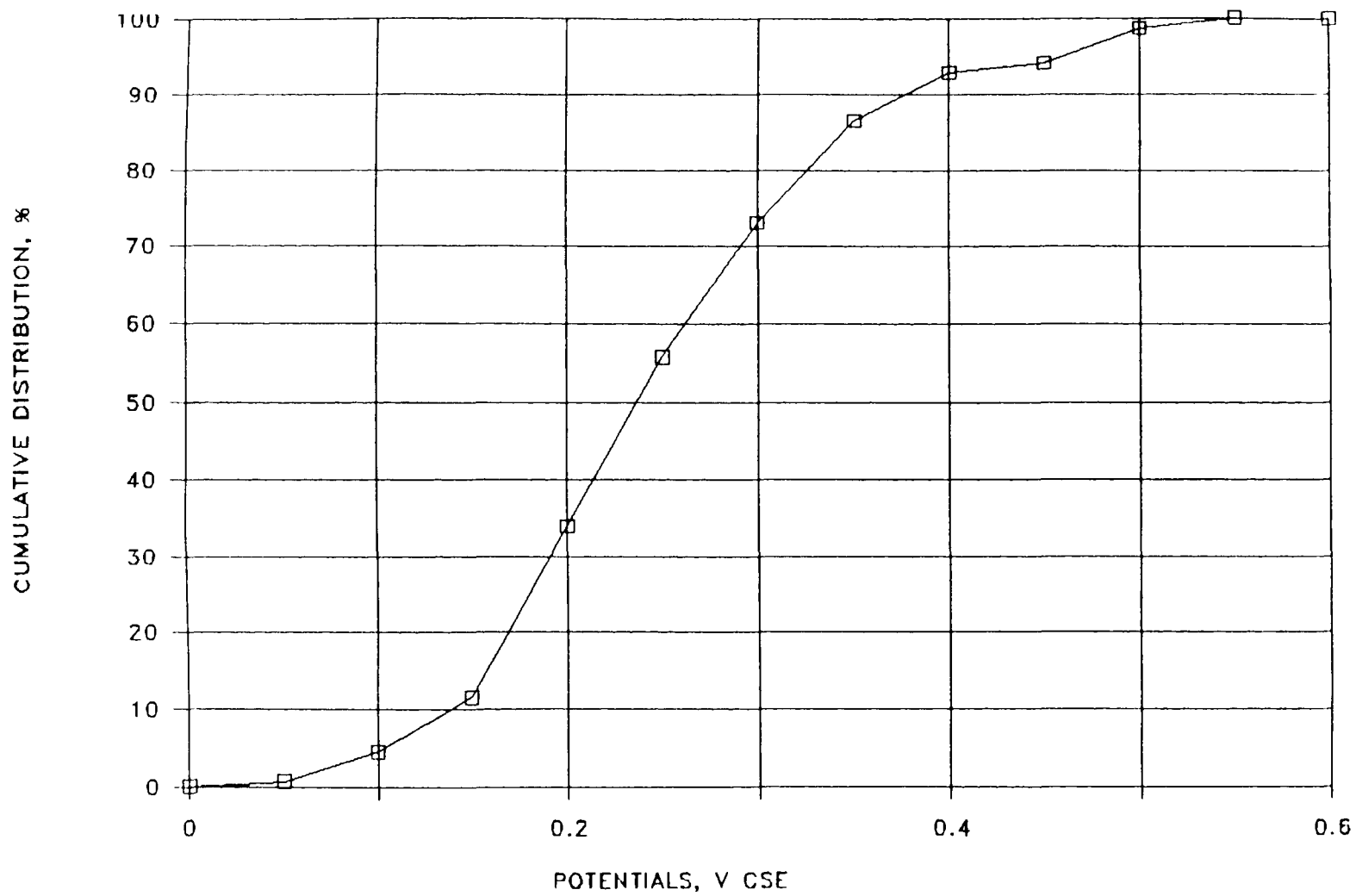


Figure 24. Cumulative frequency distribution of potential readings in Girder 3, Span 4.

There is no reason to believe corrosion activity has taken place in Girder 8.

There is greater than 90 percent probability that no steel corrosion had occurred in Girder 2, where the maximum potential measurement was less negative than -0.20 V CSE.

The percent of potential readings in Girders 1, 5, 6, and 7 in the range of -0.20 to -0.35 is extremely low, varying from approximately 1 percent in Girders 5, 6, and 7 to 3 percent in Girder 1. Therefore, corrosion activity in these girders can be rated as uncertain to unlikely.

Evaluating results of the half-cell potential survey and chloride analyses with those of the visual examination and other tests it is concluded the corrosion activity in prestressing strands is limited mainly to the of Girder 3 in Span 4. This girder exhibited the highest levels of chloride at the deepest interval, 1.5-in (38 mm), sampled.

### **Metallurgical Analyses**

The sample for metallurgical examination was obtained from Girder 3, Span 4 at 19 ft from the east end of the bridge. The sample consisted of a single wire and exhibited considerable corrosion and deterioration. The purpose of metallurgical examination was to characterize the failure mode and to identify the type of corrosion present.

**Visual and Macroscopic Examination.** The sample of wire was first subjected to visual and macroscopic examinations performed with the aid of a stereoscopic microscope capable of magnifications up to 40X. The wire displayed corrosion or rusting throughout its entire length. Diameter measurements revealed dimensions from 0.120 in to 0.030 in (3 to 0.76 mm). The corrosion product along the outside surfaces of the wire were generally red-brown in color, typical of rust. No evidence of inherent metallurgical defects were observed on the surface of the wire such as cracks, laminations, or laps. The fractured surface displayed the same rust or corrosion products observed on the remainder of the wire. The fracture was neither shiny nor crystalline in appearance.

**Scanning Electron Microscope.** The fractured end of the wire was placed within the vacuum chamber of an SR-50 scanning electron microscope. Examinations were performed in both the as-received condition and after cleaning in a solution of inhibited

hydrochloric acid. The inhibited acid solution permitted removal of some of the corrosion products from the fractured surfaces. A 15 kV electron beam was used to examine the wire at magnifications up to 20,000X.

These examinations revealed the fractured surface to predominantly display a dimpled appearance. These dimples are formed during microvoid coalescence and are indicative of a ductile overload failure. No indications of other failure modes were identified such as brittle fracture, stress corrosion cracking, or cleavage. A typical example of the fracture appearance is shown in figure 25.

**Metallographic Examination.** Metallographic sections were cut through the fractured tips of the submitted wire. After mounting the sections in bakelite molds, standard metallographic techniques were used to grind and polish the sections to a 0.05 micrometer finish. A metallurgical microscope was used to examine the cross sections at magnifications up to 2000X. Etching with a solution of 1 percent nitric acid in anhydrous ethanol (nital) provided clear definition of the microstructures.

These examinations revealed a microstructure typical of prestressing steel wire. The microstructure consisted of heavily cold worked and elongated grains of ferrite and pearlite. Near the fractured ends of the wires, similar microstructures were observed. It could be seen that the reduction in wire diameter was primarily due to corrosion rather than necking during tensile overload failure. The corrosion may be classified as a general oxidation of the wire surface. No indication of inherent metallurgical defects were observed which would have contributed to premature failure of the wire such as excessive inclusions, laps, carburizations, or unusual surface conditions developed during forming or manufacture of the wire. Illustration of the microstructure and the mode of failure exhibited by the wire sample is presented in figure 26.

**Cause of Failure.** Based on the above examinations, it appears the wire sample failed primarily due to reduction in effective cross-section caused by corrosion. Measurements on the wire indicated reductions of up to 1/4 of the original diameter. It should be noted that this will reduce the effective cross-sectional area to 1/8 of its original value. The corrosion of the wire was classified as a general oxidation. The reduction in area culminated in the failure of the wire by a ductile overload. Scanning electron micro-

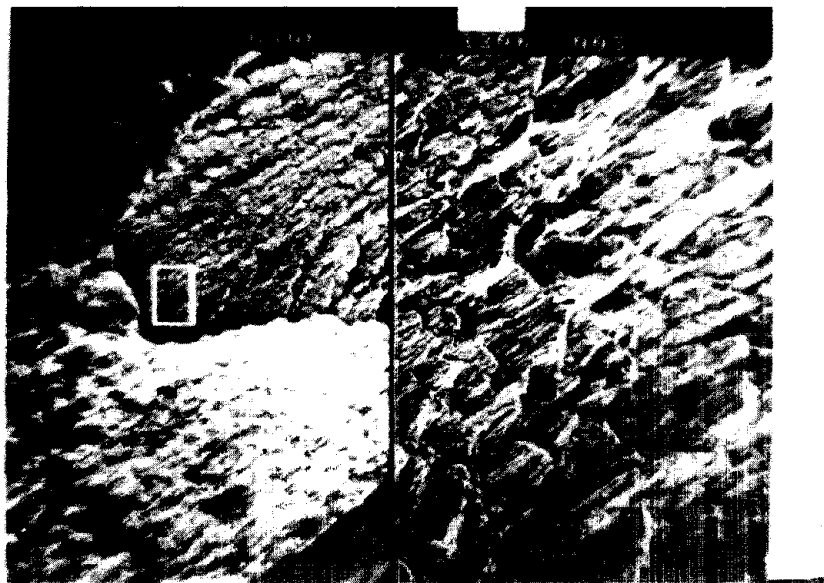


Figure 25. Fractured area of a wire at a magnification of 50X (left) and 500X (right).

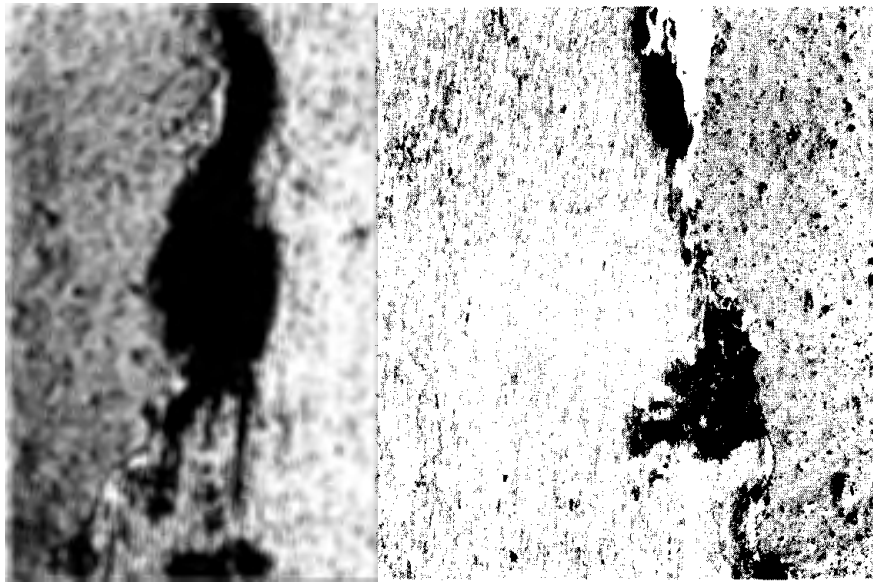


Figure 26. The significant reduction in diameter from the bottom to top.  
(Magnification: 50X. Etchant: 1% Nital.)

scope examination failed to identify any other fracture modes. No indications of defects or unusual microstructures were observed in the wire. This testing revealed the wire sample to have corroded until the remaining material was incapable of maintaining the applied load.

### **Summary**

- Distress of reinforced concrete occurred mainly in girders adjacent to the longitudinal expansion joint and at the ends of almost all girders in areas of transverse expansion and fixed joints over bridge piers and abutments.
- Deterioration of the shotcrete repair was caused by corrosion of prestressing strands due to chloride laden water penetrating through the loose patch bond as well as through the shotcrete, which apparently was not dense enough to provide sufficient protection to prestressing strands against intrusion of chlorides.
- Almost all transverse expansion joints as well as the longitudinal joint were badly deteriorated allowing chloride ions in the surface water to intrude through concrete cover and initiate corrosion of prestressing strands.
- No delaminations were noticed over prestressing strands. The only delaminations observed were over stirrups on internal vertical surfaces of girders adjacent to the longitudinal expansion joint in Spans 1 and 4.
- Concrete in prestressed girders of the bridge is of good quality and generally low permeability, without any major signs of distress.
- The highest concentration of chlorides was found in girders where the most corrosion-related deteriorations took place. Because the bridge is sloped toward its north side, the concentration of chlorides in girders on the south side of the longitudinal joint is as low as in any girder remote from this joint.

- Test results showed concrete in the prestressed girders presently has a low permeability to chloride ions.
- The average thickness of concrete cover around prestressing strands, especially on the bottom side of girders is slightly lower than the specified value.
- The noticeable corrosion activity in prestressing strands is limited mainly to the bottom side of Girder 3 in Span 4.
- It appears that prestressing strands failed by a ductile overload, primarily due to reduction in the effective cross section caused by corrosion initiated by chloride ions.
- As a result of the study, two major factors were outlined as being responsible for corrosion of the reinforcement and subsequent deterioration of concrete, they are, leaking expansion/contraction joints and inadequate concrete cover.

## **THE ROUTE SEVEN VIADUCT**

### **Viaduct Description**

The Route Seven Viaduct is located on Route 7 in Chicago Ridge (figure 27). The viaduct was built in 1959. The total length of the viaduct is 1,268 ft (386 m), the width is 50 ft (15.24 m). The viaduct consists of 23 precast prestressed box girder spans, each 50 ft (15.24 m) long, and 2 steel beam spans, 55 and 63.8 ft (16.76 and 19.45 m) long. The elevation of the viaduct and a cross section through a typical concrete span are shown in figure 28. A typical span consists of 17 precast, pretensioned box beams each 3 ft (0.91 m) wide and 2.25 ft (0.69 m) high. The beams are tied together in three locations by means of 1-in (25.4 mm) diameter transverse tie bars inserted into 2-in (50.8 mm) diameter paper tubes installed before placing concrete. Joints between box beams are dry-packed with 1:1 sand and portland cement mortar (figure 28, Detail B). Design compressive strength of concrete used for precast, prestressed beams was 5000 psi (352 kg/cm<sup>2</sup>). Specified strength at the time of prestress release was 4000 psi (281 kg/cm<sup>2</sup>).

Box beams are reinforced with a total of 28 to 34 Grade 250 high-strength, stress-relieved, seven wire strands arranged in two rows in the bottom portion of a beam, and 1 to 2 strands in each web of a beam (figure 29). The nominal diameter of a strand is 0.5 in (12.7 mm). The initial stress in each strand was 160, 000 psi (11 249 kg/cm<sup>2</sup>).

One end of each prestressed girder is fixed by means of 0.75-in (19.1 mm) diameter grouted dowels installed after beams were positioned. The other end is freely supported by graphited asbestos bearing pads. All transverse joints are filled with pre-molded joint filler.

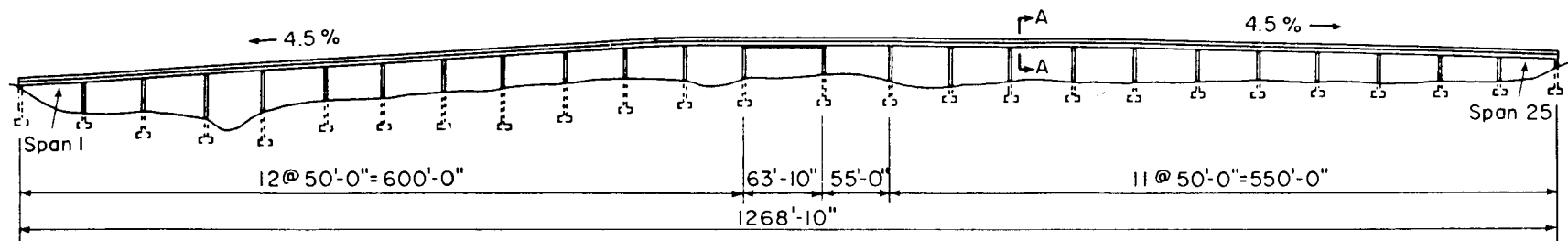
### **Visual Examination**

Typical signs of distress of reinforced concrete observed in spans of the viaduct included wet spots, deposits of deicing salt, rust stains, cracks and spalls in concrete cover, as well as corroded and failed prestressing strands. Most deterioration had

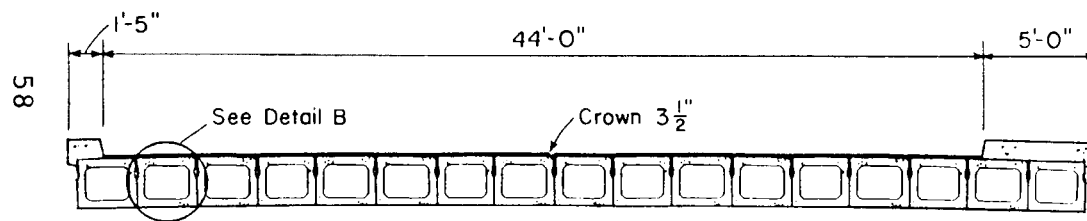




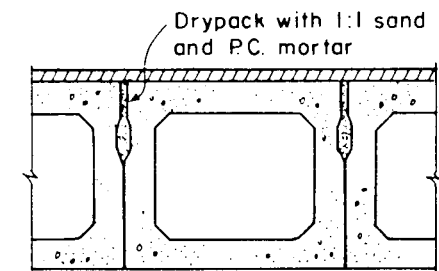
Figure 27. The Route Seven Viaduct in Chicago Ridge



ELEVATION

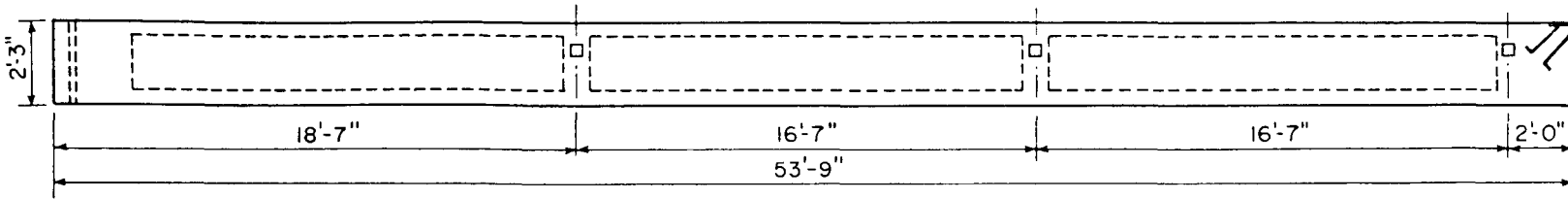


SECTION A-A

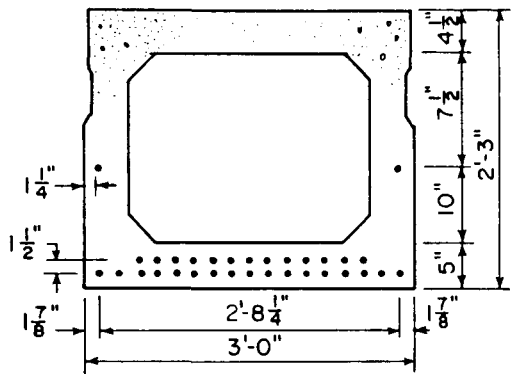


DETAIL B  
(Longitudinal joints)

Figure 28. Bridge on Route 7, Chicago Ridge.



ELEVATION



SECTION THRU BEAM NO. 7

Notes: Strand used as prestressing element shall be non galvanized, high strength, stress-relieved 7 wire strand. The nominal diameter shall not exceed 3/8" and the nominal cross-sectional area shall be 0.0799 in.

DESIGN STRESSES  
 $f_c = 5000$  psi  
 $f_{c1} = 4000$  psi  
 $f_s = 250,000$  psi  
 $f_{s1} = 160,000$  psi

Notes: 13 Strands in Top Row  
 17 Strands in Bottom Row  
 1 Strand in Each Web

Figure 29. Precast prestressed concrete beam.

occurred in the bottom surfaces of box girders, in areas adjacent to leaking longitudinal joints.

It was noticed during the visual examination that almost all joints between box girders were leaking to some extent. The rate of leakage varied from hardly noticeable, detectable only by discolorations due to evaporated water, to quite extensive accompanied by rather heavy deposits of deicing salts (figure 30). Most of the leakage had occurred in areas of Joints 2, 7, 8, 11, and 12, counting from the south side of the viaduct. Close examination of the deck concrete overlay revealed the presence of numerous cracks ranging from hardly visible random hairlines to well defined medium size cracks. It appeared the leakage of chloride-laden water started through these cracks (figure 31) and then progressed through joints between girders.

Cracks over prestressing strands varied in length from 0.5 to 7.5 ft (0.15 to 2.29 m), and in width from about 0.06 to 0.16 in (1.52 to 4.06 mm). A typical crack caused by corrosion of a strand is shown in figure 32.

The extent of spalling of concrete cover varied from moderate to very severe (figures 33, 34). Spalling of concrete cover next to transverse joints over piers was not common and was observed only in one beam, Beam 15, Span 23 (figure 35). The area of this spall was about 6 ft<sup>2</sup> (0.54 m<sup>2</sup>). Unlike spalls adjacent to leaking joints, the spalls shown in figures 36 and 37 were attributed to corrosion of external strands due to water running either along the side of a box girder or around a malfunctioning drain.

Almost all strands exposed to direct action of the atmosphere and chloride-laden water were found to be severely deteriorated. The extent of corrosion was more severe on the top surface of wires, less between wires, and less on the bottom surfaces adjacent to the steel/concrete interface. Surface corrosion appeared to be the only type of corrosion on the surface of wires composing a strand. Cases of failure of six wires surrounding the central wire or even all wires including the central wire were not uncommon (figures 38 and 39). On some occasions, no steel could be found in areas of spalled concrete cover, except for a layer of rust and imprints of corroded wires on the bond surface (figure 40).

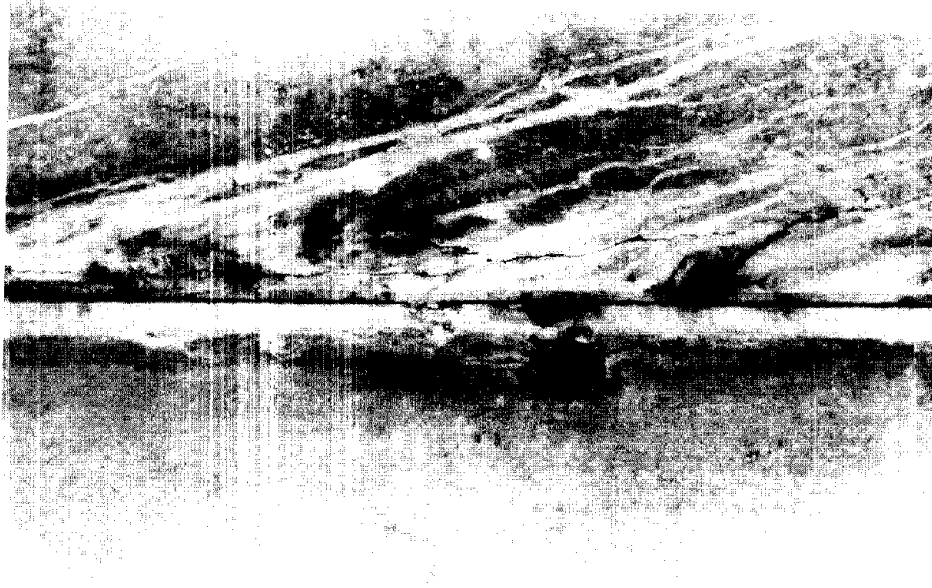


Figure 30. Signs of severe leakage of water through a joint between box girders.

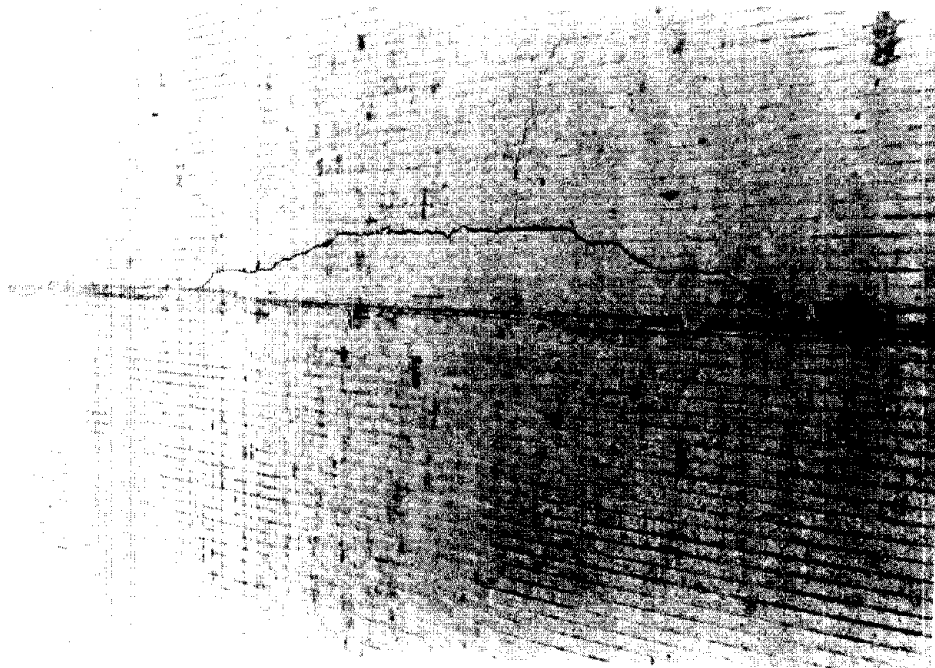


Figure 31. Cracking of concrete overlay in areas adjacent to expansion/contraction joints.

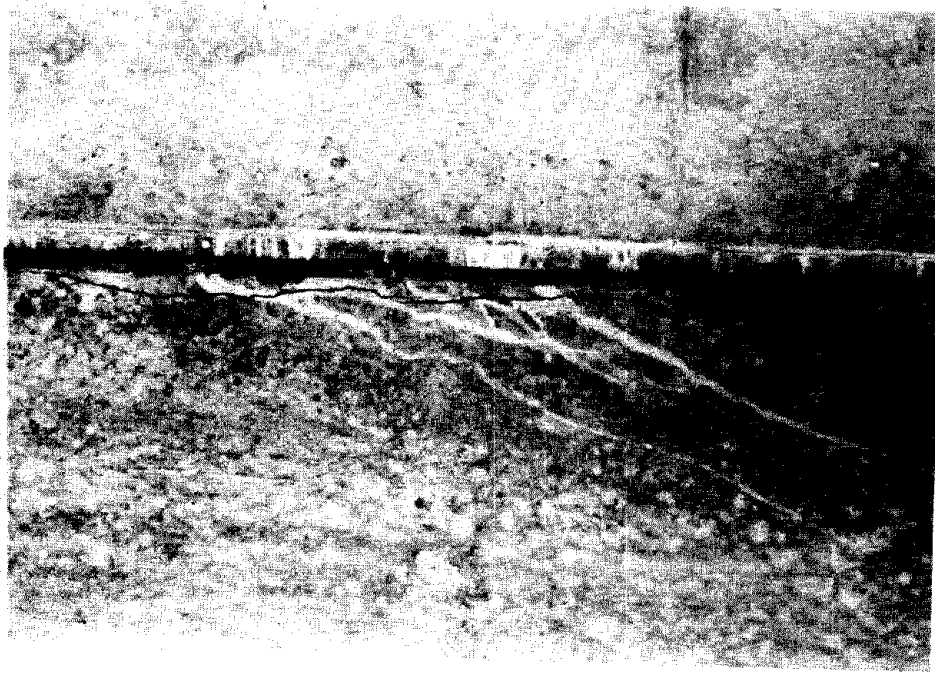


Figure 32. Typical crack caused by corrosion of a prestressing strand.

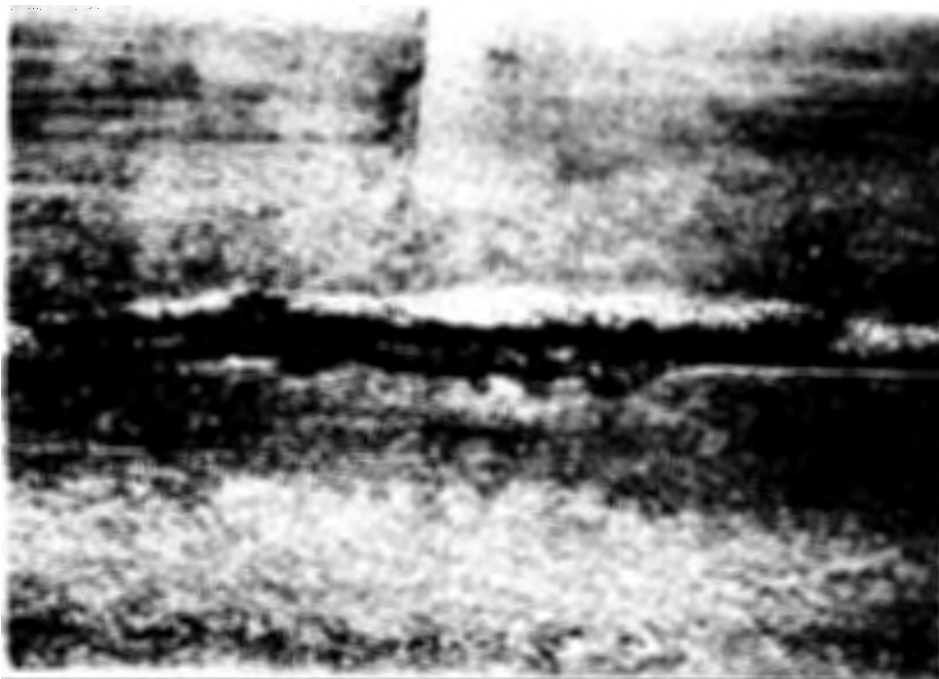


Figure 33. Moderate spalling of concrete cover over a strand.

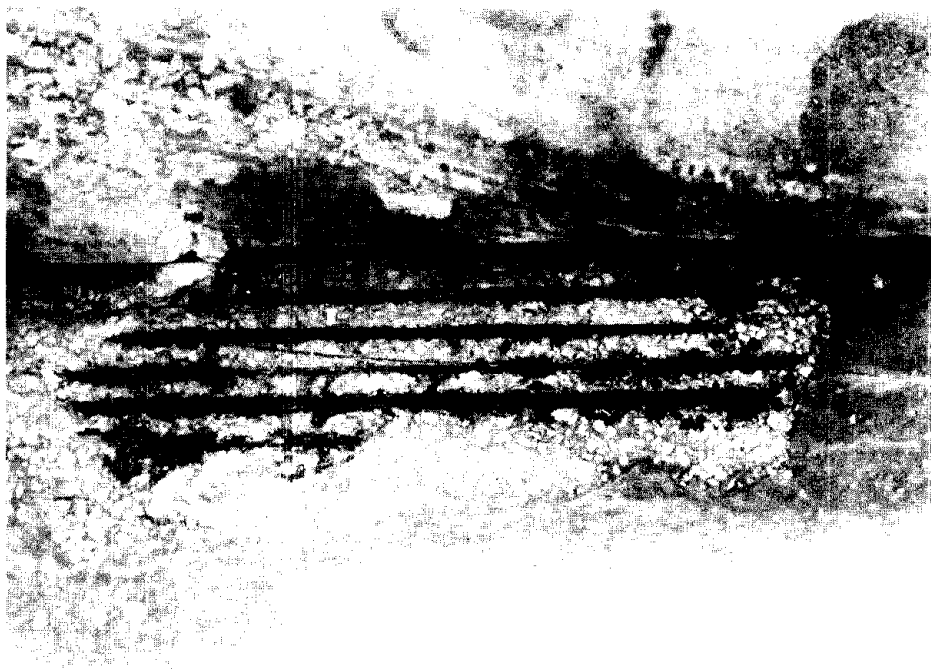


Figure 34. Very severe spalling of concrete cover over several prestressing strands.



Figure 35. Concrete spall adjacent to a leaking transverse joint.

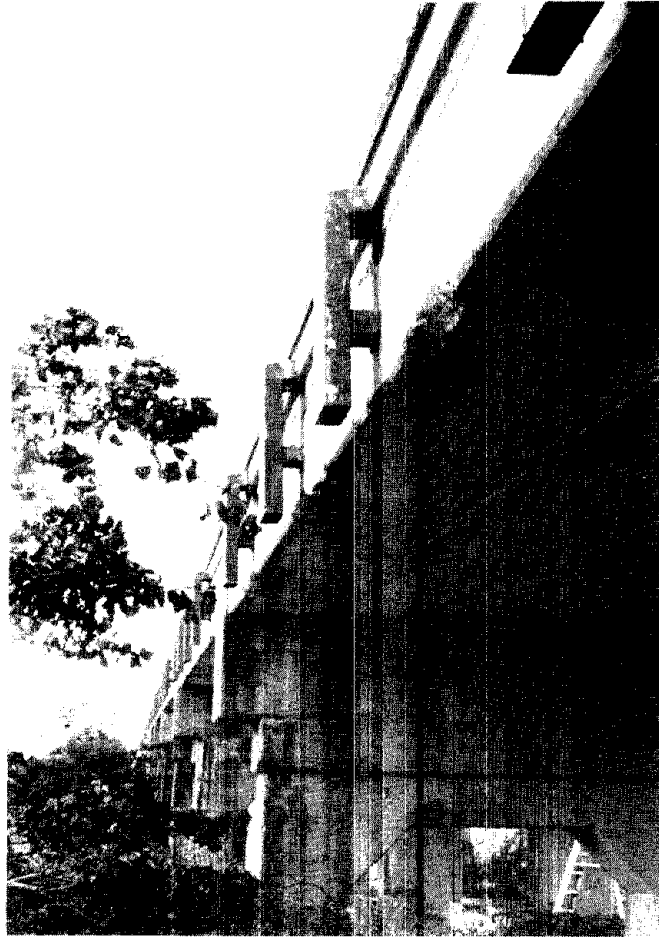


Figure 36. Corrosion related spalling of concrete cover due to water running along the side of a girder.



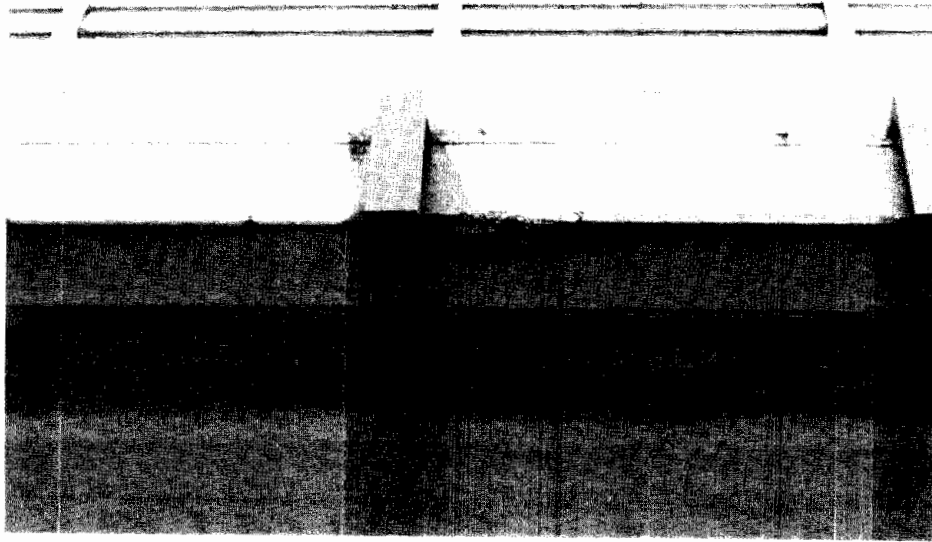


Figure 37. Corrosion related spalling of concrete cover due to water running around the malfunctioning drain.

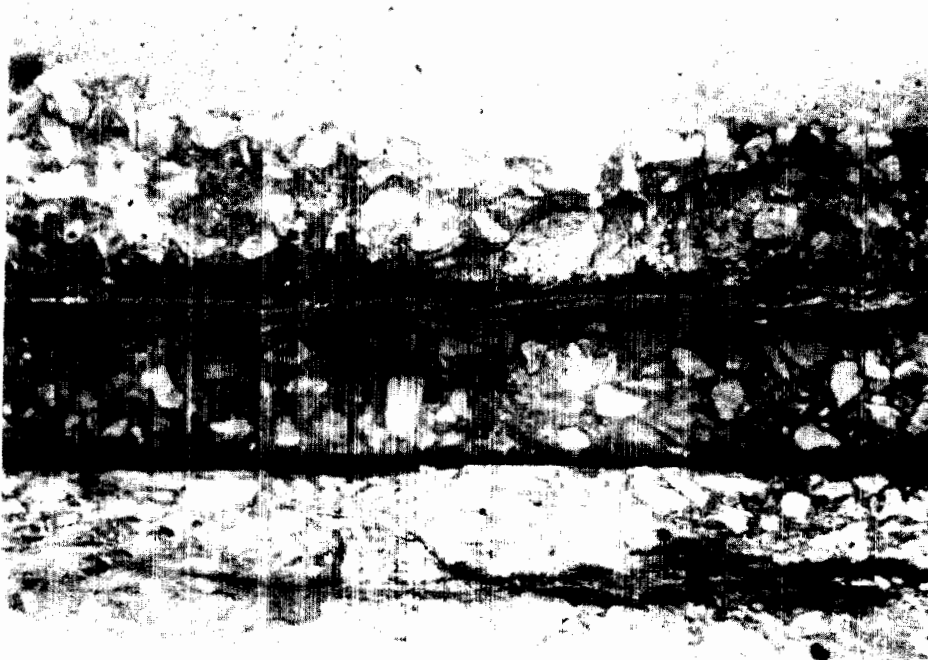


Figure 38. Failure in all six wires surrounding a central wire.

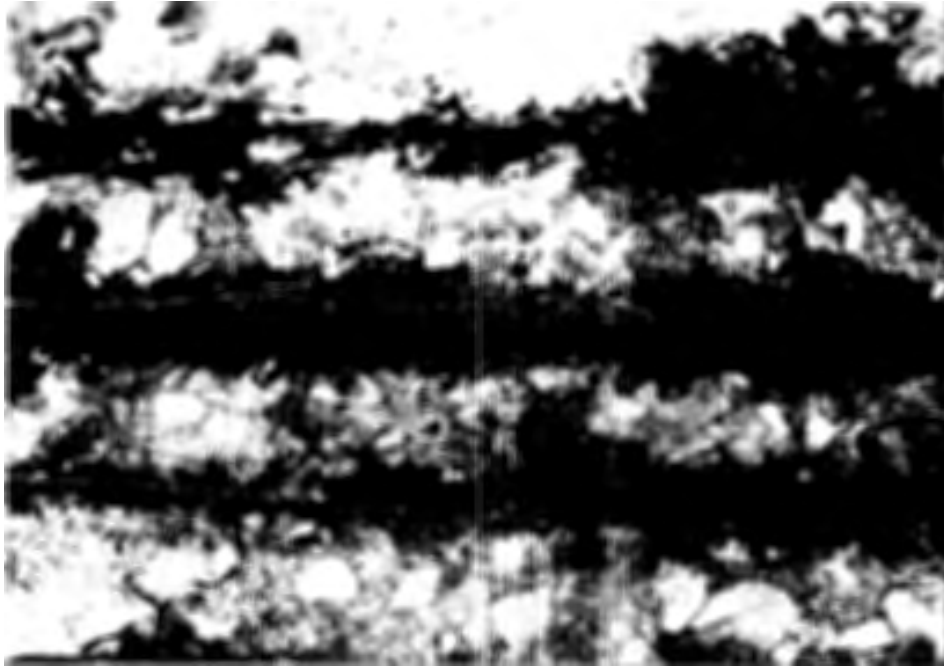


Figure 39. Complete failure of a prestressing strand.

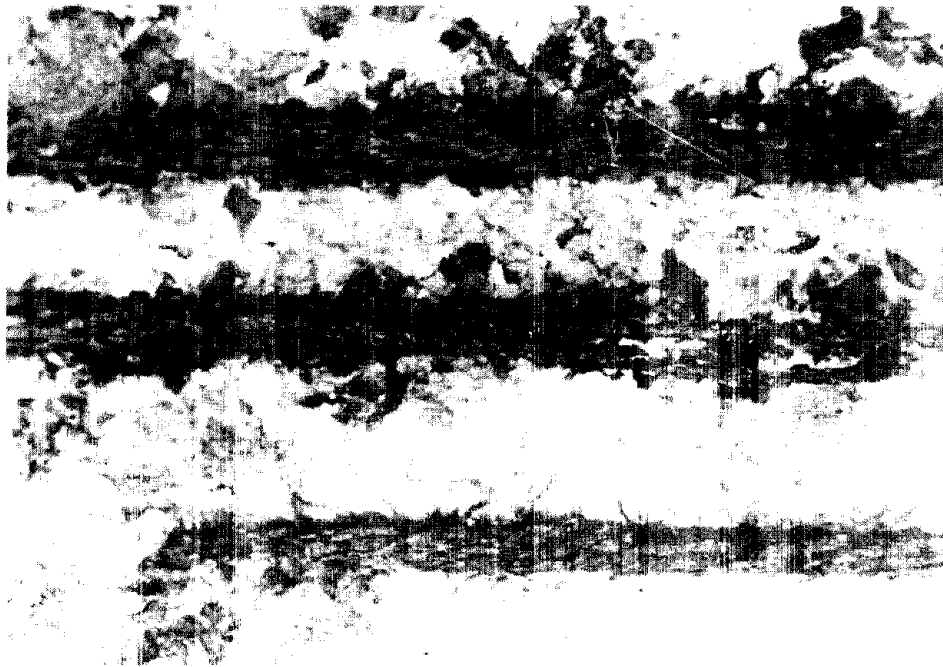


Figure 40. Imprints of corroded wires on the surface of the steel-concrete interface.

Concrete spalls in some areas were repaired with what appeared to be an epoxy based mortar. The overall condition of repairs was good, except for negligible stains of rust in some patches. There was no evidence of debonding of the mortar in examined patches. In general, this repair method seems to be quite effective and can be considered for further evaluation in the laboratory and under field conditions.

It was noted during the visual examination that some exposed prestressing strands were coated with an epoxy compound, apparently in an attempt to protect them from further corrosion. In most cases, corrosion could be seen through the epoxy coat. Since the bond between the coating and the strands was rather loose, it was difficult to say if this corrosion occurred after the strands were coated or it was not removed prior to application of the protective coat.

### **Description of Study Areas**

After the visual examination a total of 4 areas representing different extents of distress of prestressed concrete in the viaduct were selected for more detailed study.

**Study Area #1.** This area is located in Span 3 and consists of Beams 2, 3, and 4, counting from the south side of the viaduct (figure 41). The area represents a severe to very severe extent of deterioration of concrete and corrosion of the reinforcement.

The dampness in the bottom surfaces of beams in Area 1 was rated as negligible in Beam 4 and quite persistent in Beams 2 and 3. Out of 11 cracks noted in Beams 3 and 4, 10 were located along longitudinal joints 2 and 3, and only 1 crack was located in the middle of the bottom surface of Beam 3. The total length of cracks in Study Area 1 was 21 ft (6.4 m). No cracks were observed in Beam 2. The extent of spalling of concrete cover in Study Area 1 varied from none in Beam 2, moderate in Beam 4, and severe in Beam 3. The total areas of spalled concrete in Beams 3 and 4 were 2.1 and 4.7 ft<sup>2</sup>, (0.20 and 0.44 m<sup>2</sup>), respectively. The total length of exposed prestressing strands in this study area was 27.83 ft (8.48 m). At least 1 failure was recorded in 7 out of 11 exposed strands.

**Study Area #2.** This area is located in Span 22 and consists of Beams 2 and 3 (figure 42). The area represents moderate to severe deterioration. Most deteriorations in this area had occurred in Beam 2.

The dampness of concrete cover was rated as moderate to very persistent in Beams 3 and 2, respectively. There were 5 cracks in Beam 2, and 2 in Beam 3. All cracks were located along Joint 2. The total length of cracks in both Beams was about 19 ft (5.79 m). The total areas of concrete spalling in Beams 2 and 3 were 1.1 and 13.2 ft<sup>2</sup> (0.10 and 1.23 m<sup>2</sup>), respectively.

**Study Area #3.** This area is located in Span 3 and consists of Beams 10, 11, and 12 (figure 43). The area represents spans with extensive leakage, but without visible corrosion related deterioration of concrete cover. Wet spots and deposits of deicing salts were well visible along Joints 10 and 11, and partially along Joint 12. The total length of 5 cracks, all located in Girder 11 was 11.5 ft (3.5 m). Neither concrete spalls nor exposed strands were present in this study area.

**Study Area #4.** This area is located in Span 22 and consists of Girders 10 and 11 (figure 44). This area was used as a reference area since it does not have any signs of concrete deterioration or water leaking through the joints between girders.

### **Delamination of Concrete Cover**

Delamination surveys were performed on the bottom surfaces of box girders in Study Areas 1, 2, 3, and 4. In Areas 1, 2, and 3 delaminations were noticed only in concrete adjacent to leaking joints.

The extent of delamination of concrete cover varied from moderate in Area 1, moderate to negligible in Area 2, negligible in Area 3, and none in Area 4. The total areas of delamination were about 4.6, 2.8, and 0.9 ft<sup>2</sup> (0.43, 0.26 and 0.08 m<sup>2</sup>) in Areas 1, 2 and 3, respectively. The widths of delaminations in Areas 2, and 3 were in the range of 2 to 4.5 in. (50.8 to 114.3 mm). In Area 1 the width of delamination was higher reaching 11 and occasionally 15 in (381 mm). In general, delaminations in all examined girders looked more like advancing spalls.

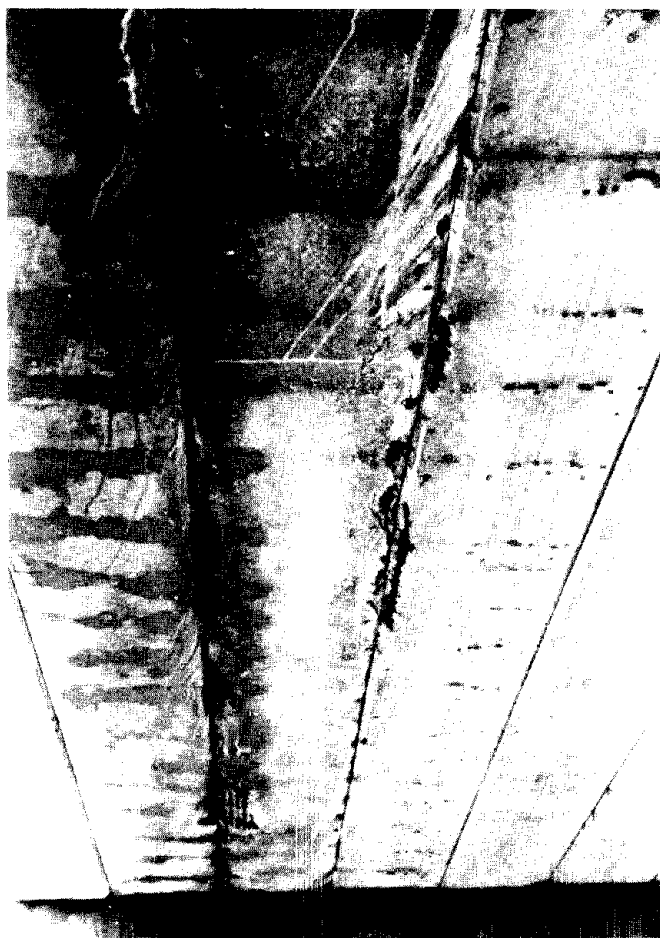


Figure 41. Study Area 1.

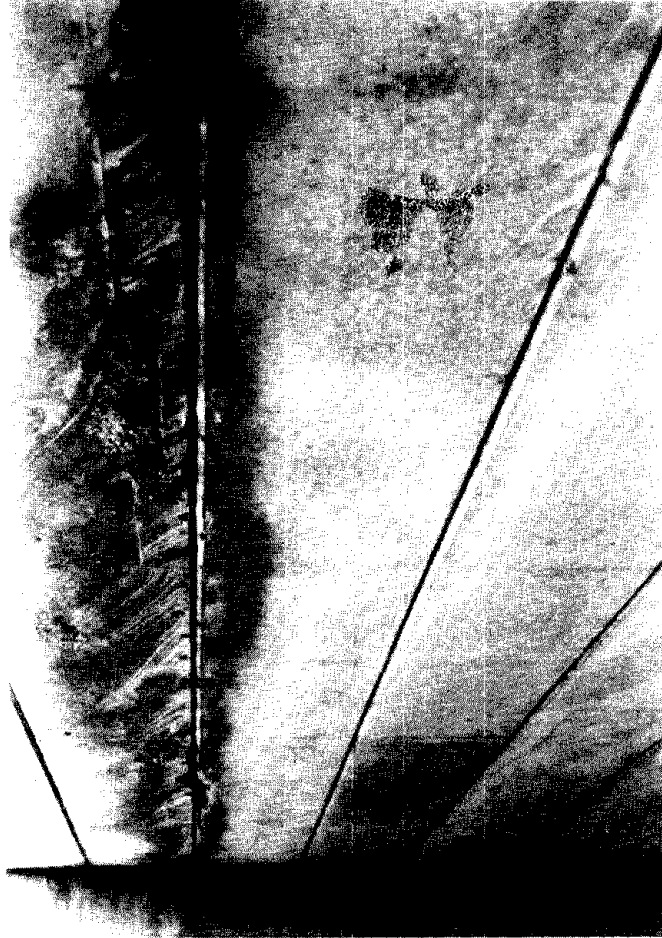


Figure 42. Study Area 2.

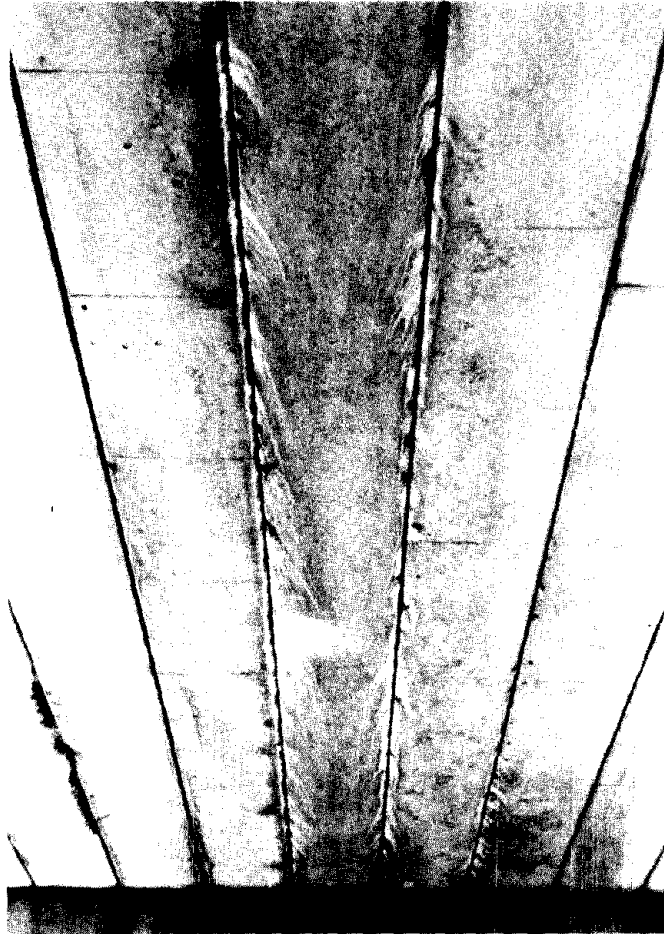


Figure 43. Study Area 3.

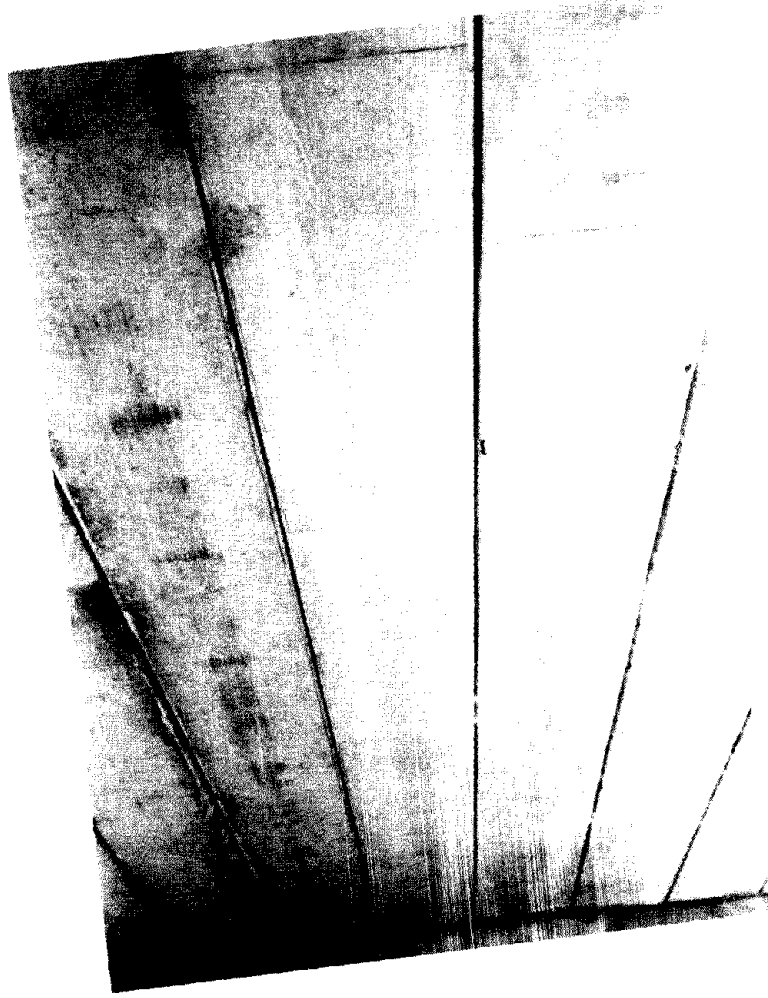


Fig. 44. Study Area 4.



## **Petrographic Examination**

**Core SP#2, BB#1.** This core was obtained from Span 2, Box Beam 1, counting from the south side of the viaduct. One core end has a weathered surface, thereby exposing fine aggregate particles. A 0.38-in (9.7 mm) diameter popout is present on the exposed weathered surface. The popout extends 0.38 in (9.7 mm) deep and occurs within a chert coarse aggregate particle located just below the exposed surface. The other core end is the imprint of a smooth surface. The smooth surface is slightly sticky and in one area paper or cardboard-like material adheres to the smooth surface.

Coarse aggregate is a crushed dolomite with occasional chert particles. Measured maximum aggregate size is 0.75 in (19.1 mm). Coarse aggregate particles are light gray, moderately hard, porous to dense, angular, spherical to prismoidal. Fine aggregate is a natural calcareous-siliceous sand containing quartz, limestone, dolomite, chert, sandstone, siltstone, granite, feldspar, ironstone, ferromagnesian minerals, and other rock/mineral types. Fine aggregate particles are variously colored, moderately hard to hard, dense, subrounded to well-rounded, and spherical to subspherical. Calcareous fines are moderately abundant. The aggregate appears slightly deficient in intermediate sizes. The aggregate is fairly well dispersed. There are no indications the aggregate particles have performed poorly in service.

Cement paste is medium brownish gray, very hard, dense, and well-bonded to aggregate particles. Paste along freshly broken surfaces exhibits a vitreous luster, microgranular texture, and irregular fracture. Paste carbonation extends 0.06 in (1.52mm) from the weathered surface. Residual cement particles and calcium hydroxide are moderately abundant. Based on interpretation of previously described paste properties, water/cement ratio is estimated to be 0.37 to 0.42. Typical microstructure of the concrete is shown in figures 45 and 46.

The concrete is air-entrained. Air content is visually estimated to be 3 to 4 percent. Most of the voids are extremely fine and spherical. The concrete appears well-consolidated. Void distribution is somewhat nonuniform with some areas containing fewer voids than other areas.

Secondary deposits are not detected in voids or aggregate sockets. Minor crazing microcracks attributed to slight shrinkage are present in the 1 mm of concrete closest to the weathered surface. There is no evidence of deterioration in concrete represented by this core.

**Core SP#23, BB#1.** This core was obtained from Span 23, Box Beam 1. One core end shows a weathered imprint of a formed surface. The opposite core end is an irregular broken surface passing primarily through aggregate particles. Steel reinforcement is not present in the core. There is no evidence of bleed channels or gaps.

Aggregate types and properties are similar to those of the previously described core. There are no indications the aggregates have performed poorly in service. Cement paste is medium brownish gray, hard, dense, and well-bonded to aggregate particles. Paste along freshly broken surfaces exhibits a vitreous luster, microgranular texture, and irregular fracture. Paste carbonation extends 0.06 to 0.09 in (1.5 to 2.3 mm) from the weathered surface. Residual cement particles are abundant. Calcium hydroxide is moderately abundant. Based on interpretation of previously described paste properties, water-cement ratio is estimated to be 0.35 to 0.40. Typical microstructure of the concrete is shown in figures 47, and 48.

The concrete is air-entrained. Air content is visually estimated to be 3.5 to 5.0 percent. Most of the voids are extremely fine and spherical. The concrete appears well-consolidated. Void distribution is somewhat nonuniform with some areas containing fewer voids than other areas. Secondary deposits are not detected in voids or aggregate sockets. There is no evidence of deterioration in concrete represented by this core.

Concrete properties identified petrographically suggest that concrete represented by the two examined cores is of good quality and generally low permeability. Core SP#2, BB#1 is judged to have a lower permeability than Core SP#23, BB#1. None of the cores exhibit major signs of distress.

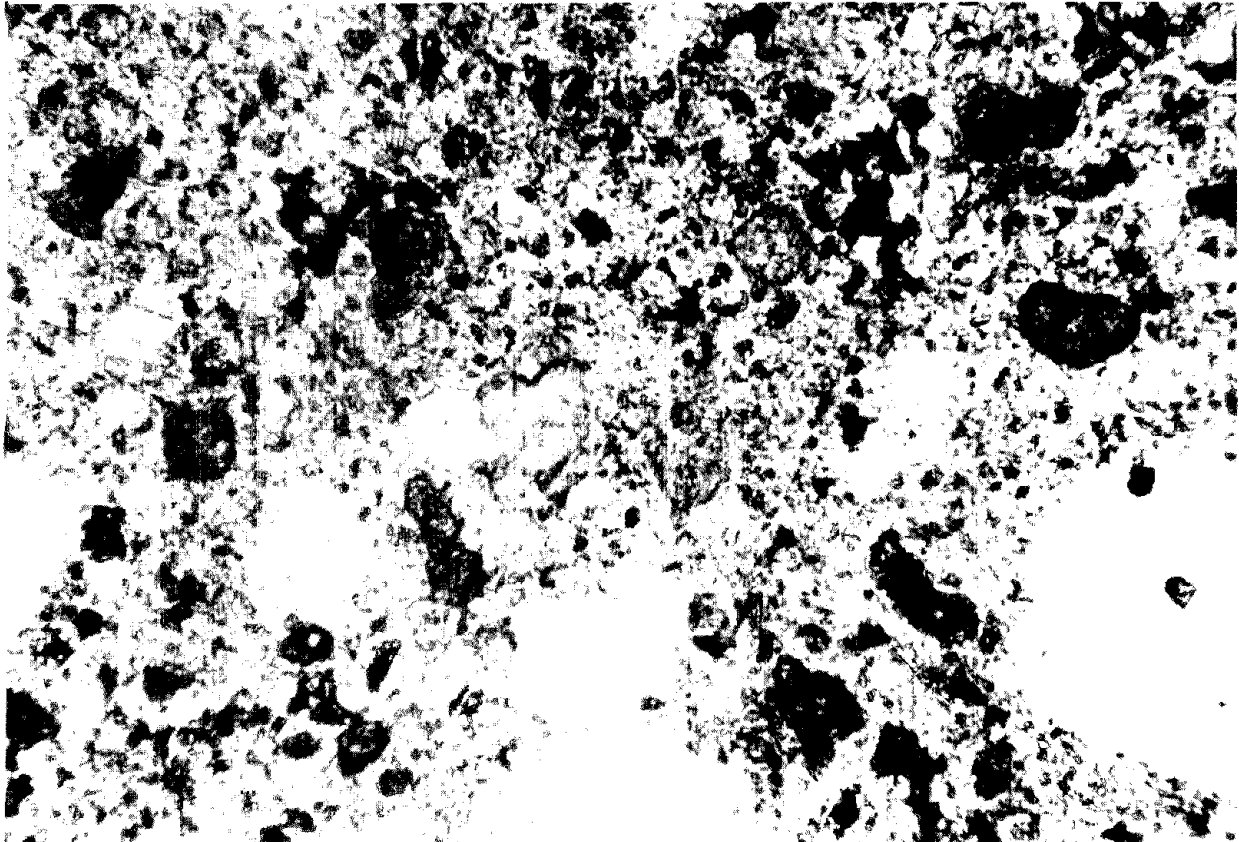


Figure 45. Microstructure of concrete in Core 2, Span 3.  
(Plane-polarized light. Magnification - 100X.  
Length of field = 1.2 mm.)

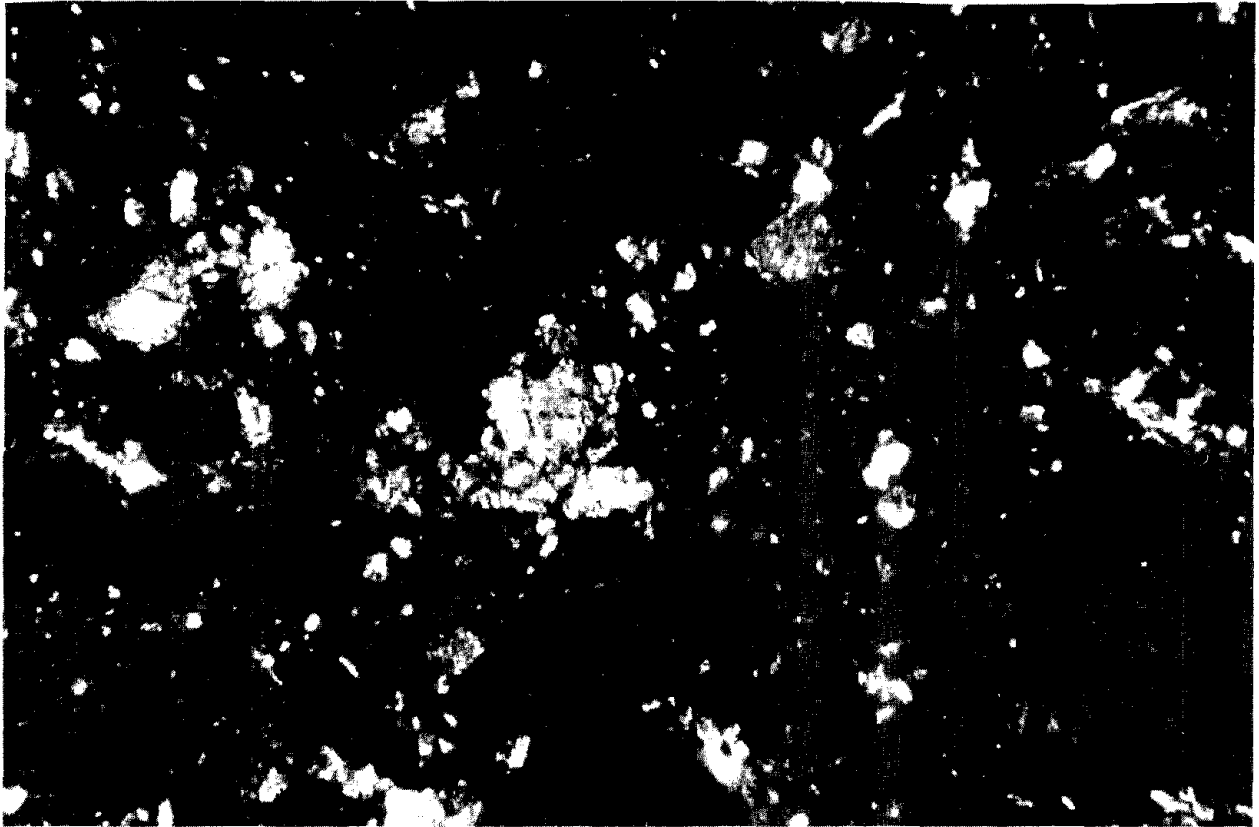


Figure 46. Microstructure of concrete in Core 2, Span 3.  
(Cross polarized light. Magnification = 100X.  
Length of field = 1.2mm.)

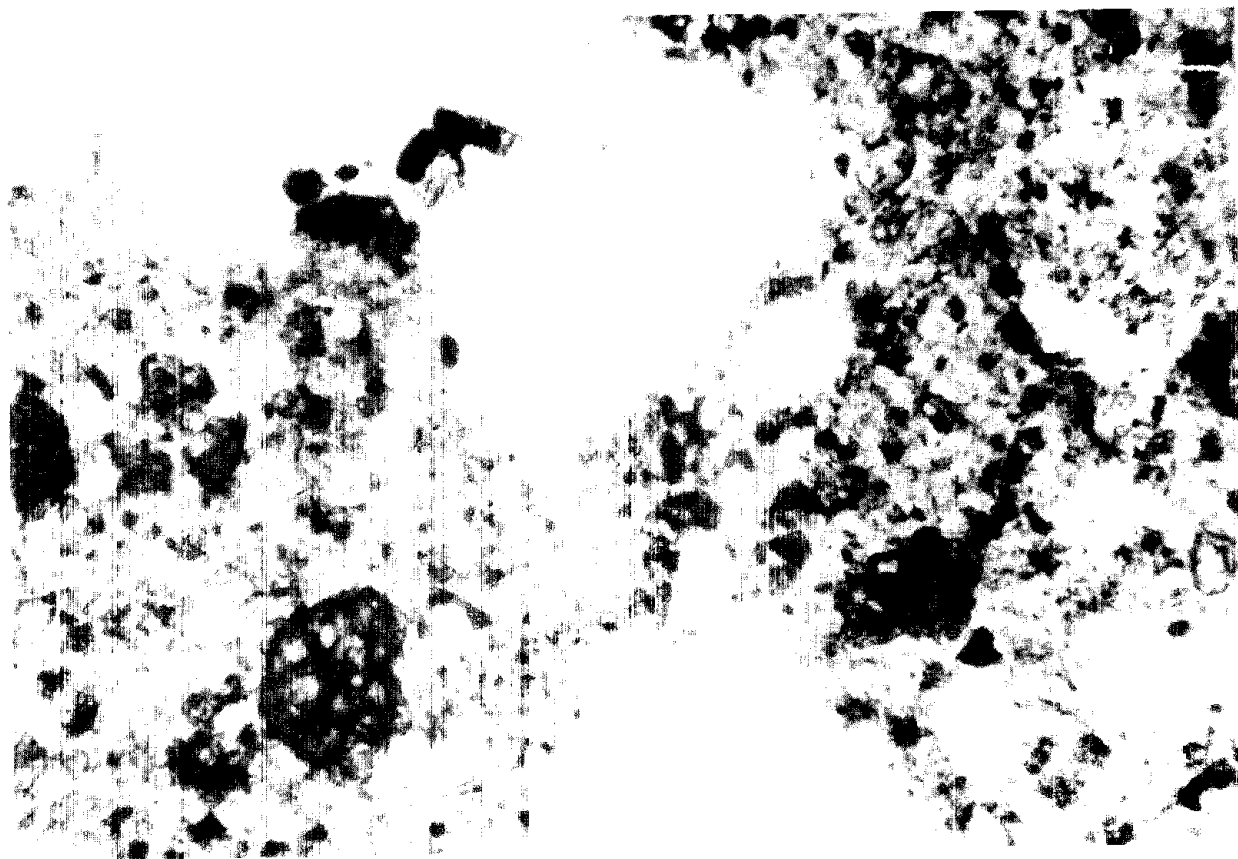


Figure 47. Microstructure of concrete in Core 2, Span 23.  
(Plane-polarized light. Magnification = 100X.  
Length of field = 1.2mm.)

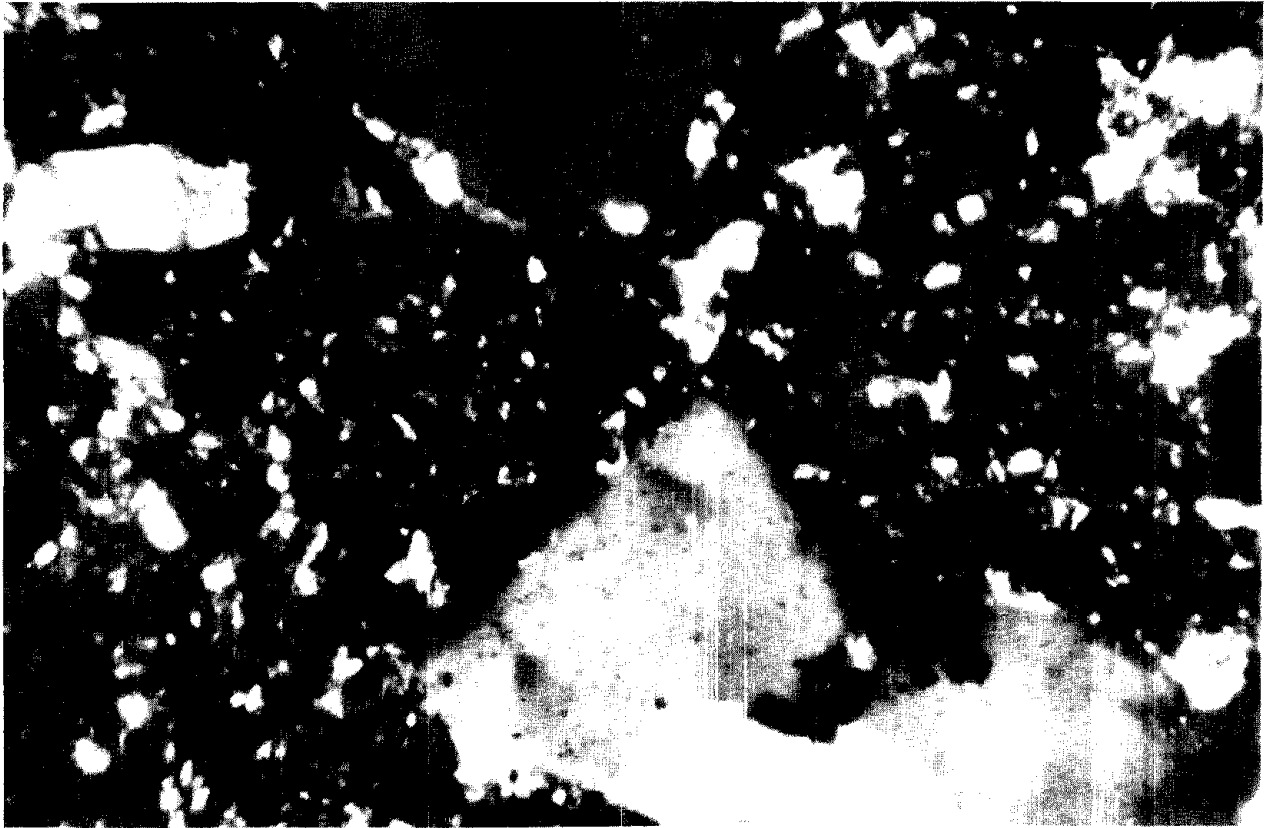


Figure 48. Microstructure of concrete in Core 2, Span 23.  
(Crossed-polarized light. Magnification = 100X.  
Length of field = 1.2mm.)

### **Concentration of Chlorides**

Concentration of chloride ions in the concrete was determined on powder samples obtained from different depths of box girders in areas adjacent to corroded and non-corroded prestressing strands. Samples in Study Area 1 were obtained at Locations 1, 2, and 3 which correspond to a distance of 0.25, 0.50 and 0.75 of the span length from the west end of the viaduct. Test results in percent by weight of concrete are given in table 6.

As expected, the concentration of chlorides was higher near the surface of a girder and lower at a depth of 1.5 in. (38.1 mm). This difference was negligible in Study Area 4, (Samples 25, 26, and 27), apparently due to higher permeability of the concrete. In Study Area 1 the concentration of chlorides at the level of the prestressing strands varied from 0.102 percent in areas of moderate deteriorations to 0.444 percent where severe deteriorations took place. In Study Area 2, values higher than 0.50 were found in Sample 24 obtained from concrete adjoining badly corroded prestressing strands.

The amount of chlorides in concrete samples taken from depths of 3.5 to 4.0 in (89 to 102 mm) was approximately the same (Samples 38, 41, and 42). These test results may reflect chlorides inherent in the aggregate, which is typical of crushed dolomite in the Chicago area.

In general, the concentration of chlorides varies greatly from point to point and thus can give rise to powerful corrosion cells, provided the moisture content of the concrete is sufficient to make it function as an electrolyte. It has been determined that corrosion related deteriorations in bridge members may occur at a resistivity of concrete of 60,000 ohm-cm and lower, which corresponds to a moisture content of approximately 3.5 percent and higher. Visual appearance indicated the moisture content in girders of the Route Seven Viaduct was fairly high.

### **Rapid Chloride Permeability**

Samples for the rapid test of chloride permeability were prepared by slicing cores obtained for petrographic analyses. Results of tests are given in table 7. The amount of current transmitted during a 6-hour test was in the range of 504 to 1661 coulombs.

Table 6. Total chloride analysis for the Route Seven Viaduct.

Sample No.	Location <sup>1</sup>	Depth, in.	Cl ions, %	Study area
34	SP3,B3,L1	1.0	0.455	1
35	SP3,B3,L1	1.5	0.444	-
39	SP3,B3,L3	0.5	0.511	1
40	SP3,B3,L3	1.5	0.102	-
19	SP22,B3,L1	0.5	0.534	2
20	SP22,B3,L1	1.0	0.480	-
21	SP22,B3,L1	1.5	0.231	-
23	SP22,B3,L3	1.0	0.610	2
24	SP22,B3,L3	1.5	0.516	-
28	SP22,B2,L2	0.5	0.493	2
30	SP22,B2,L2	1.0	0.391	-
29	SP22,B2,L2	1.5	0.145	-
31	SP3,B10,L1	0.5	0.399	3
25	SP22,B10	0.5	0.379	4
26	SP22,B10	1.0	-	-
27	SP22,B10	1.5	-	4
38	SP3,B3,L2	4.0-4.5	0.036	
41	SP3,B3,L3	3.5-4.5	0.051	
42	SP3,B3,L3	4.0-4.5	0.053	

<sup>1</sup>Note: Location designation is given as a combination of a Span, Beam, and Location number.



These tests indicate the permeability of the bridge concrete is rather low at this point in time and is not considered to be one of the major factors promoting corrosion of pre-stressing strands, although initial permeability may well have been much higher, in view of the high levels of chloride detected in the concrete.

Table 7. Rapid chloride permeability.

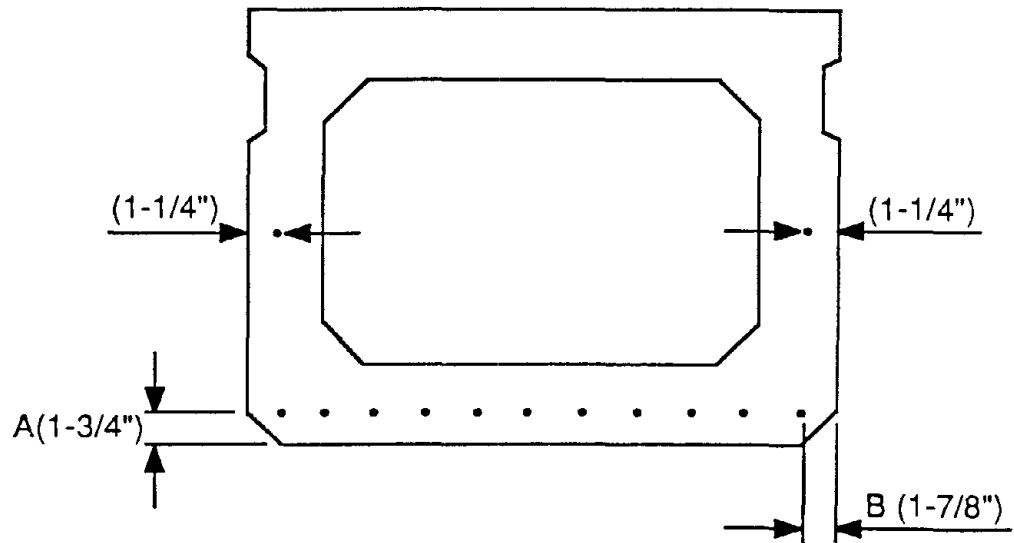
Sample No.	Location	Charge passed (coulombs)	Permeability (per AASHTO T277)
SP#2,BB#1	Span 2, Beam 1	504	Very low
SP#23,BB#1	Span 23, Beam 1	1661	Low

These results are in agreement with the findings of petrographic analysis. This indicates concrete represented by both cores is of good quality and that concrete in Core SP#2,BB#1 is less permeable than concrete in Core SP#23,BB#1.

### **Concrete Cover Survey**

Survey of concrete cover was carried out on box beams in all four study areas. Readings were taken on the bottom side (Location A, figure 49) and on both north and south sides (Location B) of each box beam. Readings on the bottom side were obtained using both the R-Meter and direct measurements. Readings on the side of a beam were obtained only by direct measurements over exposed strands.

Essential data along with a number of observations in each study area are given in figure 49. These data indicate the average thickness of concrete cover on the bottom side of beams is in the range of 1.5 to 1.62 in (38 mm to 41 mm) as compared with 2.0 to 2.63 in (51 to 67 mm) on the south and north sides of a beam over bottom prestressing strands. The average specified concrete cover on the bottom side is 1.75 in (45



#### LOCATION A

	STUDY AREA			
	1	2	3	4
n	15	18	16	17
AVG	1-3/8"	1-3/8"	1-5/8"	1-7/16"
MIN	1-1/4"	1-3/16"	1-1/2"	1-1/4"
MAX	1-7/8"	1-1/2"	1-7/8"	1-9/16"
STD	0.170"	0.106"	0.170"	0.101"

#### LOCATION B

	STUDY AREA			
	1	2	3	4
n	10	6	8	6
AVG	2-1/16"	2-5/16"	2"	2-5/8"
MIN	1-3/4"	2"	1-3/4"	2"
MAX	2-1/4"	2-3/4"	2-1/8"	3"
STD	0.165"	0.270"	0.270"	0.340"

Figure 49. Concrete cover survey.

mm), and 1.89 in (48 mm) on the north and south sides. It should be noted that the specified concrete cover over web strands is only 1.25 in (32 mm). Taking into consideration that joints between box girders are the major route for chloride-laden water, it is possible that strands in some girders have completely deteriorated. Since these strands can not be inspected their loss and therefore the loss (at least partial) of load carrying capacity of an affected girder will remain undetected. In general, concrete cover in inspected girders is not sufficient to provide proper protection to reinforcing strands. This, and also leaking joints between girders, are probably the main reasons for the rather severe deteriorations observed in the viaduct.

### **Potential Survey**

Potential surveys were conducted on 17 box beams in Spans 3 and 22. The essential information for each beam and for each study area, consisting of the minimum, maximum, average, number of observations, and population standard deviation is shown in tables 8 and 9. The summary of distribution of potential readings are given in table 9.

Analyzing test results given in tables 8, 9, and 10 it can be seen the highest average value of potential readings were found in Study Area 2. The percent of potential readings in the range of -0.20 to -0.35 V CSE was lower, but the percent of potential readings more negative than -0.35 was higher than in other study areas. These results indicate the highest extent of corrosion activity in the prestressing steel was in Study Area 2, on both sides of the leaking joint between box girders 2 and 3. This conclusion does not agree with results of the visual examination of the viaduct spans which showed the highest extent of distress was in Study Area 1. It should be noted that this is true only for Study Area 2, the other study areas showed a good correlation between results of the visual examination and the potential survey.

### **Metallurgical Analyses**

The sample for metallurgical analyses was obtained from Box Beam 2, Span 22. Prior to obtaining the sample, concrete cover over nonexposed portion of the strand was removed and the whole strand was examined visually.

Table 8. Potential readings in box beams of Span 3 and 22.

Girder No.	n		MIN		MAX		AVG		STD	
	SP3	SP22	SP3	SP22	SP3	SP22	SP3	SP22	SP3	SP22
1	72	72	0.01	0.13	0.34	0.39	0.13	0.28	0.08	0.06
2	72	64	0.20	0.36	0.60	0.49	0.37	0.41	0.06	0.03
3	72	66	0.21	0.30	0.54	0.55	0.37	0.39	0.06	0.04
4	69	72	0.13	0.18	0.43	0.50	0.24	0.31	0.09	0.09
5	72	71	0.08	0.15	0.38	0.47	0.20	0.25	0.07	0.07
6	72	69	0.12	0.31	0.40	0.50	0.21	0.39	0.07	0.05
7	72	72	0.14	0.33	0.42	0.47	0.31	0.39	0.06	0.04
8	72	72	0.26	0.20	0.44	0.52	0.34	0.38	0.04	0.05
9	72	69	0.11	0.20	0.39	0.54	0.29	0.31	0.06	0.08
10	72	66	0.04	0.15	0.33	0.40	0.21	0.25	0.06	0.05
11	72	66	0.27	0.21	0.44	0.42	0.33	0.31	0.03	0.04
12	72	72	0.04	0.22	0.35	0.43	0.22	0.33	0.07	0.04
13	72	72	0.02	0.05	0.36	0.37	0.15	0.19	0.08	0.09
14	72	71	0.01	0.00	0.35	0.38	0.09	0.09	0.07	0.09
15	72	70	0.01	0.00	0.35	0.38	0.10	0.09	0.08	0.10
16	72	69	0.03	0.00	0.40	0.33	0.19	0.16	0.10	0.10
17	72	72	0.19	0.00	0.41	0.27	0.30	0.20	0.05	0.04

Note: Results in the above table are negative values expressed in V CSE.

The sample exhibited considerable corrosion and deterioration. Failure in wires occurred at several locations. All broken ends of wires were sharp. It appeared the strand was coated with an epoxy compound after the failure had occurred. Rust could be seen through the epoxy coat.

The extent of corrosion on the surface of the freshly exposed portion was negligible. It was more extensive on the surface close to concrete cover than on the back surface

Table 9. Potential readings in Study Areas 1-4.

Statistics	Study area			
	1	2	3	4
n	213	130	216	132
MIN	0.13	0.30	0.21	0.25
MAX	0.60	0.55	0.44	0.42
AVG	0.33	0.40	0.25	0.28
STD	0.07	0.04	0.05	0.05

Note: Results in the above table are negative values expressed in V CSE.

Table 10. Percent of potential readings in study areas.

Range, V CSE	Study area			
	1	2	3	4
Less negative than -0.20	15	0	22	12
-0.20 to -0.35	40	8	69	79
More negative than -0.35	45	92	9	9

of the sample. The bond between the strand and the concrete was good. Several notches, up to 0.08 in (2 mm) deep, were observed on some wires surrounding the central wire.

After visual examination, the sample was submitted for metallurgical analyses to characterize the mode of failure and to identify the type of corrosion present.

**Visual and Macroscopic Examination.** The sample was first subjected to visual and macroscopic examinations performed with the aid of a stereoscopic microscope capable of magnifications up to 40X. All wires in this sample displayed considerable corrosion or rusting similar to that observed in the sample from O'Hare Airport Leads bridge. The corrosion, however, was primarily near the fractured end of the wire with very little corrosion or deterioration at the opposite end which had been cut. The wire diameter was measured on the clean end of the wires and all were found to have diameters of approximately 0.120 in (3.05 mm). All seven wires from this group were sequentially longer in the counter clockwise direction with the center strand displaying the greatest length. None of the wires displayed any areas of clean metal near the failed ends which did not display corrosion. Measurements of the wire in the corroded areas revealed dimensions down to 0.040 in (1.02 mm). In some of the wires, the minimum diameter was found to be near the tip of the fracture with a gradual increase in diameter typical of necking in a ductile overload failure. Other areas of the wire displayed primary reduction in dimensions of the wires near the outside of the group with considerably less material degradation near the center strand of the group. An illustration of the appearance of the wires is shown in figure 50.

**Scanning Electron Microscope Examination.** The fractured ends of the wires were placed within the vacuum chamber of an SR-50 scanning electron microscope. Examinations were performed in both the as-received condition and after cleaning in a solution of inhibited hydrochloric acid. The inhibited acid solution permitted removal of some of the corrosion products from the fractured surfaces. A 15 Kv electron beam was used to examine the wires at magnifications up to 20,000X.

These examinations revealed the fractured surface to predominantly display a dimpled appearance. These dimples are formed during microvoid coalescence and are indicative of a ductile overload failure. The areas which did not display this appearance remained covered with the plastic or glass-like material and prevented proper examination of the surfaces. No indications of other failure modes were identified such as brittle fracture, stress corrosion cracking, or cleavage. A typical example of the fracture appearance is shown in figures 51 and 52.

**Metallographic Examination.** Metallographic sections were cut through the fractured tips of several of the wires. In addition, a section was taken from near the cut end of the wires. After mounting the sections in bakelite molds, standard metallographic techniques were used to grind and polish the sections to a 0.05 micron finish. A metallurgical microscope was used to examine the cross sections at magnifications up to 2000X. Etching with a solution of 1 percent nital provided clear definition of the microstructures.

These examinations revealed a microstructure typical of prestressing steel wire. The microstructure consisted of heavily cold-worked and elongated grains of ferrite and pearlite. Near the fractured ends of the wires, similar microstructures were observed. It could be seen the reductions in wire diameter were primarily due to corrosion rather than necking during tensile overload failure. The corrosion may be classified as an oxidation of the wire surfaces. No indication of inherent metallurgical defects were observed which would have contributed to premature failure of the wire such as excessive inclusions, laps, carburizations, or unusual surface conditions developed during forming or manufacture of the wire. Illustration of the microstructure exhibited by the wire sample is presented in figures 53, 54, and 55.

**Cause of Failure.** Based upon the above examinations, it appears the wire sample failed primarily due to reduction in the effective cross section caused by corrosion. The corrosion of the wire was classified as a general oxidation. The reduction in the cross sectional area culminated in the failure of the wire by a ductile overload. Scanning electron microscope examination failed to identify any other fracture modes. No indications



Figure 50. The test sample of the seven-wire strand from Span 3, Box 2.



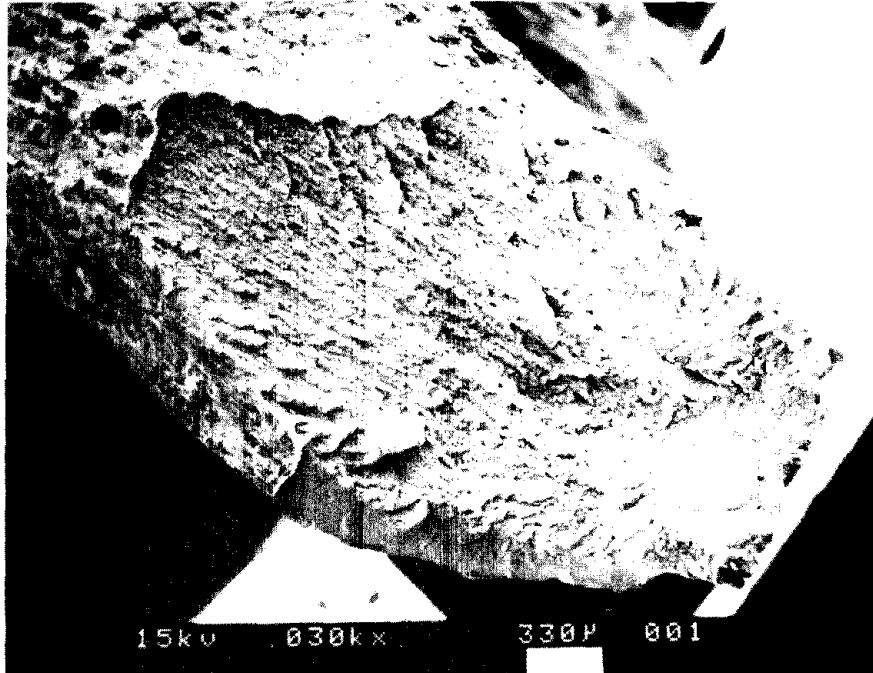


Figure 51. The fractured end of one of the sample wires. (Magnification: 30X.)

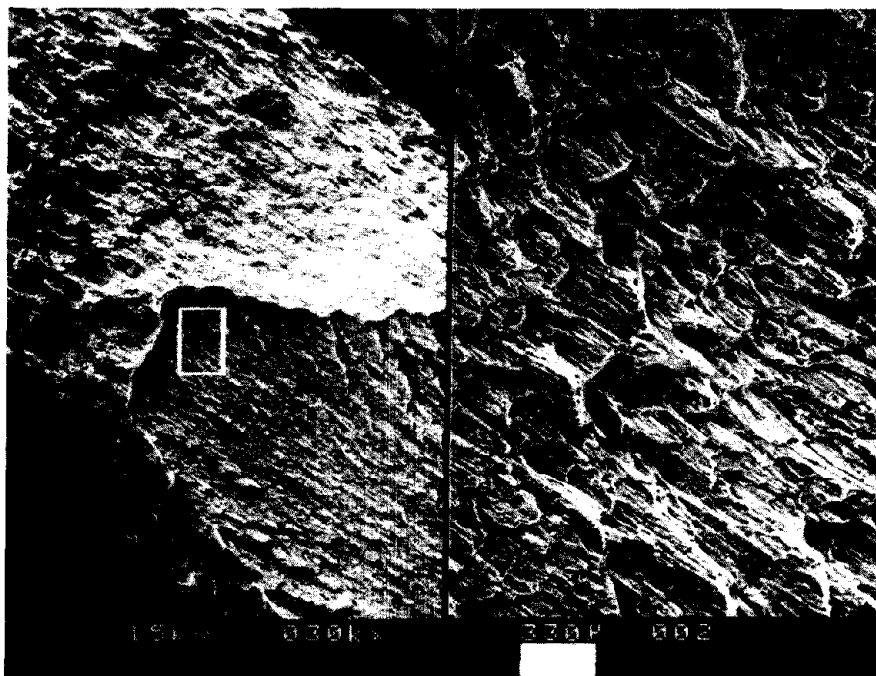


Figure 52. Fractured area of a wire at a magnification of 30X (left) and 300X (right).

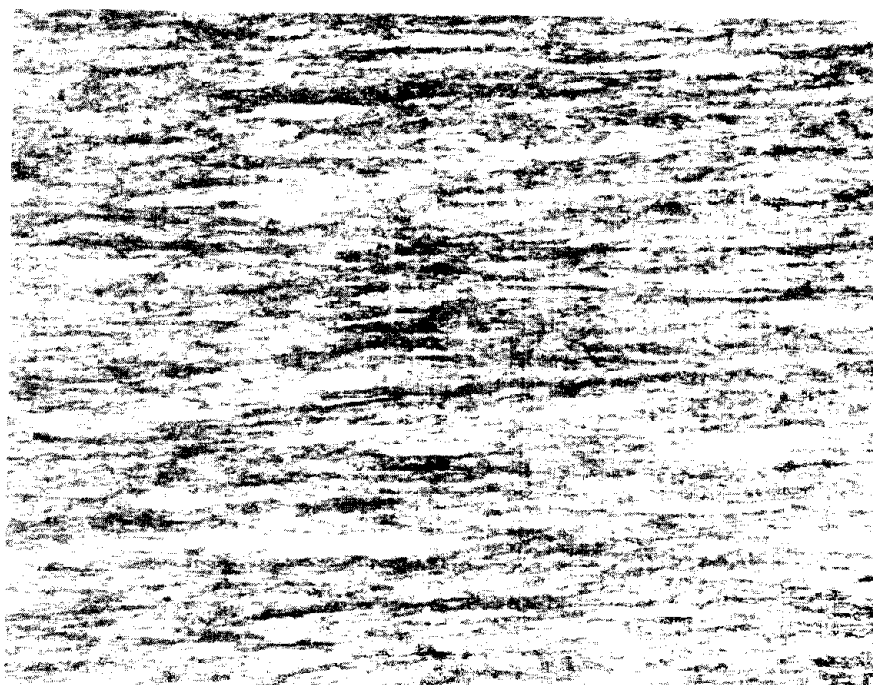


Figure 53. A typical example of the heavily cold-worked microstructure exhibited near the cut end of a wire.  
(Magnification: 200X. Etchant: 1% Nital.)

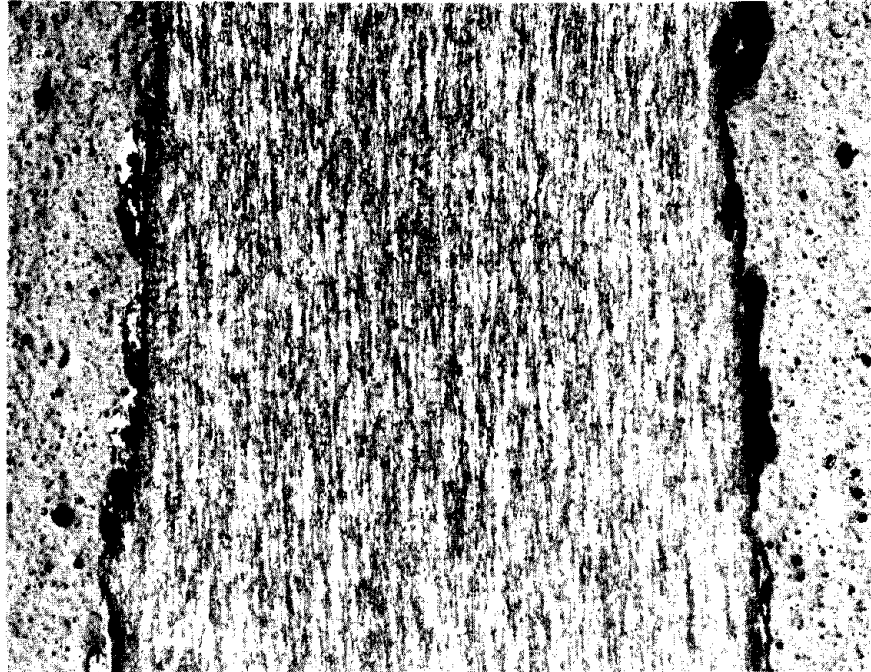


Figure 54. The microstructure of the center wire with Bakelite along the left and right edges.  
(Magnification: 50X. Etchant: 1% Nital.)

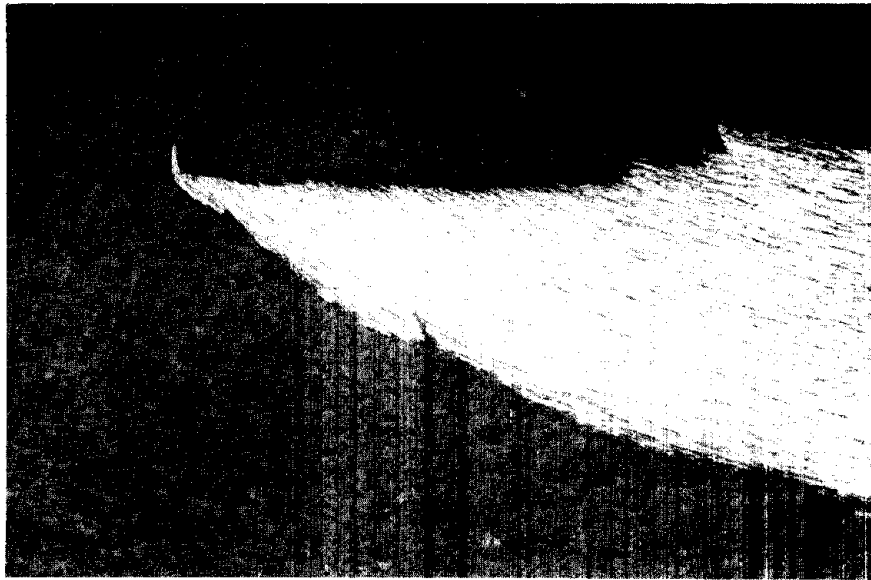


Figure 55. Microstructure near the fractured end of a wire.  
(Magnification: 50X. Etchant: 1% Nital.)

of defects or unusual microstructures were observed in the wire. This testing revealed the wire sample to have corroded until the remaining material was incapable of maintaining the applied load.

### **Summary**

- Most deterioration of concrete and corrosion of prestressing strands was observed in areas adjacent to leaking joints between box girders. It appeared the leakage occurred through cracks in the deck overlay and subsequently through joints between girders.
- Extent of corrosion of prestressing strands varied from negligible to very severe. Cases of failure of six wires surrounding the central wire or even all wires including the central wire were not uncommon.
- Overall condition of repairs made using an epoxy based mortar was good. This repair method appears to be quite effective, provided the corrosion is removed prior to application of a patch.
- Detailed study was conducted on four areas representing different extents of deterioration of concrete and corrosion of reinforcing steel in the viaduct.
- Delamination of concrete cover over prestressing strands was not common.
- Petrographic examination showed concrete represented by the two cores was of good quality and generally low permeability, without any evidence of deleterious chemical reactions.
- Concentration of chlorides and moisture content in concrete cover varied from point to point within range sufficient to give rise to powerful corrosion cells in prestressing strands.

- Concrete cover in inspected girders was found insufficient to provide proper protection to reinforcing strands.
- The most essential information to characterizing the extent of corrosion activity are the average and the percent of readings more negative than -0.35 V CSE.
- Based on results of the potential study it can be concluded that the area exhibiting a higher extent of distress not necessarily has the higher corrosion activity.
- It appears that failure in prestressing strands occurred as a result of a ductile overload due to reduction in the effective cross-section caused by oxidation corrosion.
- The main reasons for rather severe distress observed in spans of the viaduct were cracks in the deck concrete overlay, leaking joints between girders, and inadequate concrete cover.

## **THE SIXTH SOUTH STREET VIADUCT**

### **Bridge Description**

The Sixth South Street Viaduct (figure 56) is located between the 1st and 6th West Streets in Salt Lake City, Utah. The viaduct was constructed in 1962. The length of the viaduct is 2370 ft (722.4 m) of which 1500 ft (457.2 m) consist of pretensioned and post-tensioned beam spans with a total of 292 prestressed girders. The rest of the viaduct is comprised of reinforced concrete continuous slab, reinforced concrete box girder, and steel welded plate girder spans.

A typical viaduct section consists of a reinforced concrete superstructure with bearing pads, prestressed pretensioned or post-tensioned girders, diaphragms tying the girders together, and a cast-in-place deck slab. The number of girders in one span varies from 8 to 10.

**Post-Tensioned Girders.** Post-tensioned girders were prestressed by means of unbonded, unprotected tendons consisting of semirigid corrugated galvanized steel sheathing, 2 @ 1-in (25.4 mm) and 2 @ 1.5-in (38.1 mm) diameter rods anchored with end nuts seated in an end retaining steel plate. The distance from the centerline of the bottom post-tensioned bars to the bottom surface of a girder varies from a minimum of 3.5 in (88.9 mm) at mid-span to a maximum of 6 in (152.4 mm) at the ends of a girder.

**Pretensioned Girders.** All pretensioned concrete girders are AASHTO Type III girders. The reinforcement in these girders consists of 26 seven wire strands. The ends of prestressing strands are protected with portland cement mortar filling 1-in depressions in the top and in the bottom of a girder. Specified concrete cover around prestressing strands varies from 2.25 to 3 in (57.2 to 76.2 mm).

### **Nature and Extent of the Problem**

First failures of the post-tensioned tendons were noticed in 1975-1977. The steel bars generated loud noises when breaking. The noise was overheard by people in the area who reported it to the DOT personnel. The presence of fractured tendons was determined by inspecting the ends of the post-tensioned beams. Broken steel bars had





Figure 56. The Sixth South Street Viaduct, Salt Lake City, Utah.

loose ends projecting from the end of a girder and loose end nuts displaced from their original location. Cracking and spalling of end grouting caused by loosening of the tendons was also considered an indication of a possible rod fracture. There were no cracks or rust stains visible on the exterior surfaces of these particular girders. It was estimated the total number of fractured bars was about 21. Some pitting corrosion without signs of necking or loss of cross sectional area was observed on retrieved broken rods.

Failure was attributed to salt entering anchorage zones and moving inside ducts between the steel rod and sheath. All beams with fractured tendons were subsequently externally post-tensioned to restore structural capacity.

### **Visual Examination**

**Post-Tensioned Tendons.** The extent of corrosion of post-tensioned steel bars was determined by inspecting two tendons, one in Girder 3, Span 36-37 (figure 57), and the other one in Girder 10, Span 28-29 (figure 58). These tendons were exposed in November 1977 and have remained open since then.<sup>(47, 48)</sup> Neither of the two tendons was fractured. The thickness of the duct sheath in exposed tendons was 0.01 in (0.25 mm). The distance between the steel rod and the duct was about 0.04-0.06 in (1.0-1.5 mm). Neither grout nor grease were found inside the tendons.

There was some rust on exposed surfaces of the tendon in Girder 3, as well as on the sheathing and the rod (figure 59). The extent of surface corrosion was rated negligible. No corrosion pits were observed on the surface of the rod or the duct enclosing this rod.

Concrete was removed to determine the extent of corrosion of the tendon that was not exposed to the atmosphere. No corrosion was observed on the surface of the newly exposed sheathing. Also there was no corrosion on the surface of the high chair bar below the sheathing (figure 60). Concrete cover from the bottom surface of the girder to the high chair bar and to the tendon was 1.5 and 2.9 in (38.1 and 73.7 mm), respectively. Concrete cover from the north side of the viaduct was 7.1 in (180.3 mm).

After inspecting the outside surface, the duct was removed and the inside surface of the duct as well as the surface of the rod were examined (figure 61). The extent of corrosion on the inside surface of the duct gradually decreased as more concrete and more sheathing was removed. Deeper into the structure the inside surface of the tendon did not exhibit any signs of corrosion. Corrosion on the surface of the rod appeared to be more extensive than on the inside surface of the duct and was persisting as far as the rod was visible.

The extent of corrosion on outside surfaces of the tendon in Girder 10, Span 28-29 was approximately the same as in the previously described tendon. An additional 4-in (102 mm) length was exposed to determine the condition of the tendon protected with concrete cover. Thickness of concrete cover over the tendon was 3.38 in (86 mm) from the bottom, and 7.1 in (180 mm) from the north side of the girder. There was no corrosion on the outside surface of the newly exposed tendon (figure 62). The extent of corrosion on inside surfaces varied from negligible to moderate (figure 63). Some negligible pitting corrosion on the north side of the prestressing rod was also noticed. The depth of pits did not exceed 0.05 in (1.3 mm). Corrosion on the surface of the newly exposed rod was less extensive than that on the surface of the previously exposed portion of the rod. No signs of corrosion were noticed on the surface of the high chair bar below the tendon. Concrete cover over this bar from the bottom and from the north side of the girder was 1.5 in and 2.9 in, (38 and 74 mm), respectively. Concentration of chlorides in the concrete next to the exposed tendon was 0.012 percent, essentially a baseline level.

The condition of examined steel surfaces and especially high chair bars which have the lowest concrete cover suggest that the penetration of chloride ions through concrete cover and through a duct was very unlikely.

**Pretensioned Strands.** The ends of seven wire strands in pretensioned girders were covered with portland cement mortar. The mortar was found to be soft but in good condition, without any signs of deterioration (figure 64). Some strands were exposed to a depth of 2.25 in (57 mm) and examined for the presence of rust. The extent of corro-

sion varied from negligible throughout the whole exposed length to moderate at the end of the strands (figure 65).

No signs of corrosion were noticed on the surface of a newly exposed strand in Girder 5, Span 39-40 (figure 66). Concrete cover over this strand from the bottom side of the girder was 1.9 in (48.3 mm), and from the north side was 3.1 in (78.7 mm).

**Anchorage Areas.** Most extensive deterioration of concrete in post-tensioned girders occurred in areas of anchor steel plates. Cracking was noticed in almost every post-tensioned girder. Typically cracks would occur around and in the mortar filled tendon depressions (figure 67). Spalling of the mortar cover over steel plates was not uncommon (figure 68). This type of deterioration was mainly caused by corrosion of steel anchor plates and, to some extent, by corrosion of conventional reinforcing steel bars. The cause of concrete cracking in beam pedestals was not clear (figure 68).

The extent of corrosion of steel plates was rated as moderate to severe, and very severe (figures 69 and 70). It was more severe in bottom than in top anchor plates. In some cases the thickness of rust on the surface of steel plates was as much as 0.25 in (6.4 mm).

The percent of chlorides in concrete in this area was 0.324 at a depth of 2 -2.5 in (50.8-63.5 mm); and 0.272 at a depth of 2.5-3.0 in (63.5-76.2 mm), the only area with such high concentrations of chlorides. This indicates that corrosion of the anchorage system occurred due to a high concentration of chlorides in combination with a sufficient amount of moisture to cause chloride ions to migrate to a depth of 3 in (76.2 mm) The only source of chlorides in these locations is the chloride-laden water running from the deck through expansion joints.

**External Tendons.** It was estimated that of a total of 224 post-tensioned girders, 30 were reinforced with external tendons (figure 71). A typical external tendon consists of a heavy frame made of a 0.9 in (22.9 mm) steel sheet and a 2 in (50.8 mm) steel anchor plate bolted to the frame. Each tendon has a 1.5-in (38.1 mm) diameter post-tensioned rod protected with a 2.5-in (63.5 mm) diameter rigid plastic duct connected to the frame through a steel pipe (figure 72). The threaded end of the rod is coated with a

bitumen emulsion. The space between the steel frame and beam is filled with a flexible sealer with epoxy mortar on top of it.

It was noted the external tendons were detailed such that even when located next to a leaking joint, the penetration of chloride-laden water inside tendons was very unlikely. The anchor of a tendon was not covered with concrete or with mortar and therefore could easily be inspected. It appears this design provides good protection to post-tensioned rods against corrosion and can be recommended for similar projects.

**Deck Drains.** A typical bridge drain consists of a 6 in (152.4 mm) pipe extending to about 2 ft (0.61 m) above the ground. Drains were installed next to each second expansion joint, on the east side of the viaduct, about 2 ft (0.61 m) from the joint. Originally, each drain pipe was installed parallel to the bottom edge of a pier cap and had a slope of not more than 20 deg. Accumulation of water and debris on top of the deck, deterioration of concrete in areas of expansion joints and in pier elements, as well as holes in drain pipes made to increase the rate of flow of storm water suggested the drainage system was not functioning properly (figures 73, 74, and 75) . The problem was aggravated by the presence of unsealed sidewalk joints on both sides of the viaduct.

Later the original design was altered. Drain pipes were either removed completely with the exception of a short vertical portion, or slope was increased to approximately 60 deg (figures 76 and 77). Leaking deck joints were resealed and deteriorated concrete around them was replaced. The short pipes appeared to provide sufficient flow of storm water. It appears that drain grids are inspected and cleaned on a routine basis.

Expansion joints in sidewalks above pier caps are still open. Based on results of the examination of pier caps, the concentration of chlorides in the water running through these joints appeared to be sufficient to cause future corrosion of reinforcement with subsequent deterioration of the surrounding concrete.

**Cause of Corrosion.** Since a sample of a fractured rod was not available for metallurgical analyses it was impossible to determine the mode of the fracture. It is known that the fracture was brittle without any decrease in cross sectional area of steel



Figure 57. Exposed post-tensioned tendon  
in Girder 3, Span 36-37.

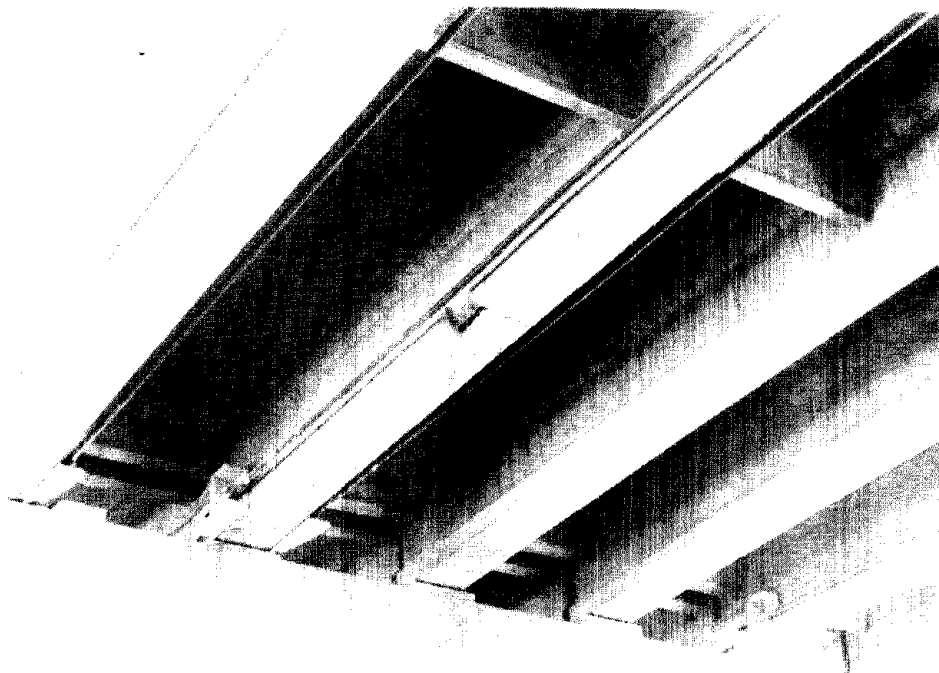


Figure 58. Exposed post-tensioned tendon  
in Girder 10, Span 28-29.

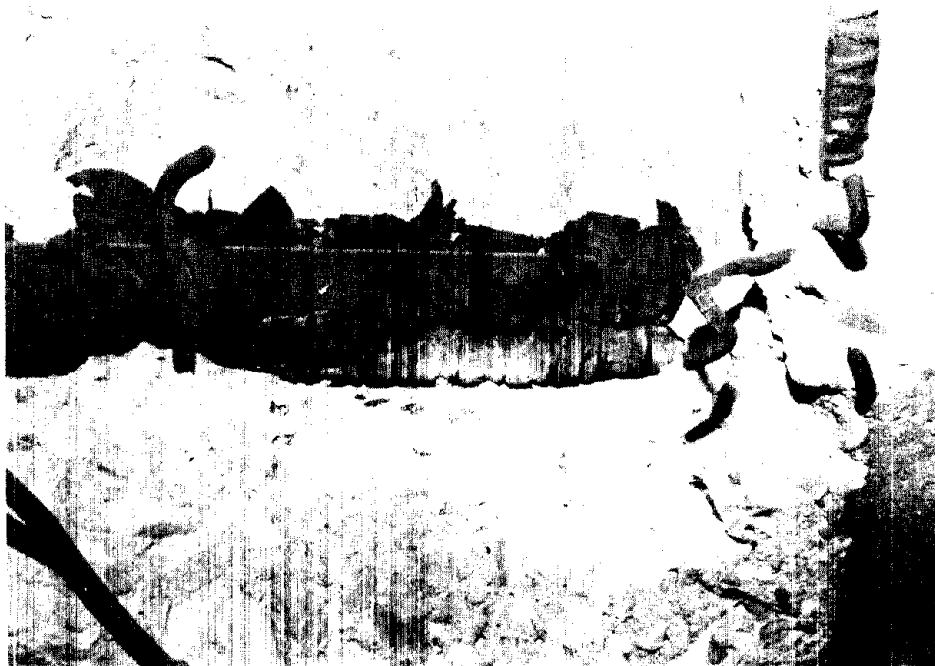


Figure 59. Surface type corrosion on exposed surfaces of the prestressing tendon in Girder 3, Span 36-37.



Figure 60. Condition of the newly exposed surfaces of the duct and the high chair rod in Girder 3.



Figure 61. Extent of corrosion on the newly exposed surface of the rod in Girder 3.



Figure 62. Condition of the tendon protected with concrete, Girder 10, Span 28-29.



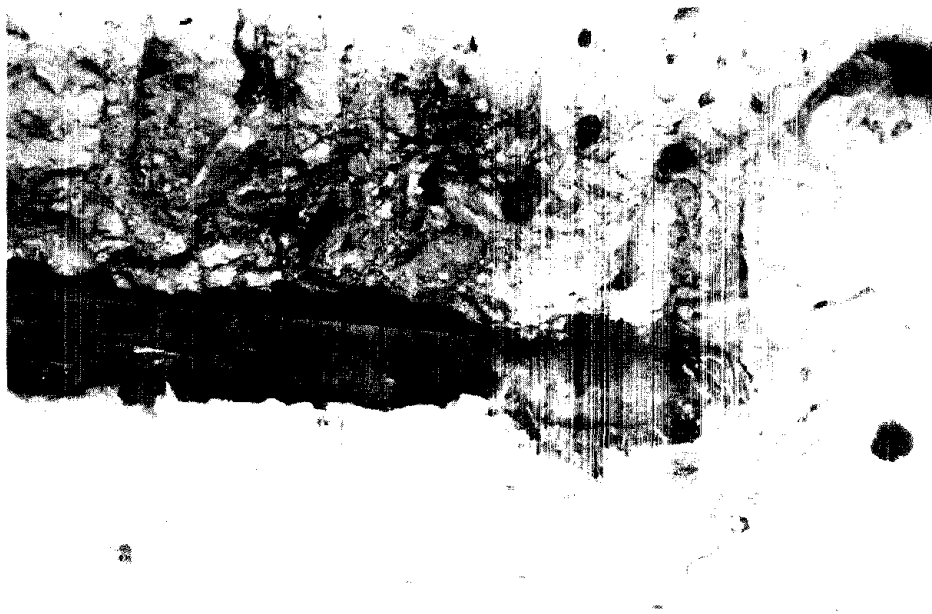


Figure 63. Negligible to moderate surface type corrosion on the newly exposed surface of the rod in Girder 10.

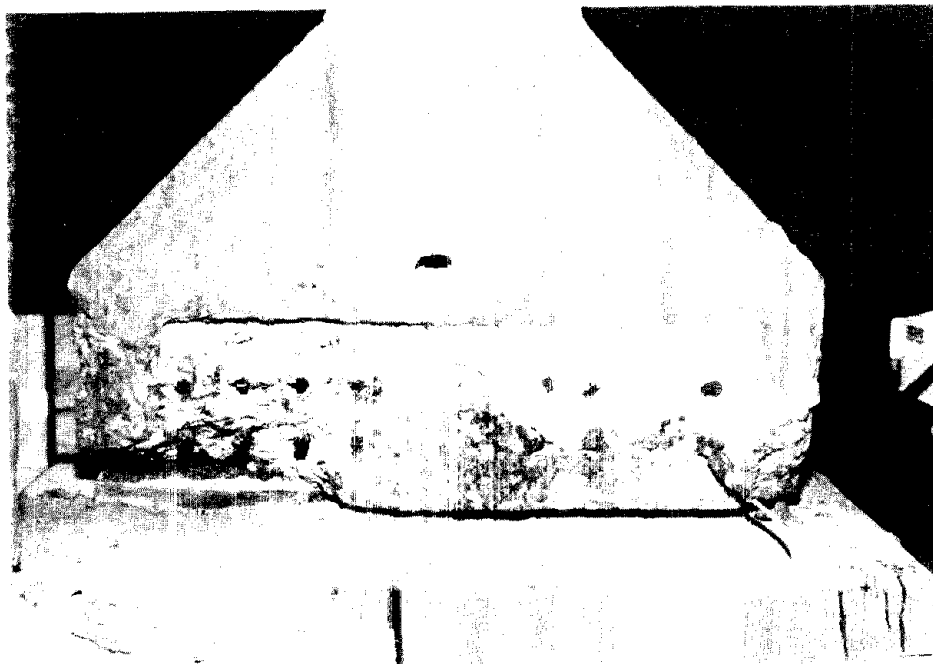


Figure 64. Corrosion protection to exposed ends of seven wire strands by means of portland cement mortar.



Figure 65. Moderate corrosion of exposed strands at the end of a girder.



Figure 66. Appearance of the exposed strand in Girder 5, Span 39-40.



Figure 67. Cracks in mortar  
and concrete in areas  
of anchor plates.

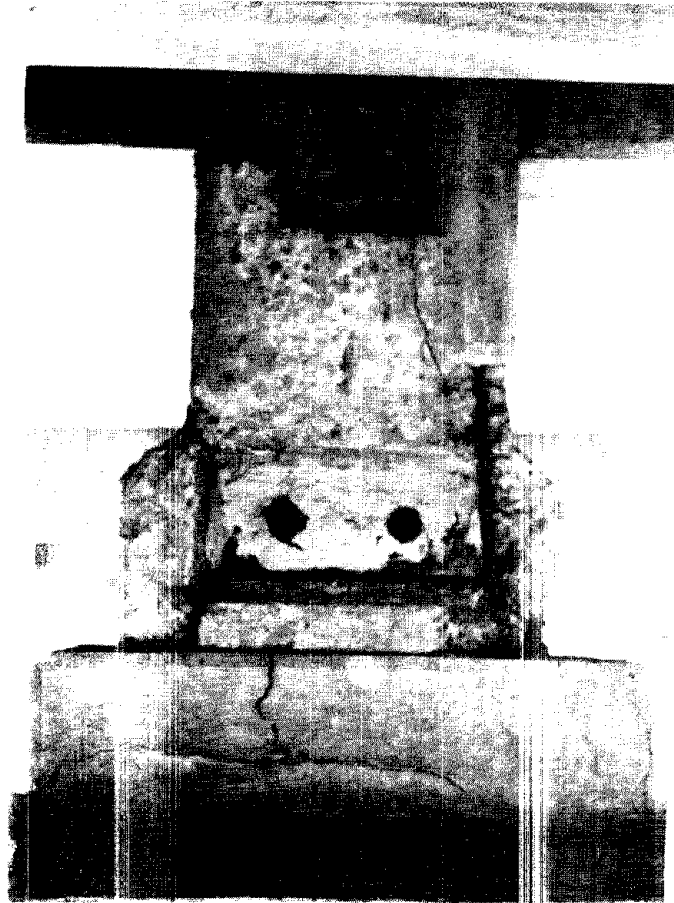


Figure 68. Spalling of the mortar cover over anchor steel plates.

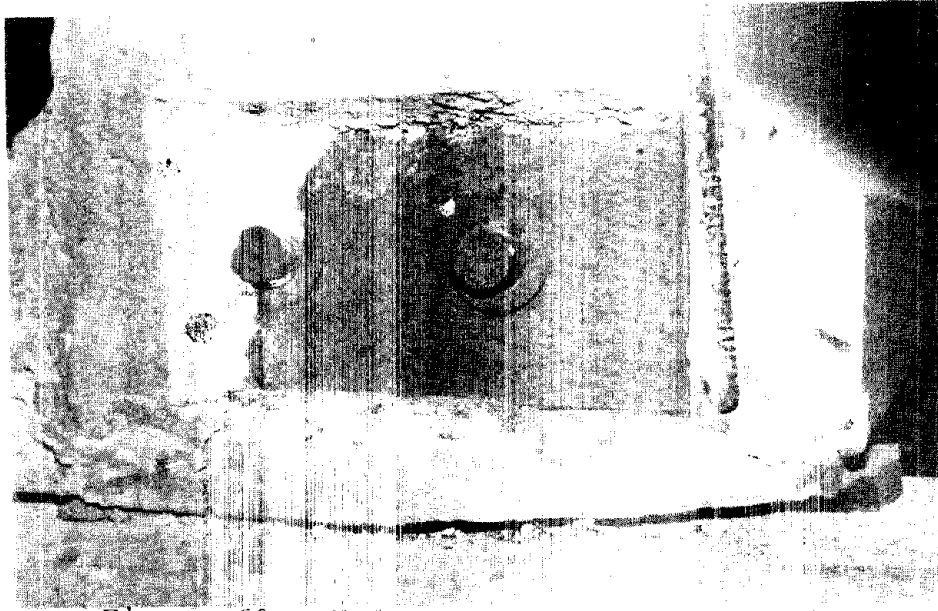


Figure 69. Moderate to severe corrosion of a steel plate.

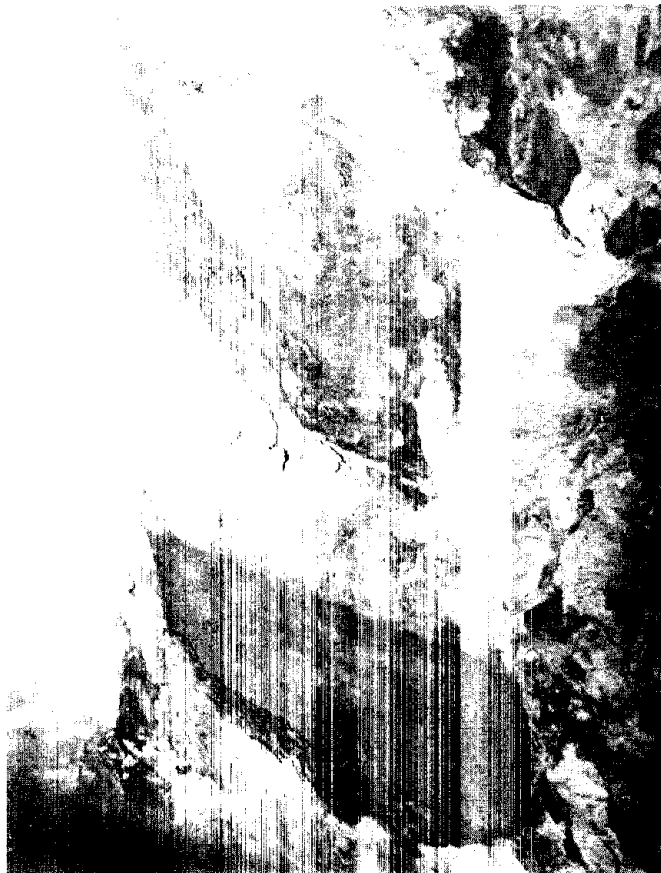


Figure 70. Very severe corrosion of an anchor plate.

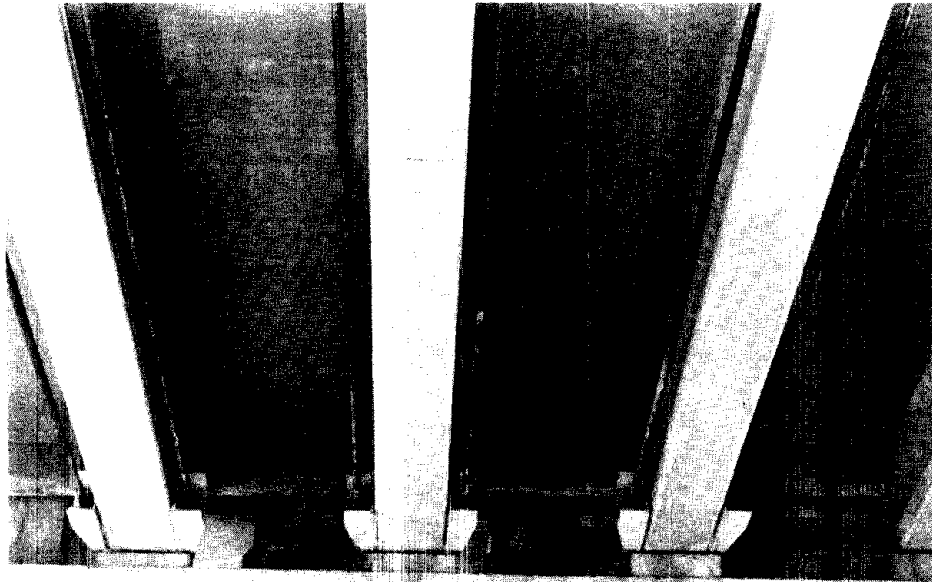


Figure 71. Post-tensioned girders reinforced with external tendons.

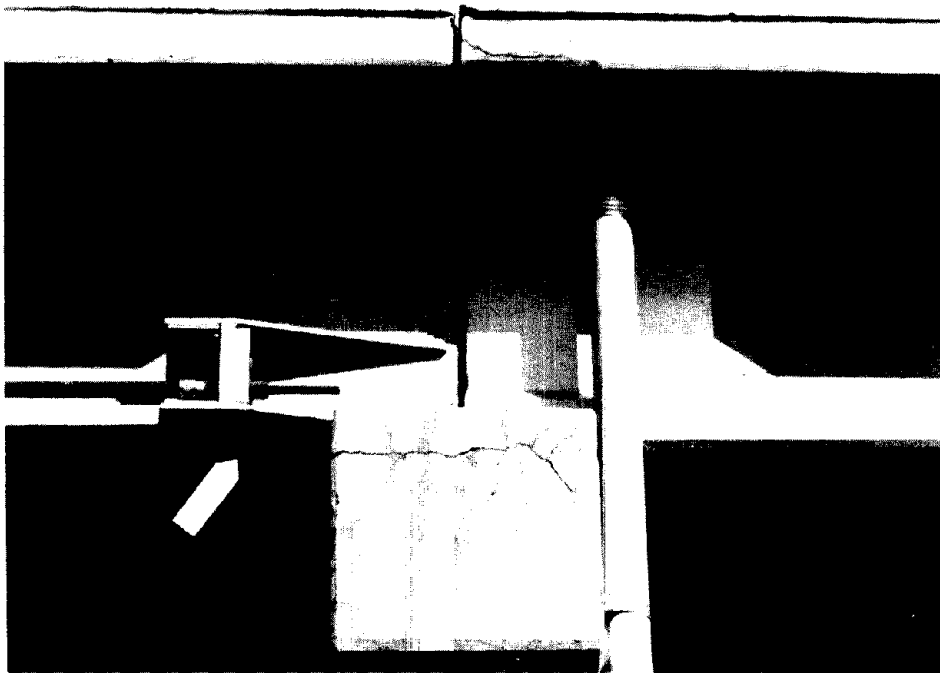


Figure 72. A typical external tendon.



Figure 73. Accumulation of debris and deterioration of concrete in areas adjacent to the open sidewalk expansion joint.

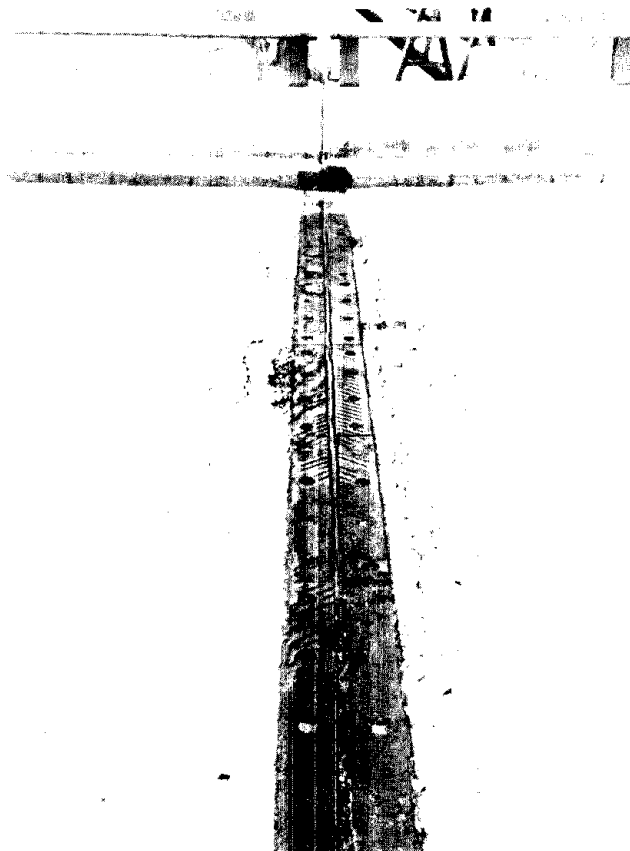


Figure 74. Deterioration of concrete in areas of expansion joints.

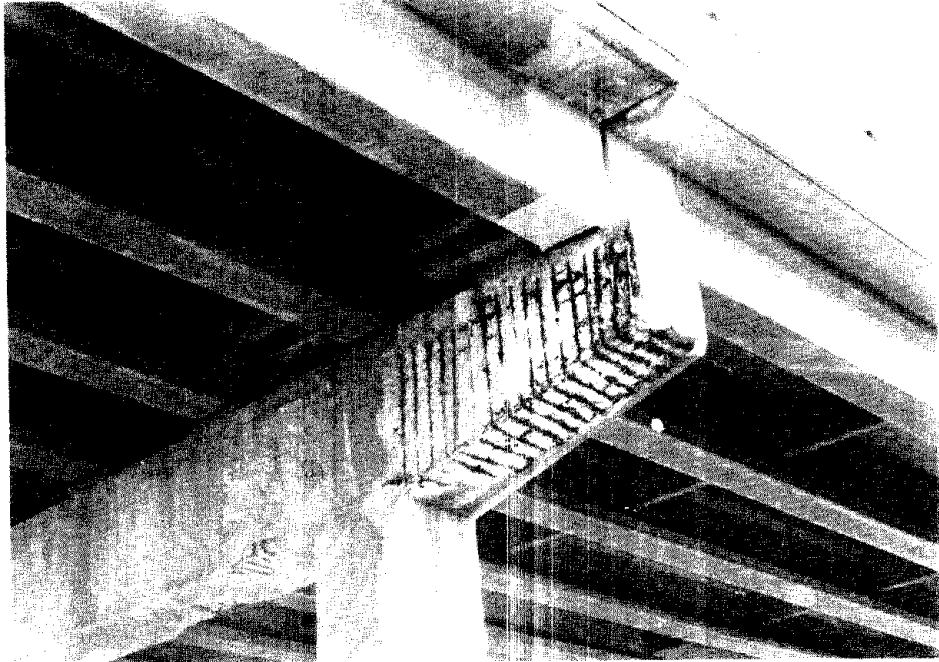


Figure 75. Corrosion-related deterioration of concrete in a pier cap.

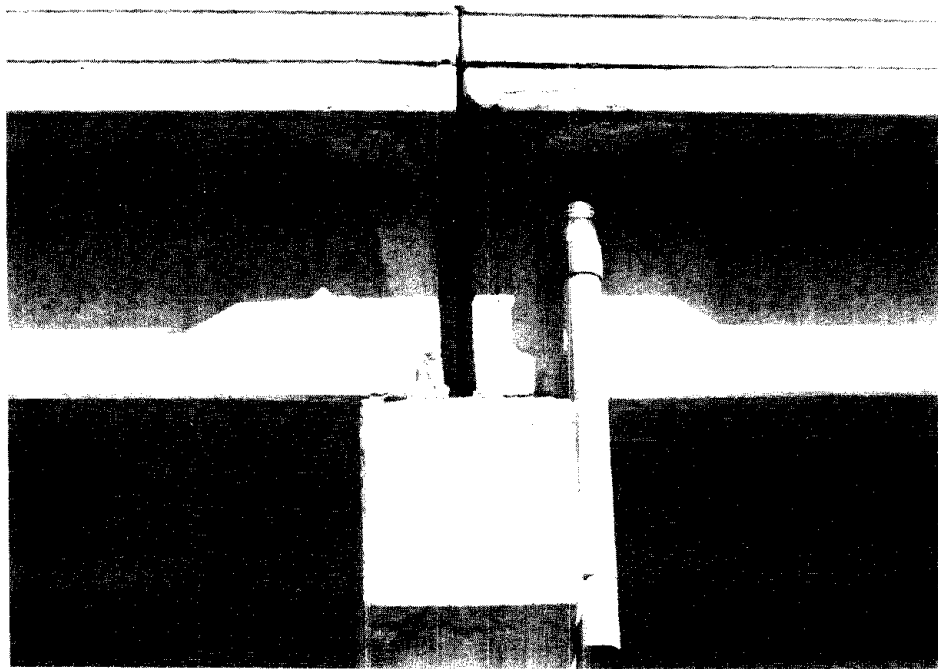


Figure 76. Remaining short vertical portion of a drain pipe.





Figure 77. Drain pipe with an increased slope.

rods. It is possible the fracture occurred due to hydrogen embrittlement, though this cannot be confirmed.

### **Petrographic Examination**

Cores labeled Bent 42-G#8 and Bent 39-G#5, and a chunk sample labeled Bent 42-G#8 were examined. Core Bent 42-G#8 was obtained from Girder 8, Span 42, and Core Bent 39-G#5 was obtained from Girder 5, Span 39. A chunk sample of Bent 42-G#8 was obtained from Girder 8, Span 42 and represented concrete adjacent to a corroded anchor plate.

**Core Bent 42-G#8.** Cross section of this core is shown in figure 78. Coarse aggregate is a partially crushed, natural siliceous gravel having a maximum size of 0.75 in (19.1 mm). Rock types present in the coarse aggregate include sandstone, chert, metaquartzite, andesite, and basalt. Coarse aggregate particles are variously colored, hard, somewhat porous to dense, spherical, and angular to well-rounded. Fine aggregate is natural siliceous-calcareous sand composed of quartz, feldspar, biotite, mica, chert, sandstone, granite, calcite, metaquartzite, basalt, and andesite. Fine aggregate particles are hard, generally dense, spherical, and subangular to sub-rounded. The aggregate is well-graded and uniformly dispersed. There are no indications the aggregate has performed poorly in service.

Cement paste is light gray, moderately soft to moderately hard, somewhat porous, and fairly well-bonded to aggregate particles. Along freshly broken surfaces, the paste exhibits a subvitreous to dull luster, microgranular texture, and irregular fracture. Paste carbonation extends to 0.5 in (12.7 mm) depth from the formed surface. Residual cement particles are infrequent. Calcium hydroxide is moderately abundant. Based on the previously described paste properties, the water-cement ratio is estimated to be 0.50 to 0.60.

The concrete is not air-entrained. Entrapped air content is estimated to be 0.5 to 1.0 percent. The few voids present are large and subspherical to nonspherical. There is no evidence of deterioration in this core.

**Core Bent 39-G#5.** A cross section of this core is shown in figure 79. Aggregate types and properties are similar to those in the previously described core, however,

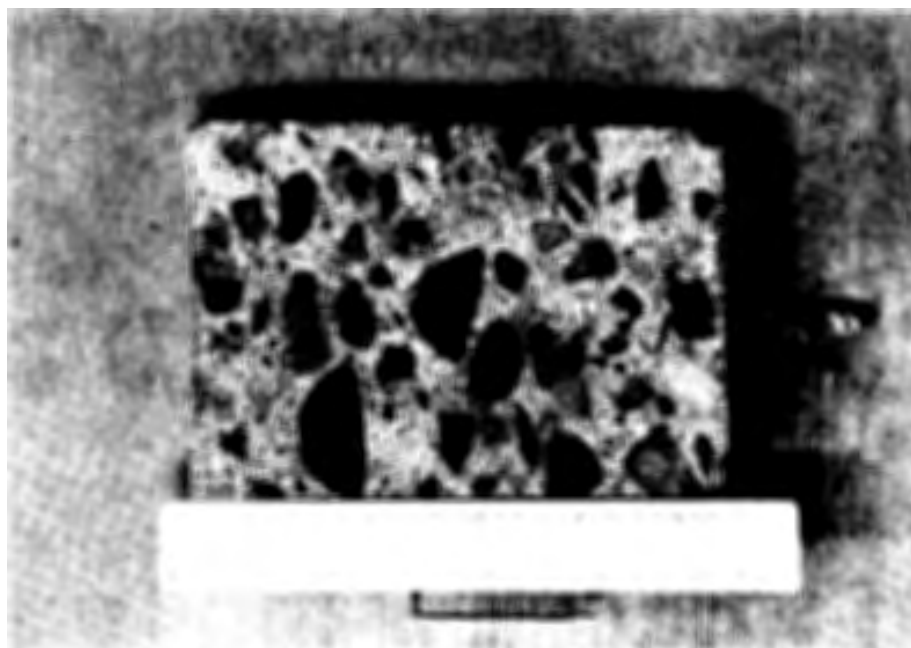


Figure 78. A lapped slice of Core Bent 42-G#8.

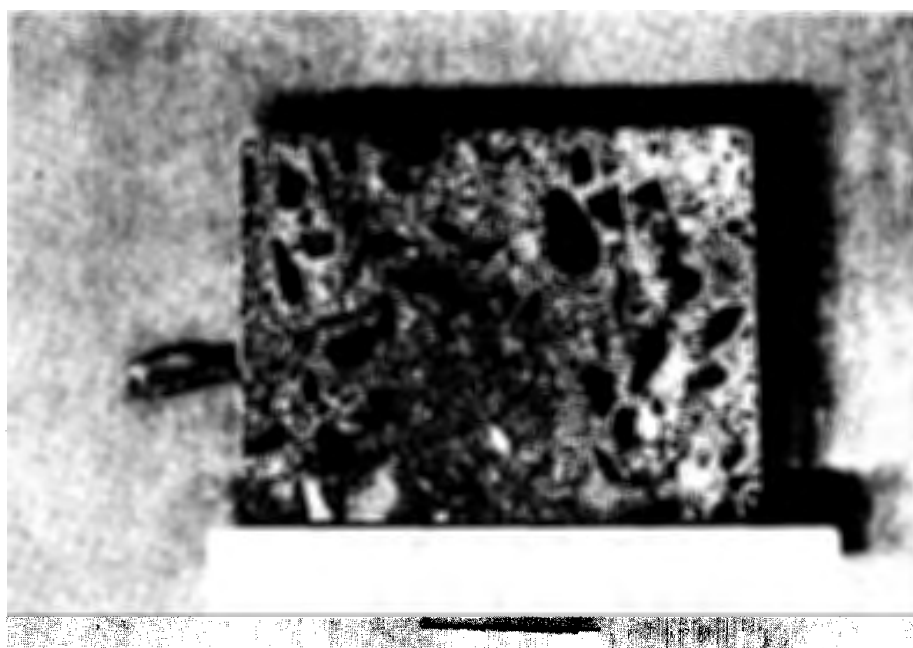


Figure 79. A lapped slice of Core Bent 39-G#5.



Figure 80. A lapped slice of Chunk  
Sample Bent 42-G#8.

larger aggregate sizes appear deficient in this core. Cement paste properties in this core are also similar to those in Core Bent 42-G#8, except that paste carbonation extends 0.5 to 0.75 in (12.7 to 19.1 mm) in depth from the formed surface and the presence of isolated microscopic particles of high water-cement ratio paste was noted mostly at fringes of aggregate particles. These zones represent trapped bleed water or possibly may be a remnant of oversaturated aggregate.

A few minor surficial drying shrinkage microcracks occur at the imprint of the formed surface. The microcracks extend up to 0.13 in (3.3 mm) into the concrete.

**Chunk Sample Bent 4-G#8.** The cross section of the specimen is shown in figure 80. The sample consists of a rectangular chunk of concrete of which two sides are broken surfaces and the remaining sides are either imprints of adjacent concrete and/or weathered imprints of formed or finished surfaces.

Along one side of the specimen is a 0.13-in (3.3 mm) thick layer of mortar adhering to the concrete. At the bottom of the sample is a piece of extremely corroded steel. The steel does not appear to be round reinforcing bar, but rather some sort of rectangular embedment. Cracks radiate from the steel into adjacent overlying concrete and pass around and through aggregate particles. Cracks up to 1.5 in (38.1 mm) from the steel are partially filled with brown corrosion product. Also cracks are filled with secondary deposits of calcium carbonate. The calcium carbonate is frequently seen deposited over the corrosion product. This suggests moisture migration through cracks. The cracks appear to be a result of expansion caused by steel corrosion. Concrete cover is 2 in (50.8 mm) from the side of the specimen and 1 in (25.4 mm) from the mortar layer.

Aggregate types and properties are similar to those in previously described cores. Paste properties are similar to those described in Core Bent 42-G#8. However, paste at the level of steel is carbonated and paste at the top of the specimen is carbonated to 0.13 to 0.25 in (3.3 to 6.4 mm). Paste carbonation appears to have migrated from the side of specimen or from the bottom mortar layer, since paste in the middle and upper portions of the specimen are only slightly carbonated to uncarbonated. No isolated patches of high water-cement ratio paste were detected.

Water-cement ratio is estimated to be 0.50 to 0.60 in all three concrete specimens. None of the cores are air-entrained. Entrapped air content is estimated to be 0.5 to 1.0 percent. The few voids present are large and subspherical to nonspherical. None of the cores exhibit evidence of distress.

### **Chloride Concentration**

A total of 14 samples were obtained from girders of the bridge to determine concentration of chlorides in concrete at various depths, with an emphasis on end sections of girders. Description of test samples and test results are shown in table 11.

Table 11. Concentration of chlorides in concrete at various depths.

Sample No.	Girder No.	Bent No.	Location	Depth (in.)	Cl ion %
1	5	32	East end	0.0- 0.5	0.635
2	5	39	East end	1.0- 1.5	0.555
3	5	39	East end	4.5- 5.0	0.007
4	5	39	Middle bottom	0.0- 0.5	0.012
5	5	39	Middle bottom	1.0- 1.5	<0.006
6	5	39	Middle bottom	1.75-2.25	<0.005
7	10	28	Exposed tendon	0.0- 0.5	<0.004
8	3	37	Exposed tendon	0.0- 0.5	0.010
9	4	42	Top mortar	0.0- 0.5	0.184
10	4	42	Top concrete	0.0- 0.5	0.016
11	4	42	Top concrete	2.0- 2.5	0.003
12	4	42	Top concrete	4.0- 4.5	0.004
13	4	42	Bottom concrete	2.0- 2.5	0.324
14	4	42	Bottom concrete	2.5- 3.0	0.272

The highest concentration of chlorides was found in the east end section of Girder 5 (pretensioned), above Bent 39 (Samples 1, 2, and 3). Samples 4, 5, and 6 were obtained from the middle of the bottom side of Girder 5. Percent of chlorides varied

from 0.012 in the top 0.5-in layer to 0.005 at the depth of the reinforcement. It is reasonable to expect that samples 4, 5, and 6 are representative of baseline chloride content of concrete cover in all pretensioned and post-tensioned girders in the viaduct.

As mentioned previously, concentration of chlorides at the level of exposed prestressing tendons in Girders 10 and 3 (Samples 7 and 8, respectively) was not higher than that in the bottom concrete cover of Girder 5.

Concentration of chlorides in mortar covering the top steel plate (Sample 9) was higher than that of concrete in the same area (Samples 10, 11, and 12). The highest concentration of chlorides was at the very bottom of the section (Samples 13 and 14).

In general, results of the chloride analysis are in agreement with results of the visual examination and appear to confirm the source of corrosion-inducing chloride ions to be from leaking expansion joints.

### **Rapid Chloride Permeability**

Samples for rapid test of chloride permeability were prepared by slicing cores obtained for petrographic analyses. Test results given in table 12 indicate the amount of current transmitted during a 6-hour test was in the range of 1823 to 1919 coulombs. These readings correspond to low permeability of concrete.

Table 12. Permeability of concrete to chloride ions.

Sample No.	Location	Charge passed (coulombs)	Permeability (per AASHTO T277)
1	Bent 39 Girder 5	1919	low
2	Bent 42 Girder 8	1923	low

### **Concrete Cover Survey**

Concrete cover was measured in both pretensioned and post-tensioned girders. The same procedure was used as described previously. Strands were exposed to measure concrete cover directly and R-meter readings were calibrated against these measurements. After obtaining bottom surface readings the R-meter was recalibrated against side surface measurements. The total number of readings over top and bottom strands of a pretensioned girder was 30.

Table 13. Concrete cover over prestressing strands in Girder 5.

Statistics	Top strands	Bottom strands (north side)	Bottom strands (bottom side)
Minimum, in	3.0	3.0	1.73
Maximum, in	3.75	3.75	2.92
Average, in	3.41	3.27	2.11
STD, in	0.23	0.23	0.34

Test results given in table 13 indicate the average concrete cover was lower over bottom than top strands, but cover over side bottom strands was still higher than the specified values of 2.25 and 3.0 in (57.2 and 76.2 mm) for north and bottom side strands, respectively.

Because of erratic readings the R-meter could not be used in post-tensioned girders. Instead, concrete cover was determined by direct measurements over exposed tendons. Average concrete cover from the bottom of a girder was 3.14 in (79.8 mm) and from both sides 7.1 in (180.3 mm). Specified bottom and side values were 5.5 and 8.5 in (139.7 and 215.9 mm), respectively.

No cracking, spalling, or delamination of concrete were noticed in any spans which could be attributed to insufficient concrete cover. Severe cracking and spalling of



concrete at ends of post-tensioned girders was due to corrosion of anchor plates. The way to eliminate this type of cracking is to protect anchor plates from chloride-laden water penetrating into girder depressions through the mortar cover.

### **Potential Survey**

A potential survey conducted on Girder 1, Span 39 showed the lowest potential reading was -0.25 V CSE. This value was measured at a distance of about 1 ft from the end of the girder. Starting at approximately 6 ft from the girder end, all readings on both sides over top and bottom tendons were positive, indicative of extremely dry concrete.

After obtaining these readings, a decision was made to limit the potential study to end portions of a girder only. The number of girders surveyed was 6, all located in Span 39.

It was noticed that in almost all cases readings were positive at approximately 1.5 ft (0.46 m) from the end of a girder. Of a total of 90 observations for all girders, the percent of readings less negative than -0.20 V CSE was 69, with the rest lying in the range of -0.20 to -0.35 V CSE.

This pattern of distribution of potential readings can be explained by several reasons: a) higher amount of conventional reinforcement in end areas, b) low concrete cover over steel plates and stirrups, about 1.5 in. (38.1 mm) as compared with up to 7 in. (177.8 mm) over prestressing tendons, and c) relatively high moisture content of concrete at anchorages due to constant supply of water from expansion joints. By breaking out chunk samples and subsequent overdrying, it was determined that moisture content of concrete in the end area of a typical girder was 2.8 percent compared with 1.6 percent in the middle of the same girder.

It appears that in post-tensioned girders the potential survey is not a reliable method for assessment of corrosion activity on the surface of prestressing reinforcement.

## **Summary**

The presence of fractured tendons was indicated by loud noise generated during failure, by loose ends projecting from the end of a girder, loose end nuts displaced from their original location, and by cracking and spalling of the mortar cover over anchorages:

- Failure was attributed to chlorides entering anchorage zones and moving inside unbonded ducts between a steel rod and a sheath.
- Girders with fractured tendons were subsequently externally posttensioned.
- Condition of examined steel surfaces in exposed tendons and high chairs suggest the penetration of chloride ions through concrete cover and through a duct was very unlikely.
- No evidence of corrosion was noticed on the surface of a typical prestressing seven-wire strand, except for moderate corrosion at the ends covered with mortar.
- No corrosion-related distress of concrete was noted in post-tensioned girders except for end areas adjacent to leaking expansion joints due to corrosion of steel anchor plates and to some extent corrosion of conventional reinforcement.
- The extent of corrosion of steel anchor plates varied from moderate to very severe. In some cases, the thickness of rust on the surface of steel plates was as much as 0.25 in (6.35 mm).
- Corrosion of anchorage systems occurred due to a high concentration of chlorides in combination with a sufficient amount of moisture to cause chloride ions to migrate to a depth of 3 in (76.2 mm).

- External tendons were detailed such that even when they were located next to leaking joints, it is very unlikely that chloride-laden water could have penetrated into the conduit to cause corrosion of the post-tensioned rod.
- The malfunctioning drainage system was largely responsible for accumulation of water on top of the deck with subsequent penetration of this water through leaking joints.
- It is possible that fracture in prestressing rods occurred due to hydrogen embrittlement.
- Concrete in viaduct girders is non air-entrained, has an estimated water-cement ratio of 0.50 to 0.60, and did not exhibit any signs of distress.
- The highest concentration of chlorides was found in areas adjacent to leaking joints. Concentration of chlorides at the level of reinforcement in both types of girders was negligible.
- The source of corrosion-inducing agents in girders of the viaduct was chloride-laden water coming from the deck through leaking expansion joints.
- No cracking, spalling, or delamination of concrete was noticed in any spans which could be attributed to insufficient concrete cover.
- The potential survey in this type of girder does not appear to be a reliable method to assess corrosion activity in prestressing tendons.
- There were two obvious drawbacks in this design of post-tensioned girders: (1) it does not allow the inspection of prestressing tendons, thus fractured rods may remain undetected creating a safety problem; (2) it allows a rather easy excess of chloride-laden moisture to the prestressing rods.

## THE GANDY BRIDGE

### **Bridge Description**

The Gandy Bridges, also known as Bridge No. 100068 and Bridge No. 100300 are located on US-92 over Old Tampa Bay in Tampa, Florida (figure 81). Bridge No. 100068 carrying westbound traffic and Bridge No. 100300 carrying eastbound traffic were built in 1954 and in 1967, respectively.

This study was concerned with Bridge No. 100068 only. The overall length of this bridge is 13,770.5 ft (4197.2 m). It consists of a total of 252 @ 48.0-ft (14.6 m) spans, 20 @ 72.0-ft (21.9 m) spans, 2 @ 74.0-ft (22.6 m) spans and 1 @ 86.5-ft (26.4 m) span. Elevation of the bridge above the water varies from 2 ft (0.61 m) at end spans to 45 ft (13.7 m) in the middle span.

A typical bridge superstructure is composed of precast prestressed I-shaped girders, transverse diaphragms and a cast-in-place conventionally reinforced deck slab. The superstructure is supported by cast-in-place bents resting on composite 20-by 20-in (508 by 508 mm) precast, prestressed piles. The maximum length of piles is 75 ft (22.9 m). Each pile is reinforced with a total of 20 @ 0.375-in (9.5 mm) diameter stress relieved strands. Each strand was prestressed to 14,000 psi (984 kg/cm<sup>2</sup>). The specified thickness of concrete cover over prestressing strands is 3 in (76.2 mm).

Bridge girders are prestressed with post-tensioned 1.125-in diameter high-strength alloy steel bars, each bar positioned in a 1.5-in diameter grouted corrugated metal duct. The total number of steel rods in 48 - and 72-ft long (14.6 and 21.9 m) beams is 4 and 6, respectively. Each bar is stressed to 100, 000 psi (7031 kg/cm<sup>2</sup>) and anchored in a 3.5 in. (89 mm) deep recess. All steel parts in a recess are painted with 2 coats of bitumen. Additional protection to steel bar ends is provided by filling recesses with portland cement mortar. Specified compressive strength of concrete in prestressed girders is 4000 psi (281 kg/cm<sup>2</sup>) at transfer of the prestressing force, and 5000 psi (352 kg/cm<sup>2</sup>) minimum at 28 days. An elevation and a cross section of a typical 48 ft (14.6 m) girder are shown in figure 82.

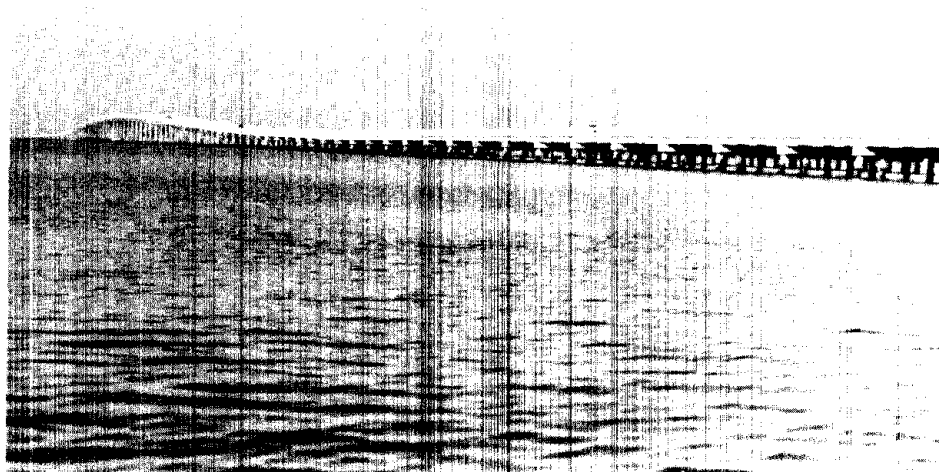
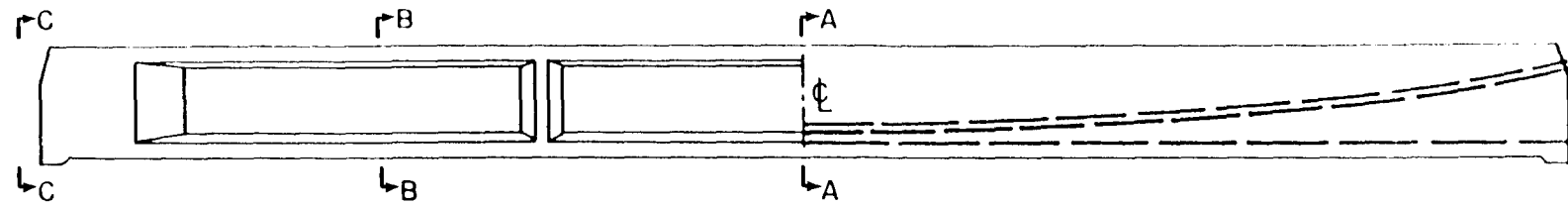


Figure 81. The Gandy Bridges.



DETAIL OF PRESTRESSED GIRDER

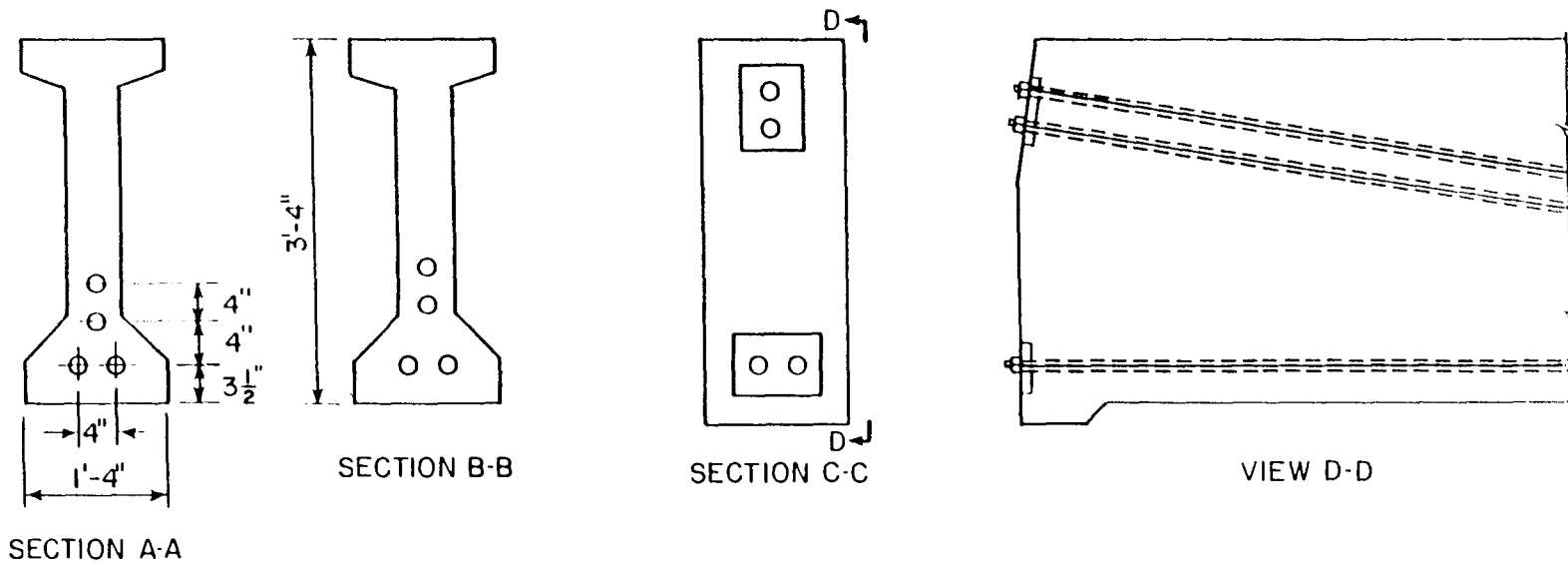


Figure 82. 48-ft Prestressed girder.

## **Visual Examination**

Visual examination was conducted to determine the type, extent and cause of deterioration in prestressed members, and to select areas for more detailed study. Visual examination was carried out on the entire bridge. Structures were examined by observing them from a boat moving along the bridge. Both sides of the bridge, the north and the south sides, were examined. After spotting a deterioration a brief study was made to describe it and to take measurements.

The most common types of deterioration observed in the bridge structure included extensive cracking and spalling of concrete cover over corroded tendons at flange, and in prestressed piles.

Cracking in prestressed beams was observed in two major areas: in beam webs and on the bottom side of beams. Cracks in beam webs were rather continuous and were located directly over draped reinforcing tendons (figure 83). Cracks appeared to be wider close to the bottom of the beam. Often these cracks could be traced over the full length of a tendon.

Cracks on the bottom side of beams were slightly different in appearance, they consisted of several short cracks and did not align with prestressing tendons (figure 84). The length of these cracks varied from 25 in (635 mm) to several feet. Cracks 7 to 9 ft (2.13 to 2.74 m) long were not uncommon. The distance between bottom side cracks was in the range of 4 to 5.5 in (102 to 140 mm). The widths of both, web and bottom side cracks varied from 0.03 to 0.13 in (0.76 to 3.3 mm), and on occasion up to 0.25 in (6.4 mm). In most cases cracks did not penetrate beyond tendons, but in some very severe cases they penetrated through the whole thickness of a web or a flange (figure 85).

Rust stains around cracks were not common and were noticed only in Beam 1, Span 274 (figure 86).

In most cases cracking was accompanied by spalling of concrete cover exposing a tendon to direct contact with salt water spray (figures 87 and 88). Spalling over web tendons appeared to be less severe than over bottom tendons. This, probably, happened because the thickness of concrete cover over top tendons was, in general, less

than that over bottom tendons. Normally, the width of spalls varied from 3 to 13 in (76 to 330 mm), occasionally reaching 16 in (406 mm) when spalling occurred over both bottom tendons. The length of spalls in the range of 6.3 to 7.9 ft (1.92 to 2.41 m) was not uncommon. Spalling was never less deep than the concrete cover over reinforcing tendons. Severe to very severe spalling was noticed in Beam 2, Span 2; Beam 2, Span 92; Beam 1, Span 122, Beam 2, Span 130; Beam 2, Span 135; Beam 3, Span 186; and Beams 1 and 2 in Span 274.

The pattern of deteriorations in relation to prevailing winds was less obvious in spans over deep water than in the end shallow water spans 2 and 274. In the end spans most concrete deterioration and steel corrosion had occurred in beams facing oncoming waves, that is in Beams 1 and 2. There was less or no deterioration in Beams 3 and 4, which were located further from the water. Observations made in end spans led to the conclusion that salt water spray, not water vapor, is the major carrier of chloride salts in an amount sufficient to cause corrosion of prestressing steel.

Cracks in prestressed piles were observed on all four sides, irrespective of the prevailing wind. In severe cases cracking was accompanied with stains of rust and spalling of concrete cover. Normally cracks were located parallel to the pile corners, running from a bent cap down under water. The length of cracks above the water level was in the range of 2.7 to 3.7 ft (0.82 to 1.13 m), the width varied from 0.06 to 0.5 in (1.5 to 12.7 mm). The number of cracks on the side of a pile was normally two or less. Figure 89 shows typical cracks in a prestressed pile. This figure also shows the remains of a fiberglass jacket used to isolate prestressing strands in the pile from direct exposure to the sea water and thus to eliminate the source of corrosion. The jacket was filled with epoxy based mortar and coated on top with an epoxy paint. The remains of this type of protection system was seen on other piles (figure 90). Based on the number of cracked and repaired piles observed during visual examination of the bridge, the extent of cracking of concrete cover in piles can be rated as severe to very severe. Similar cracks were observed in prestressed piles of the out-of-service Sunshine Skyway bridge, where the same type of piles were used (figure 91).



The beam ends were also examined for cracks, spalls, and rust stains. It was suspected that the salt water may have penetrated through the ends of beams into prestressing tendons and caused corrosion of steel rods. No corrosion related deterioration was noticed in these locations.

**Corrosion Survey.** Corrosion surveys were carried out visually on prestressing tendons in Span 92, 130, and 274.

Two types of corrosion were observed on rods: rather uniform surface corrosion and pitting corrosion. The surface corrosion was more common. The extent of surface corrosion varied from moderate (figure 92) to severe and to very severe with the thickness of corrosion in the range of 0.25 to 0.50 in (6.4 to 12.7 mm) (figure 93). Pitting corrosion was noticed in Beam 2, Span 92 only. The extent of pitting corrosion varied from moderate to severe with the depth of pits in the range of 0.04 to 0.12 in (1.0 to 3.0 mm).

Corrosion of tendons was more severe in shallow water end spans than in spans over deep water. In end spans, Beams 1 and 2, exhibited a higher extent of corrosion than Beams 3 and 4. The most severe corrosion was observed in Beam 2, Span 274, where the length of corroded tendon was 8 ft (2.44 m) (figure 94).

In almost all examined tendons a duct was found to be completely corroded. Because of corrugations there was generally a relatively good bond between the duct and the grout. No bond was noticed between the grout and the steel rod. As a rule, a duct would debond together with the grout. In some instances it was difficult to tell the difference between these two components. The thickness of grout varied from 0.20 to 0.25 in (5.0 to 6.4 mm). The grout was dense and sound. In all examined tendons the thickness of grout appeared to be rather thin compared to the diameter of a steel rod.

After cutting the steel rod from the fractured tendon in beam 2, Span 130 at 4 ft from the west end of the beam, the cross-section of the remaining duct was examined for the presence of voids. It was noticed that the steel rod was displaced to the top of the conduit and that about 50 percent of the cross-sectional area of the space between the steel bar and the conduit was not filled with grout.



Figure 83. Cracking of concrete cover over a top tendon.

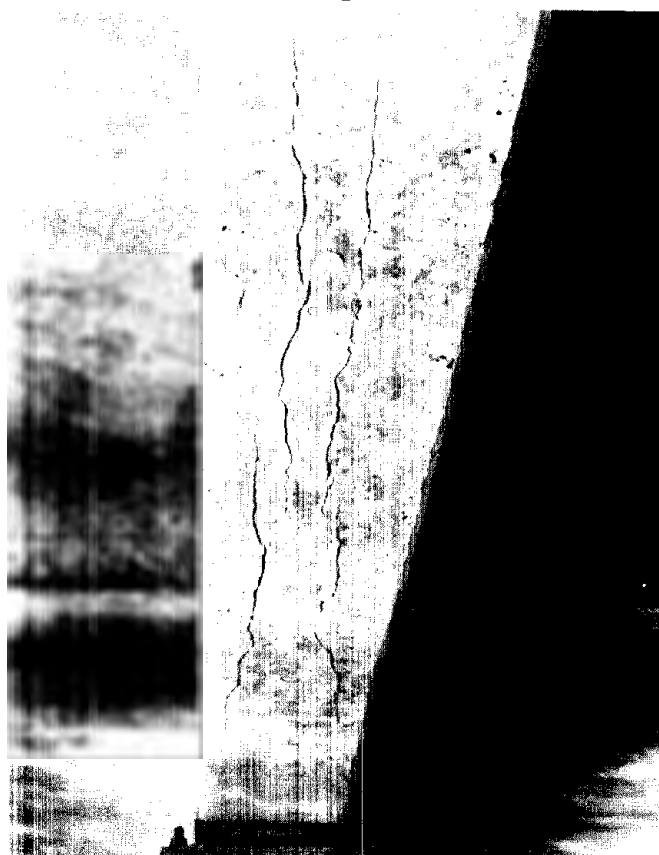


Figure 84. Cracks on the bottom side of a beam.



Figure 85. Cracking through the flange of a beam.



Figure 86. Rust stains around cracks in the bottom surface of a girder.



Figure 87. Spalling of concrete cover over a top tendon.



Figure 88. Spalling of concrete cover over the bottom tendon.



Figure 89. Typical cracks in a prestressed pile.



Figure 90. Remains of the protection system on prestressed piles.



Figure 91. Cracks in prestressed piles of out-of-service Sunshine Skyway Bridge



Figure 92. Moderate surface type corrosion.

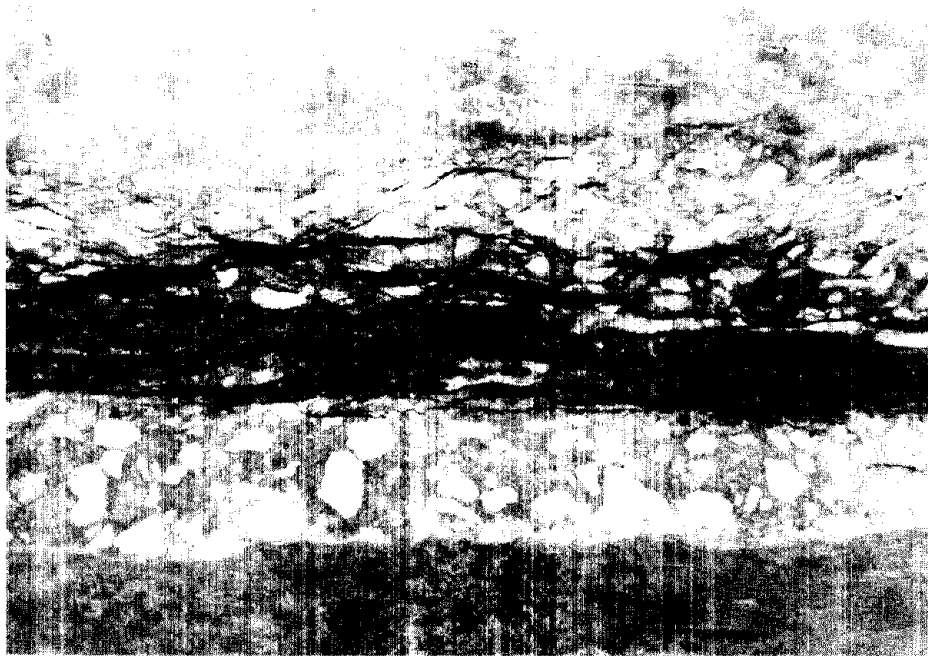


Figure 93. Very severe extent of corrosion of the prestressing rod.

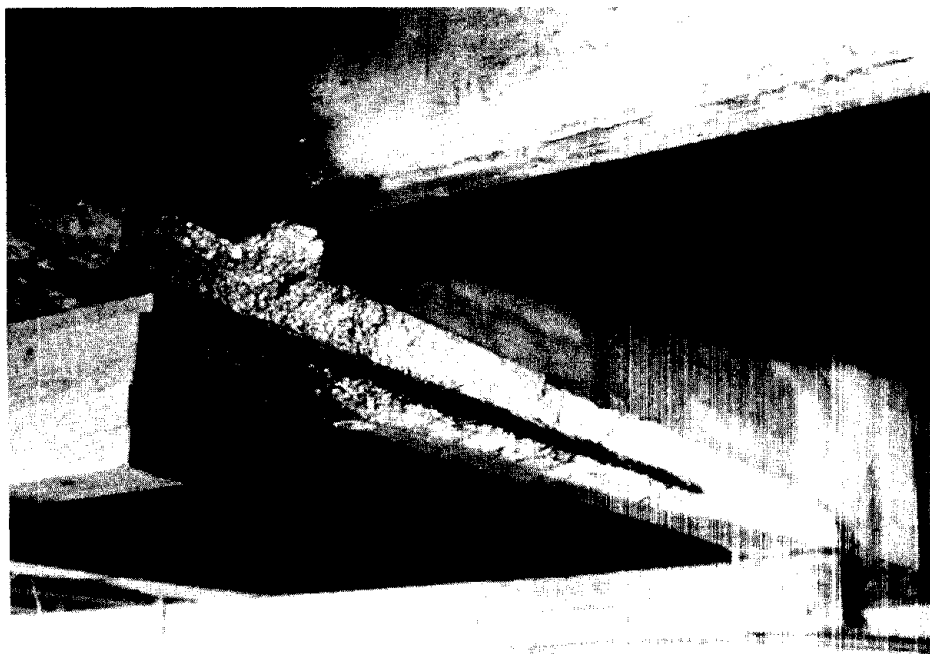


Figure 94. Severe corrosion of the prestressing rod in Beam 2, Span 274.

### **Delamination Survey**

Delamination surveys were conducted on Spans 2, 130 and 274. These were the spans selected for detailed evaluation. Some negligible delamination was noticed in Beam 2, Span 2 along the south bottom tendons and in the flange above this delamination. No delaminations were observed in other beams of this span. In Span 130 some delamination was noted in Beam 2 only, in areas of cracking and spalling of concrete cover over corroded tendons. In Span 274 moderate delamination was noted next to the exposed tendon. In general, delaminations in surveyed beams looked more like spalls, they were deep and small in areas. The beams without any visible signs of concrete deterioration did not exhibit delaminations.

### **Petrographic Examination**

Two concrete cores labeled G-3 and G-4 were petrographically examined to determine the nature of concrete materials and to evaluate the condition of concrete in situ. Core G-3 was obtained from the web of Beam 3, Span 274, at a distance of 17 ft from Bent 274. Core labeled G-4 was obtained from the bottom side of Beam 4, Span 130, at a distance of 11 ft (3.35 m) from Bent 131.

**Core G-3.** Coarse aggregate in concrete represented by Core G-3 is a crushed limestone having a maximum size of 0.75 in (19 mm). Coarse aggregate particles are beige to tan, moderately soft to moderately hard, somewhat porous to porous, angular, and spherical to prismoidal. Fine aggregate is a natural siliceous sand containing primarily quartz and a minor amount of feldspar. Fine aggregate particles are translucent, hard, dense, spherical, and well-rounded. Intermediate aggregate sizes, 0.375 in (9.5 mm) to No.8 appear low, but are compensated by finer sand sizes. The aggregate is uniformly dispersed. There is no evidence the aggregate has performed poorly in service.

Cement paste is light to medium gray, moderately hard, somewhat porous, and well-bonded to aggregate particles. Paste along freshly broken surfaces exhibits a vitreous to subvitreous luster, microgranular texture, and irregular fracture. Paste carbonation extends from the formed surface to 0.125 to 0.25 in (3.2 to 6.4 mm) depth.



Calcium hydroxide and residual cement particles are present in moderate amounts. Calcareous fines presumed to be derived as crushed fines from the coarse aggregate are moderately abundant. Water-cement ratio is estimated to be 0.40 to 0.50.

The concrete appears to be air-entrained due to presence of tiny, spherical voids. Air content is estimated to be 2 percent. The voids are uniformly distributed. Secondary deposits are not detected in voids or aggregate sockets. No evidence of deterioration is observed in concrete of this core.

**Core G-4.** Concrete represented by this core is similar to that in Core G-3, except for the amount of coarse and fine aggregates, which seems to be higher in Core G-4. Aggregate types and properties are similar to those in Core G-3. Intermediate sizes (0.375 in to No. 8) are somewhat low. The aggregate is uniformly dispersed. There is no evidence that the aggregate has performed poorly in service.

Cement paste is light gray, hard, slightly porous (less porous than in Core G-3), and well-bonded to aggregate particles. Paste carbonation extends from the formed surface to 0.375 in (9.5 mm) depth. Paste along freshly broken surfaces exhibits a vitreous to subvitreous luster, microgranular texture, and irregular fracture. Residual cement particles, calcium hydroxide, and calcareous crushed fines are moderately abundant. Water-cement ratio is estimated to be 0.40 to 0.45.

Due to presence of numerous, microscopic voids, the concrete is judged to be air-entrained. Air content is estimated to be 3.5 to 4.5 percent. Voids are uniformly distributed. Secondary deposits are not detected in voids or aggregate sockets. No evidence of deterioration is observed in concrete of this core.

Based on results of petrographic examination it can be concluded that concrete represented by the two cores is of good quality without any evidence of distress. Concrete is air-entrained and has a low water-cement ratio. Concrete represented by Core G-3 is judged to have a higher permeability than that represented by Core G-4, although both concretes appear to be of relatively low permeability.

### **Concentration of Chlorides**

A total of 14 samples were obtained from girders of the bridge to determine concentration of chlorides in concrete at various depths. Description of test locations and test results are shown in table 14.

Table 14. Concentration of chloride ions.

Sample No.	Span No.	Beam No.	Location No.	Depth in.	Cl ions %
6	2	1	10	0-0.5	0.316
7	2	1	10	1-1.5	0.167
8	2	1	10	1.5-2	0.094
10	2	3	12	1.5-2	0.073
15	130	1	13	1-1.5	0.018
16	130	1	13	1.5-2.25	0.018
11	130	2	14	0.-0.5	0.417
12	130	2	14	1-1.5	0.443
13	130	2	14	1.5-2.25	0.319
1	274	1	15	0-0.5	0.305
2	274	1	15	1-1.5	0.043
3	274	1	15	1.5-2	<0.018
4	274	2	16	1.5-2	0.046
5	274	3	17	1.5-2	0.018

There was not much difference in concentration of chlorides between external and internal beams in the middle and in end spans. The concentration of chlorides in the top surface of concrete cover was approximately the same in all tested beams, varying from 0.305 to 0.318 percent in the end span beams to 0.417 percent in Beam 2, Span 130. At the level of reinforcement, the concentration of chlorides was also rather uniform

varying in the range of 0.018 to 0.094 percent, irrespective of span location. An unusually high concentration of chlorides was found in Beam 2, Span 130, where it reached 0.319 percent.

### **Rapid Chloride Penetration**

Determination of the rate of chloride permeability was carried out on the same specimens used for petrographic analysis. Test results shown below indicate concrete Core G- 3 is more permeable than Core G-4.

Table 15. Rapid chloride permeability in core G-3 and core G-4.

Sample	Charge Passed (coulombs)	Permeability (per AASHTO T277)
G-3	2616	Moderate
G-4	1164	Low

### **Concrete Cover Study**

A survey of concrete cover was conducted on two beams in Span 2, on two beams in Span 130, and on two beams in Span 274. In addition, concrete cover was measured in areas of exposed prestressing tendons during visual examination. Readings were taken on north and south sides of the beam over top and bottom tendons, and also on the bottom side of the beam over bottom tendons.

As in previous investigations, prior to determining the thickness of concrete cover, the R-meter was calibrated against direct measurements in areas of exposed tendons. Results of the survey are shown in table 16.

Table 16. Concrete cover (inches) over prestressing tendons.

Span No.	Girder No.	Location Ft.	Top tendons		Bottom tendons				
			NS	SS	NS	SS	BNS	BSS	
2	2	36(EE)	-	-	5.75	6.75	1.75	2.00	
2	3	8(EE)	1.75	1.75	6.00	6.75	2.25	2.25	
2	3	19(EE)	-	2.75	5.50	6.50	1.75	1.65	
2	3	27(EE)	1.25	2.25	5.25	7.25	1.50	1.50	
2	3	36(EE)	1.50	1.75	5.75	6.75	1.50	1.50	
92	2	24(WE)	-	-	-	-	1.75	-	
122	1	-	-	-	-	-	1.50	2.75	
130	1	2(WE)	-	-	6.25	6.00	2.25	2.00	
130	1	4(WE)	-	-	6.00	6.25	2.25	2.25	
130	1	6(WE)	-	-	5.75	6.00	1.75	1.75	
130	1	8(WE)	-	-	5.00	6.50	1.50	1.75	
130	2	4(WE)	-	-	6.00	5.75	2.05	2.15	
130	2	5(WE)	-	-	6.00	6.00	2.00	-	
130	2	6(WE)	-	-	6.00	-	1.75	-	
130	2	8(EE)	2.75	2.25	6.00	6.00	2.50	2.00	
130	2	16(WE)	-	-	-	-	-	1.75	
130	2	19(EE)	2.50	2.50	6.00	6.00	2.50	2.50	
130	2	27(EE)	-	2.50	5.50	5.75	2.50	2.50	
274	1	4(WE)	-	-	-	5.00	-	3.50	
274	1	10(WE)	-	-	-	6.50	-	2.25	
274	1	17(WE)	-	-	5.00	-	1.50	-	
Minimum	1.25	1.75	5.00	5.00	1.25	1.50	Maximum	2.75	2.75
6.25	7.25	2.50	2.50	Average	1.95	2.25	5.75	6.20	1.90
2.10									

Note: EF-East end; WF-West end; NS-North side; SS-South side; BNS-Bottom North side; BSS-Bottom South side.

Concrete cover on the bottom side of beams varied in the range of 1.25 to 2.5 in (32 to 64 mm), average being 2.10 in (53 mm). Second row tendons (from the bottom side of a beam) are better protected against corrosion. The average thickness of concrete cover in these areas is about 6.00 in (178 mm). The largest concrete cover measured on both sides of bottom tendons ranged from 6.25 to 7.25 in (159 to 184 mm). It should be noted that most corrosion-related deterioration of concrete was observed on the bottom side of beams, less in beam web areas, and none on both sides of bottom tendons. These observations suggest insufficient concrete cover is probably the major cause of corrosion of reinforcing tendons.

### **Potential Survey**

Potential surveys were conducted on Girders 1, 2, and 3 of Span 2, Girders 1 and 2 of Span 130, and Girders 1, 2, and 3 of Span 274.

The minimum, maximum, average, number of observations, and population standard deviation for each girder are shown in table 17. Percent of potential readings is given in table 18. It should be noted that these readings represent the extent of total corrosion activity in both steel ducts and rods.

Table 17. Potential readings in girders of Spans 2, 130, and 274.

Statistics	Span 2			Span 130		Span 274		
	G#1	G#2	G#3	G#1	G#2	G#1	G#2	G#3
Minimum	0.013	0.002	0.018	0.000	0.007	0.001	0.072	0.002
Maximum	0.234	0.452	0.274	0.143	0.423	0.502	0.466	0.288
Average	0.140	0.190	0.110	0.055	0.168	0.193	0.225	0.139
STD	0.047	0.127	0.057	0.038	0.106	0.133	0.089	0.067

Note: Results in the above table are negative values expressed in V CSE.

Table 18. Percent of potentials in girders of Spans 2, 130, and 274.

Range, V CSE	Span 2			Span 130		Span 274		
	G#1	G#2	G#3	G#1	G#2	G#1	G#2	G#3
Less negative than -0.20	88	57	95	100	68	53	45	82
-0.20 to -0.35	12	23	5	-	30	33	43	18
More negative than -0.35	-	20	-	-	2	12	12	-

Analyzing test results in tables 17, and 18, it is seen the most extensive corrosion of steel ducts occurred in Girders 1 and 2 of Span 274, less extensive in Girder 2, Span 2, and less in Girder 2, Span 130. There was not much corrosion activity in Girder 3, Span 2 and in Girder 3, Span 274. High percent of low potential readings in these girders can be explained by the fact these girders are not located above water.

It is interesting to note there appears to be less corrosion activity in Girder 1 than in Girder 2 in all inspected spans. This difference was especially noticeable in Spans 2 and 130. This may be because Girder 1 in all spans is less exposed to the splashing action of waves created by prevailing winds than Girder 2 in the same zone.

### **Metallurgical Examination of Prestressing Steel**

A sample rod for metallurgical analysis was obtained from the fractured tendon in Beam 2, Span 130 at 4 ft from the west end of the beam (figure 95) using a coring machine (figure 96).



Figure 95. Sampled tendon in  
Beam 2, Span 130.

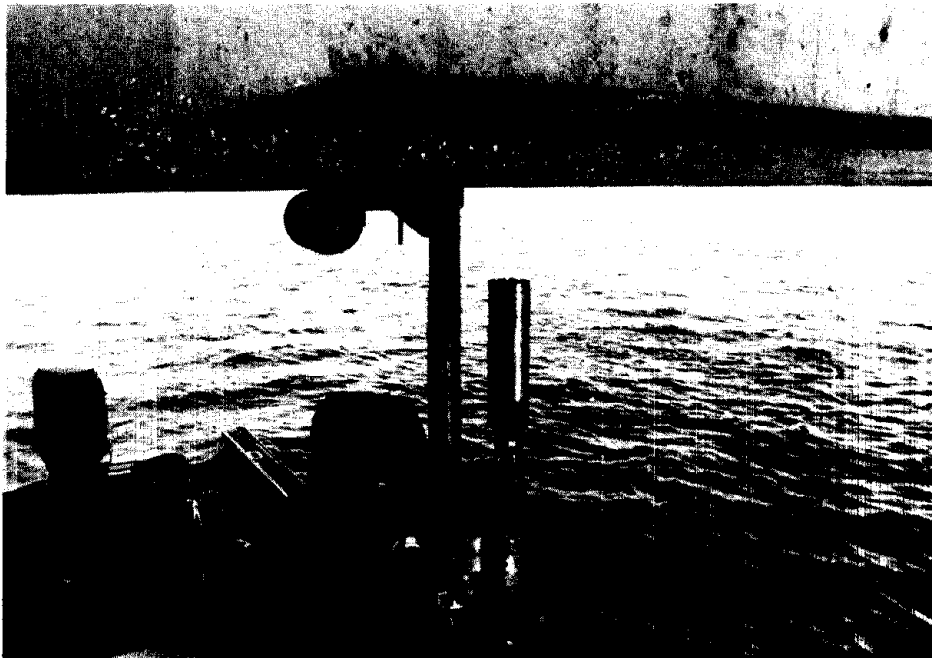


Figure 96. Obtaining a sample tendon using  
a coring machine.

**Visual and Macroscopic Examination.** The prestress rod was subjected to visual and macroscopic examinations performed with the aid of a stereoscopic microscope capable of magnifications up to 40X. These examinations revealed a uniform rust layer on all outside surfaces except at the sheared end (figure 97). The fractured end and the entire circumference displayed rust up to 0.125 in (3.2 mm) thick (figure 98).

Several areas were cleaned and measured to determine the diameter of the bar. Away from the fractured end, the diameter was found to measure 1.09 to 0.93 in (27.7 to 23.6 mm). No indications of defects or irregularities were observed on the bar such as cracks, laminations, or areas of concentrated corrosion. The fractured surface displayed the same rust deposit and interfered with characterization of the failure.

**Scanning Electron Microscope Examination.** The fractured end of the bar was cut to fit within the vacuum chamber of an SR-50 scanning electron microscope (SEM). A 15 Kv electron beam was used to examine the fractured surface at magnifications up to 20000X. Characteristic x-rays emitted by the examined areas were analyzed with the aid of a TN-5500 microprocessor system. Energy dispersion spectroscopy (EDS) techniques were used to obtain semi-quantitative chemical analyses. Examination were performed in both the as-received condition and after cleaning in a solution of inhibited hydrochloric acid in an attempt to remove the rust layer. These examinations could not characterize the mode of failure. The rust and oxidation were extensive and appeared to have completely consumed the original fractured surface. EDS analysis of the scale identified it to consist primarily of iron and oxygen, typical of rust. Small amounts of other elements were identified including sodium, aluminum, silicon, sulfur, chlorine, calcium, and manganese. The chlorine may act as an accelerator for corrosion or rusting. No evidence of any other unusual elements or conditions were identified during this testing. A typical EDS spectrum is shown in figure 99.

**Metallographic Examination.** Metallographic cross sections were taken to represent longitudinal and transverse directions from an area away from the fracture. A longitudinal section was taken also across the fracture. These sections were mounted in bakelite molds to facilitate grinding and polishing to a 0.05 micron finish. Examina-



tions were performed in both the as-polished and etched conditions using a metallurgical microscope capable of magnifications up to 2000X. Etching with a solution of 1 percent nital provided clear definition of the microstructures.

These examinations revealed microstructures typical of prestressing carbon steel bar. The structure consisted primarily of pearlite grains surrounded by ferrite. The outside surfaces of the bar displayed evidence of rusting and oxidation occurring in a pitting mode. On the fractured surface, the scale or rust was observed to be as extensive as that seen on the outside circumference. The oxidation penetrated the fractured surface preferentially along nonmetallic inclusions. No indications of deformation, dimples, embrittlement, or evidence of secondary fracturing was observed on the failed end of the bar. All the examined sections, including the fractured end, were free of inherent metallurgical defects or unusual conditions such as excessive inclusions, secondary cracks, lamination, intergranular corrosion, stress corrosion cracking, or evidence of improper handling or manufacturing techniques. Illustrations of the microstructures exhibited by the examined sections and rust are shown in figures 100 and 101.

**Tension Tests.** A round, reduced-section tensile test specimen was machined from near the center of the submitted bar. The sample was subjected to a standard tensile test performed in accordance with ASTM E8. Test results are shown below.

Tensile Strength, psi	157,000
Yield Strength, psi (2% Offset)	138,000
Elongation in 2 in., %	13.0
Reduction of Area, %	28.9

Based on the above tests and examinations, it is difficult to classify or determine a cause for fracturing of the submitted bar sample. Extensive rusting and oxidation has occurred on the circumference of the bar and on the fractured surface. This oxidation has destroyed the material which would provide evidence concerning the cause of

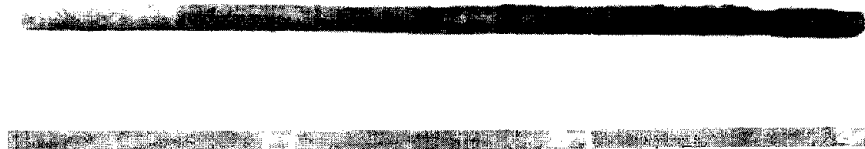


Figure 97. Visual appearance of the test prestressing rod.

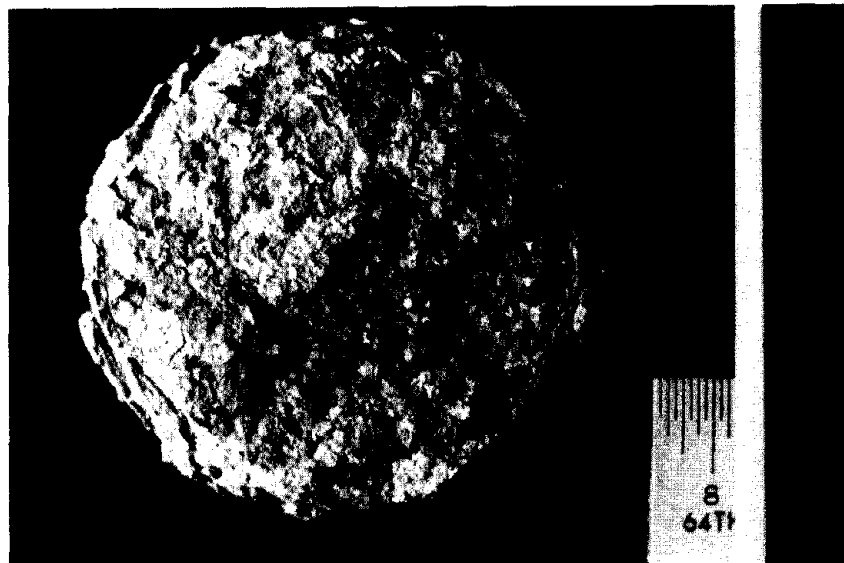


Figure 98. Extensive rust observed on the fractured surface of the rod.  
(Magnification: 3X.)

Cursor: 0 000keV = 0

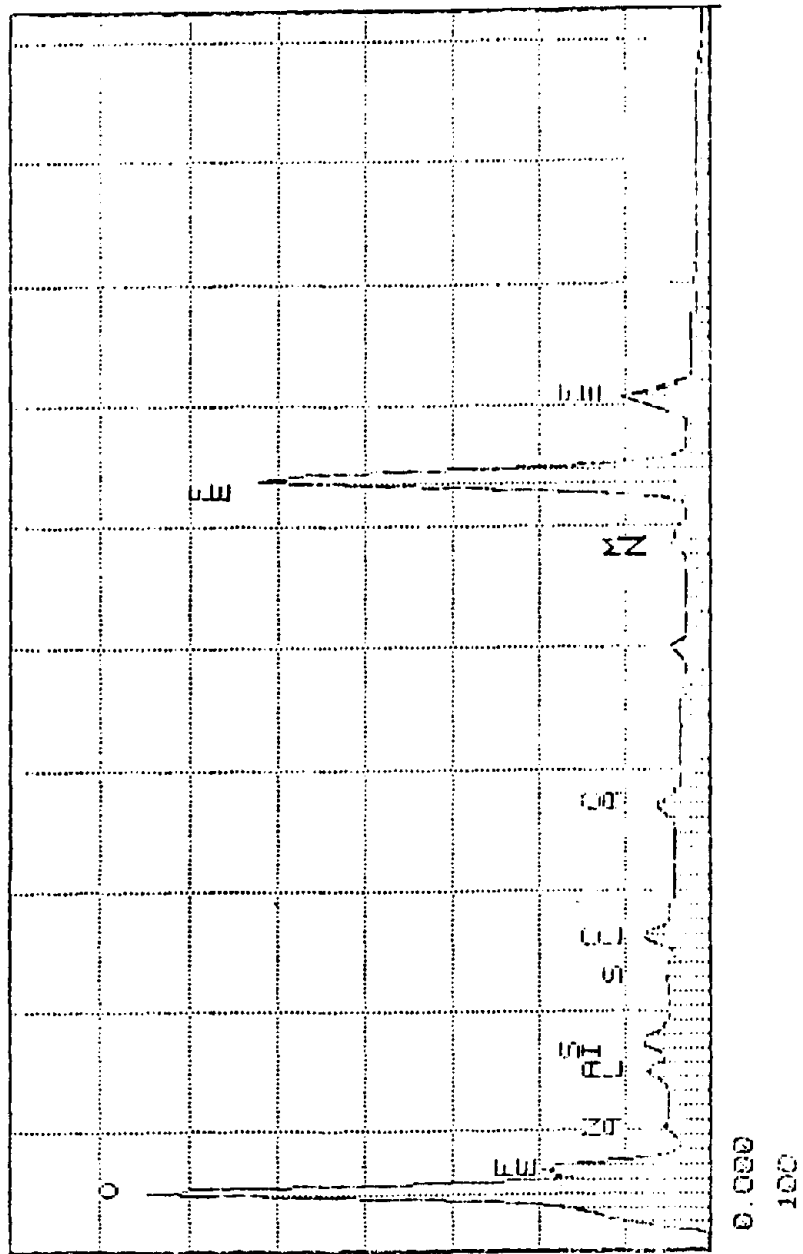


Figure 99. Typical EDS spectrum of rust.

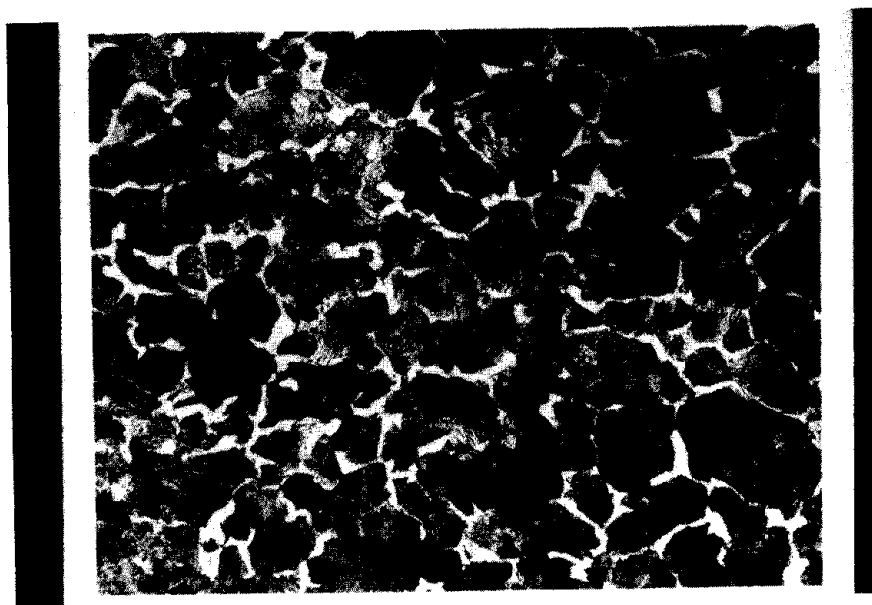


Figure 100. A typical example of the microstructure of pearlite and ferrite observed throughout the metallographic section.  
(Magnification: 400X. Etchant: 1% Nital).



Figure 101. Appearance of the metallographic cross section through the fractured end of the bar. (Extensive rusting can be observed in this section.  
Magnification: 50C).

failure. Tests and examination did not identify any significant defects or unusual conditions in the submitted bar.

Very little reduction in diameter was observed at the fractured end. If more reduction had been present at the fractured end, the failure may have been classified as a ductile overload. It appears the failure may have been more brittle in nature and may have resulted from an impact or sudden application of load. The extent of rusting on the fractured surface indicates that the failure may have occurred during construction or early in its service and is not likely to be a recent event. An impact load can cause rapid crack propagation with little material deformation. No evidence of any other failure modes such as stress corrosion cracking, or secondary fatigue cracks were identified in any of tests.

### **Summary**

- Observations made in end spans led to the conclusion that the water spray, not water vapor is the major carrier of chloride salts in an amount sufficient to cause corrosion of prestressing steel.
- Cracking of concrete cover in prestressed piles was observed on all four sides, irrespective of prevailing winds.
- Distress of concrete in girders and in piles was due to corrosion of the prestressing steel caused by chloride-laden water penetrating through concrete cover.
- Extent of corrosion on the surface of prestressing rods varied from moderate to very severe with the thickness of rust layer in the range of 0.25 to 0.50 in (6.4 to

12.7 mm). The extent of pitting corrosion varied from moderate to severe with the depth of pits in the range of 0.04 to 0.12 in (1.0 to 3.0 mm).

- Fiberglass jackets applied to bridge piles did not provide sufficient protection to the prestressing strands against chloride induced corrosion.
- Delaminations in prestressed girders were negligible. Girders without visible signs of concrete deterioration did not exhibit any delaminations.
- Concrete in the prestressed members of the bridge is of good quality and does not exhibit any evidence of distress. The concrete is air-entrained, and has a low water-cement ratio.
- Concentration of chlorides in the top surface of concrete cover and at the level of the reinforcement in all tested girders was approximately the same, except for Girder 2, Span 130, where it was found to be rather high.
- Rapid chloride permeability of concrete varied from low to moderate.
- Concrete cover on the bottom side of beams varies in the range of 1.25 to 2.5 in (32 to 64 mm), average being 2.10 in (53 mm) as compared with the specified value of 2.75 in (70 mm).
- The most extensive corrosion activity had occurred in girders exposed to the splashing action of waves created by prevailing winds.
- Because of extensive rusting and oxidation which occurred on the fractured surface of the bar, the cause of failure was difficult to classify. The failure appeared to be more brittle in nature than a ductile overload failure and may have resulted from an impact or sudden application of a load.

- Major factors that contributed to the extent of corrosion-related distress in prestressed bridge members were: exposure to direct action of the sea water, relatively high ratio of steel to concrete cross sectional area, insufficient concrete cover, permeability of concrete, and poor grouting.

## INTRACOASTAL CANAL BRIDGE

### **Bridge Description**

Intracoastal Canal Bridge is located on Padre Island Drive (figure 102). The bridge was constructed in 1972. Overall length of the bridge is 3280 ft (1000 m). It consists of 36 prestressed beam spans each 80 ft (24.4 m) long and a post-tensioned 400 ft (13.1 m) segmental box girder unit in the middle of the bridge (figure 103). A typical pretensioned beam span is comprised of a total of seven I-shaped precast pretensioned beams supported by cast-in-place piers, end diaphragms, prestressed 3.5-in (106.7 mm) thick deck panels between beams and a 4.25-in (108 mm) thick cast-in-place deck slab on top of the prestressed panels (figure 104). Precast prestressed beams were designed in accordance with AASHO 1969 Standard and Interim Specifications for Highway bridges.

The beams are prestressed with Grade 270 seven wire stress relieved deflected strands with a nominal diameter of 0.5 in (12.7 mm). All prestressed beams regardless of a span position have a total of 26 strands. Specified minimum 28-day compressive strength of concrete in prestressed beams was 6,300 psi (443 kg/cm<sup>2</sup>). The stress in strands was released when concrete gained minimum 5,300 psi (373 kg/cm<sup>2</sup>).

The segmental box unit is comprised of a total of 40 post-tensioned match-cast segments placed by the balanced cantilever method starting from two single piers. Each segment is provided with web shear keys to allow transverse alignment and to temporarily transfer shear stresses during construction. The segments are glued with an epoxy resin to lubricate their surfaces, to properly match adjoining segments, and to provide water tightness and durability at the joints. The superstructure was erected by





Figure 102. Intracoastal Canal Bridge.



Figure 103. Post-tensioned segmental box girder unit.

first, stressing temporary top tendons, and then, after end box girders had been placed, the whole unit was prestressed with the bottom permanent tendons. The bottom tendons consist of a grouted semi rigid conduit with a total of 3 seven-wire 0.5-in (12.7 mm) diameter stress-relieved strands.<sup>(49, 50)</sup> Prestressed panels were placed between pretensioned I-shaped girders to serve as permanent forms during construction and as part of a composite deck slab later during service life. A typical prestressed panel is reinforced with a total of 24 seven wire strands spaced at 4.25 in (108 mm), having a nominal diameter of 0.5 in (12.7 mm). The thickness of concrete cover over the strands from the bottom surface of a panel is 1.75 in (44.5 mm).

### **Visual Examination**

Bridge spans were visually inspected for wet spots, rust stains, cracking and spalling of concrete cover, as well as the presence of the exposed prestressing steel. Photographs were taken to record the condition of the bridge. Special attention was given to areas adjacent to leaking joints and drains. Regardless of the source of chlorides, it was expected that corrosion of steel and corrosion-related deterioration of concrete would be more pronounced in these areas because of more favorable conditions for steel corrosion to occur due to a supply of moisture.

**Concrete Cracking.** Concrete in prestressed beams appeared to be in a good condition. No cracks were noticed in beams except for beam ends adjacent to expansion/contraction joints at transition bents separating pretensioned spans from segmental box spans. Cracks were located above a top row of prestressing strands (figure 105) and in the bottom corner of a beam (figure 106). The length of cracks varied from 5 to about 13 in (127 to 330 mm). This type of crack was observed in approximately 50 percent of all such beams. The most probable cause of this cracking was corrosion of prestressing steel due to chloride-laden moisture penetrating through the joints. Because of the lack of access to these areas no further study was conducted.

No concrete deterioration was noticed in prestressed planks between pretensioned beams.

Severe cracking was observed inside segmental boxes in Spans 19 and 21. Cracks were located over top prestressing tendons on both the north and the south side of a box. A total of 12 cracks were found in 10 segmental boxes of Span 21. They began at about 5 to 6 in (127 to 152 mm) from an anchorage and propagated parallel to the prestressing force to an upper corner of a segmental box (figure 107). Length of a typical cracks was about 4.5 ft (1.4 m). The most probable cause of cracking was excessive tensile stresses developed in concrete by the concentrated forces during prestressing operations. Normally, these stresses occur when the transverse reinforcement is not designed properly or is not placed according to the design.<sup>(51-53)</sup> The visual examination conducted in June 1972 showed most of these cracks were noticed during or soon after construction. All cracks detected during the survey were repaired with an epoxy resin paste (figure 108). Because of the lack of access to external surfaces of segmental boxes, it was impossible to determine if these cracks existed on both sides of prestressing tendons or were limited to internal surfaces only.

**Drains.** The drain system of the bridge consists of a 4-by 6-in drain with a 0.75 in (19.1 mm) drip bead around a drain and a continuous 0.75-in (19.1 mm) drip bead along an end beam on both sides of each span except for spans over roadways (figure 109). Traces of water running down a beam side adjacent to a drain hole were noticed in almost all spans. No evidence of corrosion-related deterioration of concrete was noticed in these areas.

It should be noted this type of bridge drain is common in the vicinity of Corpus Christi. To install just a drain without a drain pipe is probably sufficient in this environment, but obviously would create a serious problem in a deicing salt environment.

One advantage of this drain system is there is no danger of accumulating water on the surface of the deck in areas of drains. Also, drains are located sufficiently far from expansion/contraction joints not to cause corrosion of reinforcing steel with subsequent corrosion-related deterioration of concrete in adjacent bridge components.

**Deck Surface.** Deck surface was examined for cracking and spalling that would make it permeable to water. Numerous map cracks and transverse hairlines were observed spaced at about 4.5- 5 ft (114-127 mm). No signs of moisture or salt deposits were present on the bottom surface of the deck panels, but were visible on both sides of a span on the bottom surface of a cast-in-place deck slab. Apparently, these cracks propagated through the cast- in-place deck slab only, without affecting precast prestressed planks.

**Joints.** Joints over all bents are armored joints filled with a preformed joint sealer. The joint sealer is a vulcanized elastomeric compound with a polymerized chloroprene as its basic component. The sealer was placed in a continuous extruded strip. No signs of water penetrating through joints over bents were noticed during a visual examination of the bottom surface of spans. All joints over bents were found to be in good condition (figure 110), except for joints at transition bents. The joint sealer in these joints became loose and later was removed (figure 111). As mentioned previously, this was the only location where concrete cracking due to corrosion of prestressing strands had occurred.

Joints in the segmental box unit were inspected for wet spots, bond, and matching. No signs of moisture penetrating through a joint was noticed. There was a good bond between the epoxy compound and concrete in areas of joints without any visible signs of distress. In general, matching between segments was adequate, except for two box girders S2 and S3 in Span 19. These box girders seemed to have a smaller cross sectional area than the rest of girders.

**Corrosion of Reinforcement.** No rust stains were observed in prestressed elements of the bridge except for minor stains due to corrosion of high chairs supporting strands in pretensioned girders.

During the survey, one seven wire strand was exposed in a top tendon of Box Segment 9, Span 21. The strand was located by observing cracks over tendons. The strand was found to be inserted in a preformed duct that later was filled with grout. The thickness of concrete cover over the exposed strand was about 5 in (127 mm). There was no corrosion observed on the surface of the strand. Concrete around the tendon

was dry, dense and appeared to be of good quality. The concentration of chlorides in the grout sample obtained from the area of the exposed duct at a depth of 5.5-6 in (140-152 mm) was 0.004 percent (Sample 13, table 19).

Two bottom ducts in Segment 9, Span 21 were exposed to determine the extent of corrosion of the sheathing and prestressing strands. The sheathing of the tendon was made of galvanized corrugated steel. A core obtained from concrete cover over these tendons had a good imprint of the sheathing, thus indicating that consolidation of concrete during manufacture of segmental boxes was adequate. No signs of corrosion were observed on the surface of the ducts (figure 112). The galvanized surface appeared to be bright, intact, and free from any evidence of corrosion. No signs of corrosion were observed on the surface of the strand (figure 113) that was examined after removing the duct. The interstices between strand wires were filled with grout. Both examined tendons appeared to be well protected against corrosion.

An anchorage system was exposed in Segment 9, Span 21 and examined for the presence and extent of corrosion. The anchorage system consisted of a 5-by 5-in (127 by 127 mm) steel plate and a total of 3 wedge type anchors (figure 114). The thickness of the steel plate was 2 in (50.8 mm). The ends of strands appeared to be cut with a torch. There were no signs of corrosion on the surface of any elements of the anchorage system. Grout surrounding the anchorage system was dry, dense, strong and did not exhibit any signs of distress, such as cracking or spalling. There was good bond between the grout and the surrounding concrete.

In general, it appears this design provides good protection against corrosion not only to prestressing tendons but also to the anchorage system.

### **Delamination Survey**

Delamination surveys were conducted on all prestressed beams in Spans 1, 3, 6, and 7, on prestressed Beams 1, 4, 6 and 7 in Span 39, and on post-tensioned box Girders S-1 through S-8 in Span 21. Delamination surveys in post-tensioned box girders were carried out on the north and south sides inside boxes. Neither prestressed nor

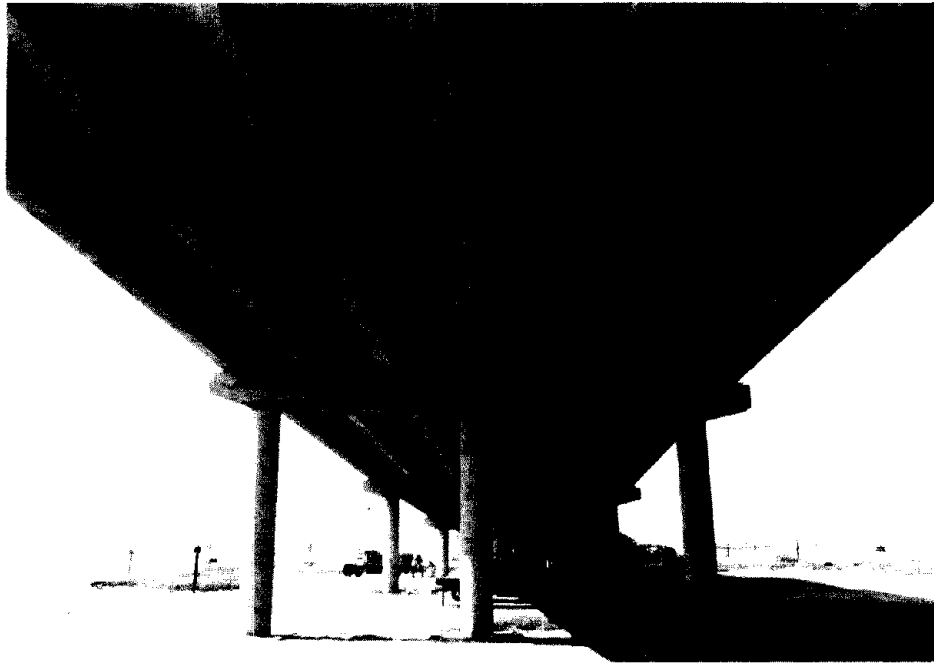


Figure 104. Typical pretensioned beam span.

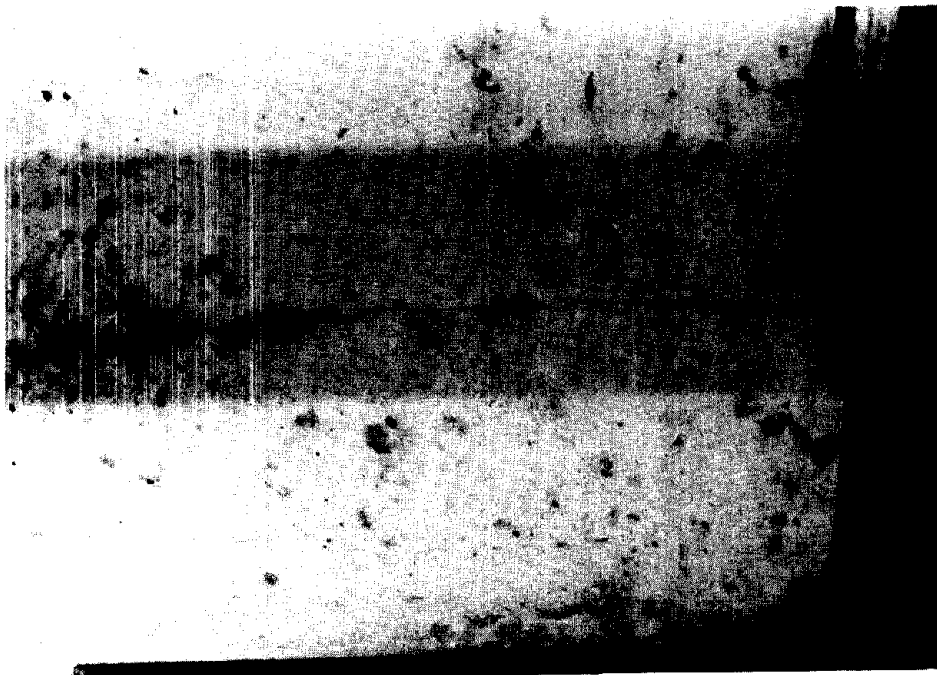


Figure 105. Crack in concrete cover above  
a top row of prestressing strands.

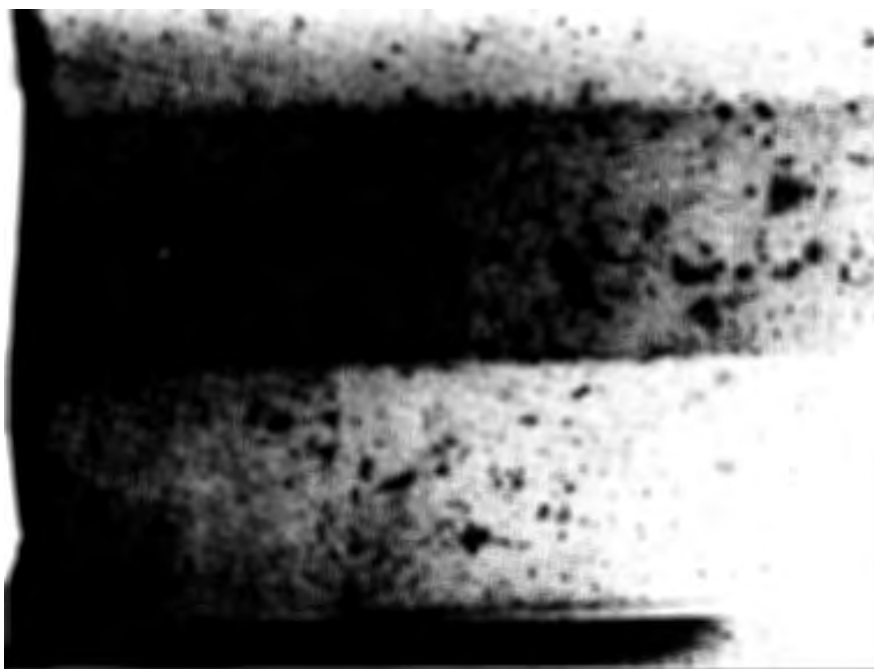


Figure 106. Cracking of concrete in the bottom corner of a beam.

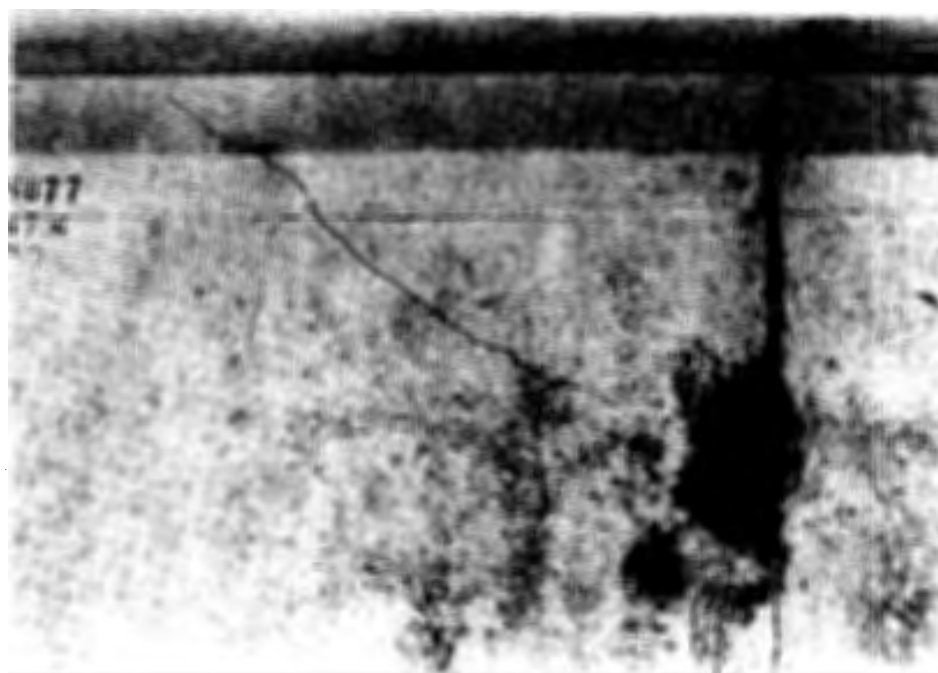


Figure 107. Severe concrete cracking inside segmental boxes.



Figure 108. Crack repaired with an epoxy resin paste.

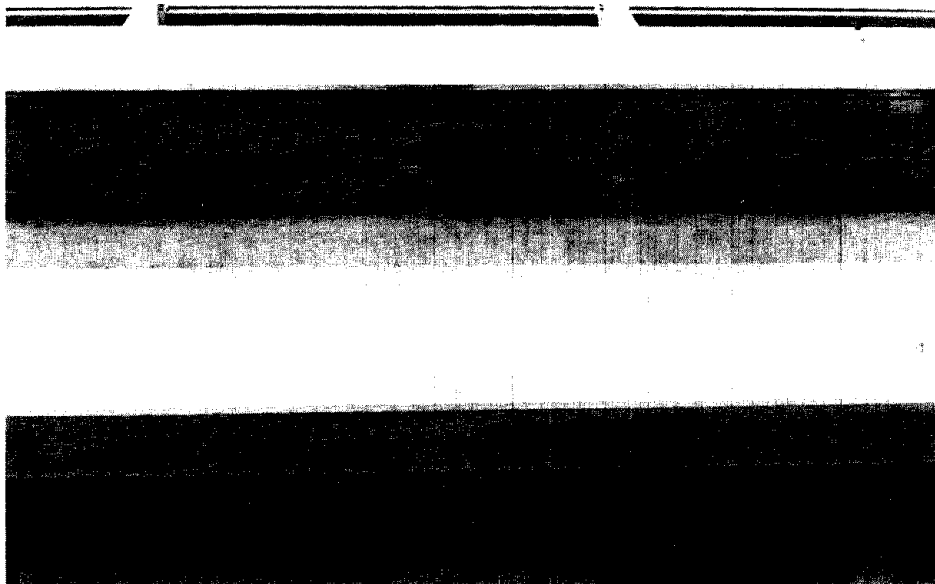


Figure 109. Typical span drain.



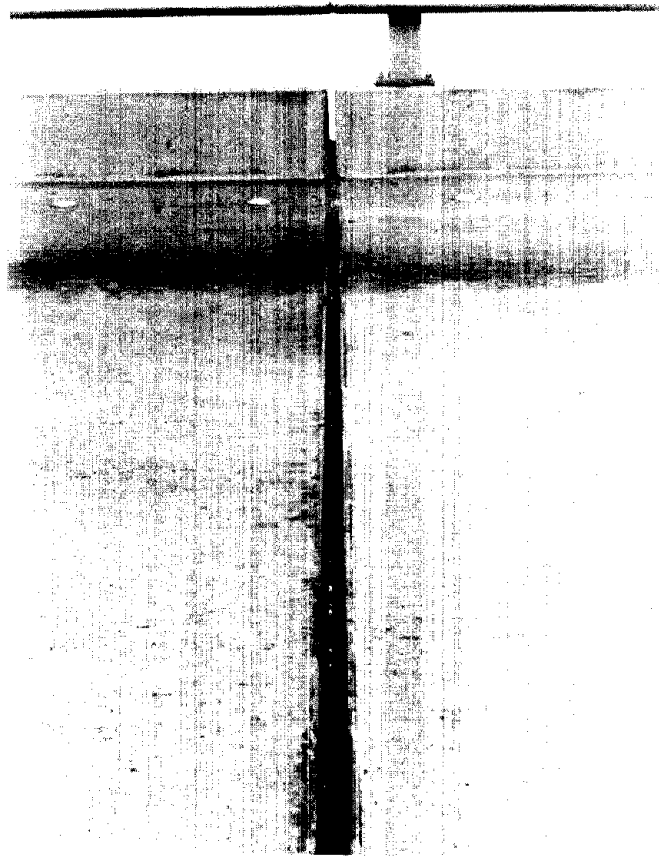


Figure 110. Typical expansion/contraction joint.

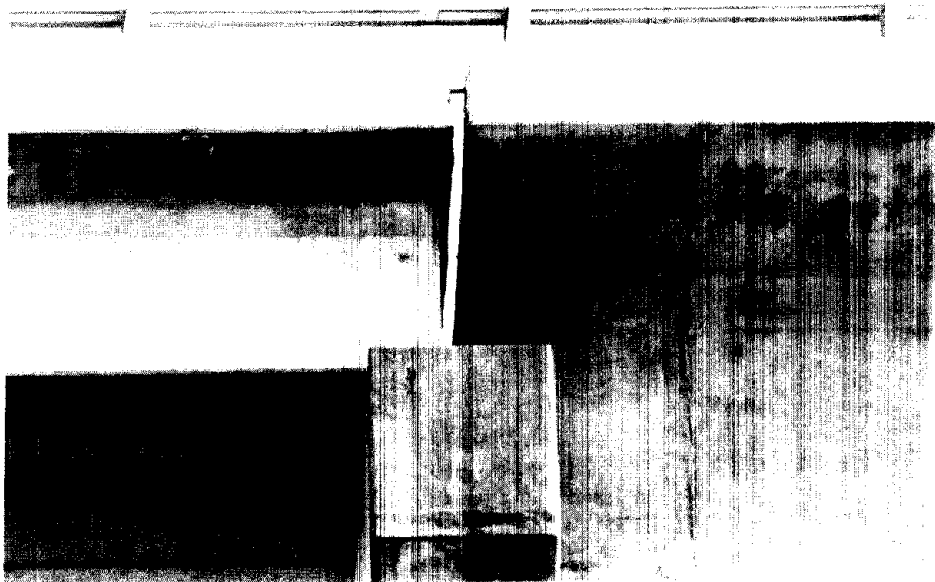


Figure 111. Expansion joint at the transition bent.

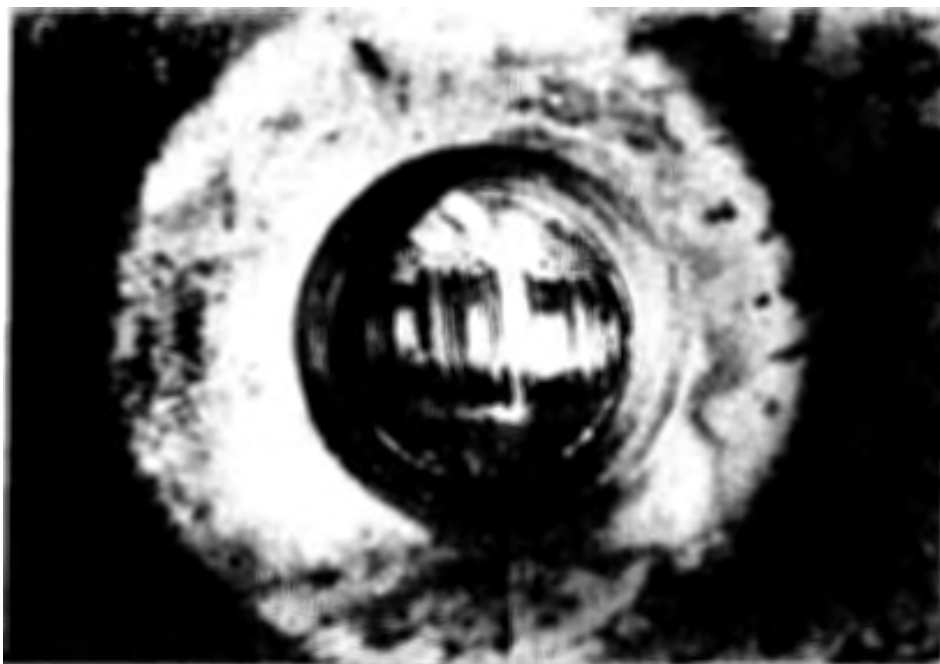


Figure 112. Condition of the sheathing  
in the bottom ducts.



Figure 113. Exposed seven wire strand.



Figure 114. Typical prestressing anchorage system.

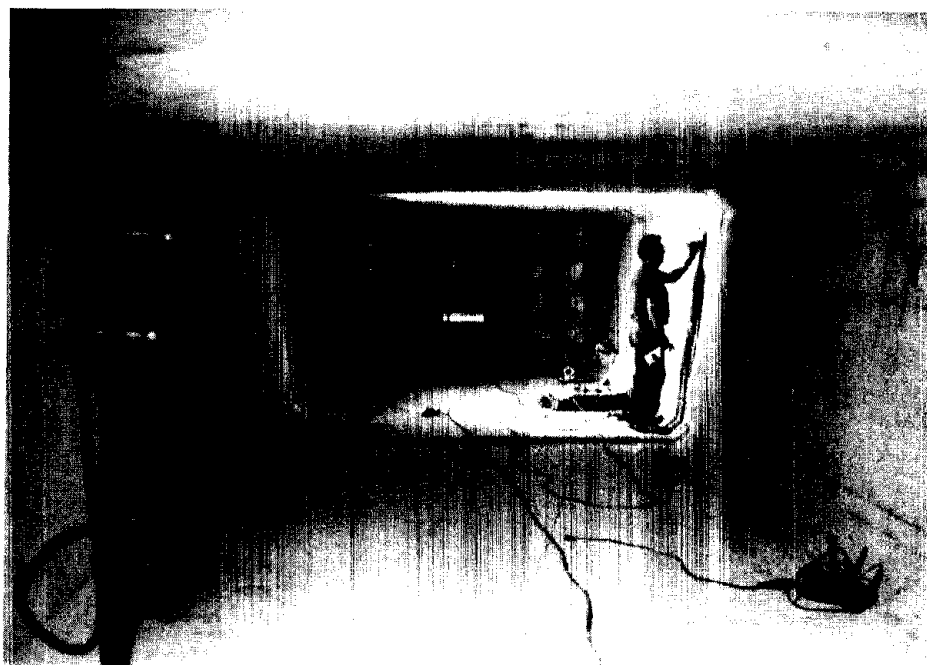


Figure 115. Potential survey on post-tensioned box girders in Spans 19 and 21.

post-tensioned girders exhibited any signs of delamination of concrete cover over the prestressing steel.

### **Petrographic Examination**

Cores labeled Beam 1 and Box S9 were examined. Core Beam 1 was obtained in Span 1 (West End), from pretensioned Beam 1 (North Side). Core labeled Box S9 was obtained from post-tensioned Box Girder 9, Span 21, counting from the West side of the bridge.

**Core Beam 1.** Coarse aggregate is a crushed limestone having a maximum size of 0.75 in (19.1 mm). Coarse aggregate particles are cream to light brownish gray, soft to moderately hard, porous to somewhat dense, frequently fossiliferous, angular, and spherical to less commonly prismoidal.

Fine aggregate is natural siliceous sand containing quartz, chert, chalcedony, feldspar, and less commonly limestone. Fine aggregate particles are variously colored, hard, dense, subrounded to well-rounded, and spherical. The aggregate is well-graded and uniformly dispersed. There are no indications that the aggregate has performed poorly in service.

Cement paste is light gray, hard, fairly dense, and well- bonded to aggregate particles. Paste along freshly broken surfaces exhibits a vitreous luster, microgranular texture, and irregular fracture. Paste carbonation is very slight, extending 0.03 in (0.76 mm) from the formed surface. Residual cement particles are present in moderate amounts. Calcium hydroxide is moderately abundant. Calcareous fines, presumed to be crushed fines derived from the coarse aggregate, are present in minor amounts. Based on interpretation of previously described paste properties, water-cement ratio is estimated to be 0.37 to 0.42.

There is no evidence of distress in concrete of the core. A few minor drying shrinkage cracks are observed along the formed surface. Random microcracks are also observed in interior portions of the core. The microcracks occur in the paste and pass around aggregate particles. The concrete is not air-entrained.

**Core Box S9.** Aggregate types, cement paste, composition, and properties of the cement paste are similar to those in the previously described core, although cement paste in this core is slightly darker.

Random microcracks are observed in interior portions of the core. As in the previously described core, these microcracks pass around aggregate particles, are present in minor to moderate amounts, and are not filled with secondary deposits. The microcracks could be due to minor drying shrinkage or thermal stresses.

The concrete is not air-entrained. Entrapped air content is estimated to be 0.5 to 1.0 percent. The few voids present are fairly large and subspherical to nonspherical.

Concrete in both cores appears to be of relatively low permeability. Neither of the examined cores exhibit evidence of progressive deterioration.

### **Concentration of Chlorides**

Ten concrete samples and 1 grout sample were obtained from the bridge and analyzed for concentration of chlorides. Test results are summarized in table 19.

Samples 1-4 were obtained from Girder 7 in Span 1 (West end of the bridge). The samples were obtained approximately in the middle of the girder at depths 0-0.5, 0.5-1.0, 1.0-1.5, and 1.5- 2.0 in (0-12.7, 12.7-25.4, 25.4-38.1, and 28.1-50.8 mm).

In general, the concentration of chlorides in pretensioned girders was low. It was lower closer to the reinforcement. The surrounding atmosphere is the only source of chlorides for the concrete of the bridge.

Even though the post-tensioned segmental unit is located directly over sea water, the concentration of chlorides in the concrete of this unit (Samples 8-12) was lower than that in the concrete of pretensioned girders. This may be because the post-tensioned unit has a higher elevation over the sea water where concentration of chlorides in the atmosphere is lower.

Table 19. Concentration of chlorides.

Sample No.	Bridge No.	Span No.	Girder No.	Depth in.	Cl ions %
1	1	1W	7M	0-0.5	0.078
2	1	1W	7M	0.5-1.0	0.071
3	1	1W	7M	1.0-1.5	0.026
4	1	1W	7M	1.5-2.0	0.012
8	1	21	S-8	0-0.5	0.037
9	1	21	S-8	0.5-1.0	0.011
10	1	21	S-8	1.0-1.5	0.003
11	1	21	S-8	2.0-2.5	0.003
12	1	21	S-8	4.5-5.0	0.003
13	1	21	S-9	5.0-5.5	0.004
14	1	39	1	1.0-1.5	0.003

The concentration of chlorides in the grout sample was negligible (Sample 14). The only source of chlorides in the grout was materials used to prepare grout. At the time this bridge was constructed, the adverse affect of chlorides on prestressing steel was well known.

#### **Rapid Chloride Permeability**

Test samples for rapid tests of chloride permeability were prepared by slicing cores obtained for petrographic analyses. The sections sawed off Core Beam 1 and Core Box S9 were designated B-1 and B-S9, respectively. Test results given in table 20 indicate the amount of charge transmitted during a 6-hour test varied from 1564 in

Sample B-1 to 2168 coulombs in Sample B-S9. These values correspond to low and moderate permeability, respectively, for concrete represented by these samples. In a highly corrosive environment the extent of protection provided by this concrete to the prestressing steel would probably vary from good to satisfactory.

Table 20. Rapid chloride permeability test results.

Sample No.	Location	Charge passed (coulombs)	Permeability (per AASHTO T277)
Core Beam 1	Beam 1, Span 1	1564	Low
Core Box S9	Box 9, North Wall	2168	Moderate

### **Concrete Cover Survey**

Concrete cover surveys were performed on all prestressed beams in Spans 1, 3, 6, and 7. Because of the lack of access, concrete cover in posttensioned box girders was not determined. The minimum, maximum, average, and the population standard deviation for each examined span are given in table 21. The specified concrete cover for prestressed beams is 2 in (50.8 mm).

Table 21. Concrete cover (inches) over prestressing strands.

Statistics	1	3	Span No. 6	7
MIN	1.75	1.88	1.75	1.63
MAX	2.25	2.13	2.25	2.00
AVG	2.08	2.00	1.93	1.94
STD	0.18	0.10	0.17	0.15
n	8.00	8.00	8.00	8.00

### **Potential Survey**

Potential surveys were conducted on prestressed beams in Spans 1 and 39, and on post-tensioned box girders in Spans 19 and 21. A total of 5 prestressed and 2 post-tensioned beams were surveyed. Prestressed beam potential readings were taken in a grid pattern at a spacing of 2 ft (0.61 m). In post-tensioned girders potential readings were obtained on the internal surface of the walls (figure 115).

The minimum, maximum, average, number of observations, and the population standard deviation for each girder are given in table 20.

Table 22. Half-potential readings in prestressed and post-tensioned girders.

Statistics	Girder No.						
	S1-B1	S1-B4	S1-B6	S1-B7	S39-B1	S-19W	S-21E
MIN	0.000	0.002	0.000	0.000	0.000	0.000	0.000
MAX	0.118	0.144	0.123	0.128	0.100	0.073	0.132
AVG	0.053	0.071	0.053	0.060	0.027	0.040	0.064
STD	0.034	0.032	0.028	0.038	0.018	0.032	0.033
n	78	136	132	96	75	55	40

Note: Results in the above table are negative values expressed in V CSE.

Analyzing these test results, it is seen maximum potential readings in all examined girders were less negative than -0.20 V CSE. Based on results of the potential survey it is concluded there is greater than 90 percent probability that no corrosion activity had occurred in any of the examined girders. This conclusion is in agreement with findings of the visual examination.



## **SHIP CHANNEL BRIDGE**

### **Bridge Description**

Ship Channel Bridge is located in Corpus Christi on Hwy 181 (figure 116). It was built in 1955. The bridge consists of precast prestressed and steel girder spans. A typical prestressed girder span is shown in figure 117.

The prestressing girder system is composed of a flexible 1.5-in. (38.1 mm) diameter metal conduit with enlargements at both ends, a 1.75-in (44.5 mm) thick bearing plate recessed flush with end of girder, and a total of 10 to 12 parallel prestressing wires anchored with Freyssinet type anchors. All conduits are filled with grout. Anchors and bearing plates are protected with cast-in-place concrete. Concrete cover from the bottom surface of a girder varies from 3 in (76.2 mm) in the middle to 6 in (152.4 mm) at the end of the girder.

### **Visual Examination**

Prestressed girder spans were examined at both ends of the bridge for signs of corrosion of prestressing steel and corrosion related deterioration of concrete. The presence of algae and mildew on the surface of girder ends, end diaphragms, and pier caps indicated that concrete in these areas was moist. No signs of salt deposits were observed in examined spans.

After visual examination of the bridge, more detailed study was conducted on Span 9 (counting from the North end of the bridge). Visual examination of this span revealed the presence of some minor spalling and cracking of concrete over conventional reinforcing steel bars and bearing steel plates at the ends of almost all girders in the span (figure 118). The extent of corrosion of steel bars and bearing plates varied from severe to very severe. A close examination showed the thickness of concrete cover over steel bars and steel plates did not exceed 1 and 0.5 in (25.4 and 12.7 mm), respectively.

The extent of corrosion in prestressing wires was evaluated on an exposed tendon, found in Girder 7 from the West side of the span (figure 119). This duct appeared

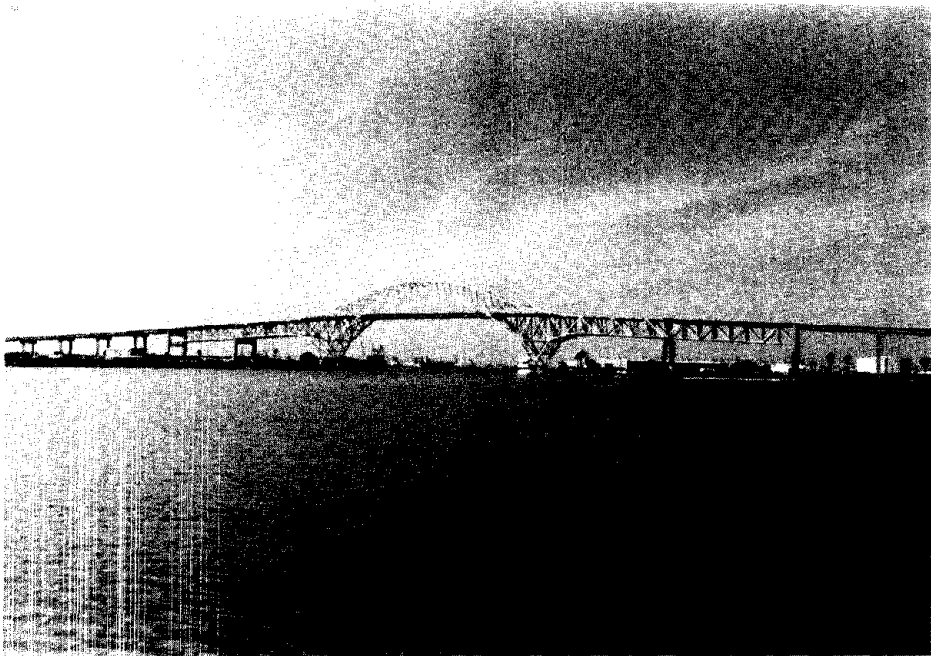


Figure 116. Ship Channel Bridge.



Figure 117. Typical prestressed girder span.

to be exposed from the time of construction of the bridge. There was a rather heavy layer of rust on the external surface of the duct (figure 120). Two wires exposed during sampling of the grout for chloride concentration did not exhibit any signs of corrosion (figure 121).

### **Chloride Concentration**

Three samples were obtained from Span 9 to determine concentration of chlorides. Test results are summarized in table 23. Sample 15, was obtained from the north end of Girder 2 (from the west side), above a corroded steel bar, at a depth of 1-1.5 in (25.4-38.1 mm). Sample 16 was also obtained from Girder 2, but in the middle of the girder. The depth of sampling from the bottom surface was 3.5 in (88.9 mm), at the level of the bottom post-tensioned tendon. Sample 17 was obtained from the grout in the exposed tendon.

Table 23. Concentration of chlorides in Span 9.

Sample	Cl ions %
15	<0.150
16	0.003
17	0.005

### **Concrete Cover Survey**

Concrete cover over conventional steel bars at the end of a girder, determined on three sides of the girder varied from 0.75 to 1.5 in (19.1 to 38.1 mm). Concrete cover over prestressed tendons was in the range of 2.25 to 3.5 in (57.2 to 88.9 mm). There was no delamination of concrete over conventional steel bars or over prestressing tendons. In general, concrete cover in prestressed girders appeared to be adequate.



Figure 118. Spalling of concrete cover over conventional reinforcing steel bars.

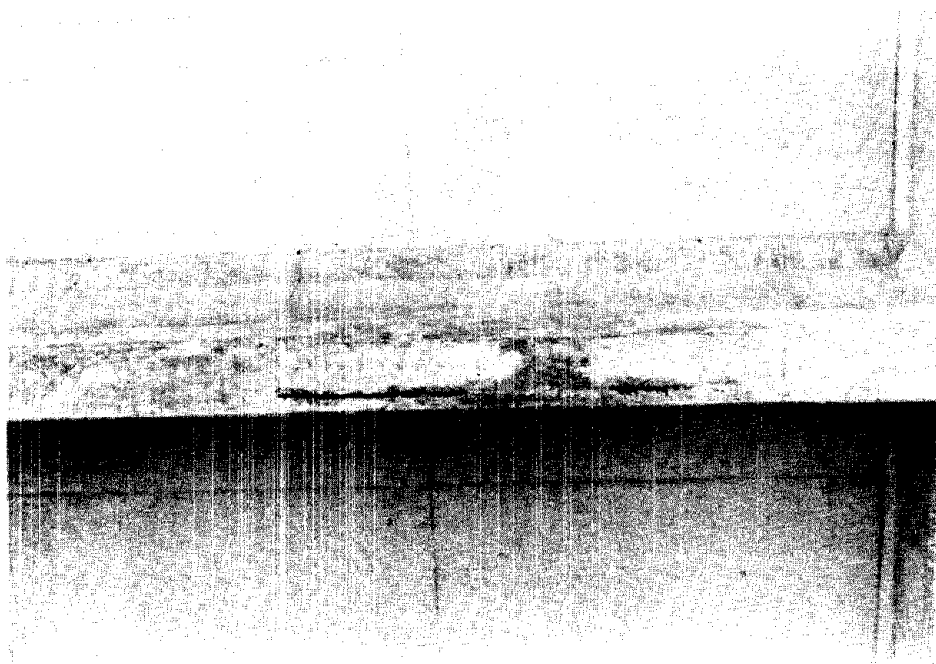


Figure 119. Exposed tendon in the bottom of Girder 7.

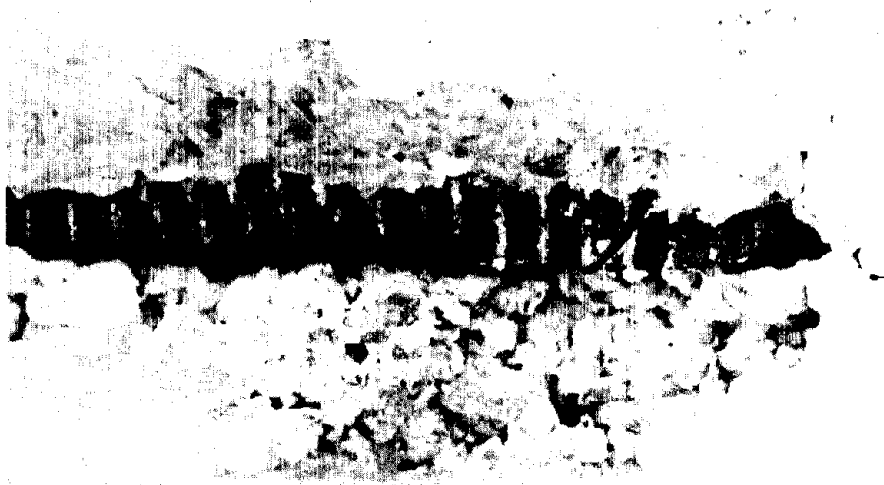


Figure 120. Heavy layer of rust on the surface of the tendon.



Figure 121. Condition of prestressing wires inside the tendon.

### **Potential Survey**

An attempt was made to determine the extent of corrosion in prestressing steel by conducting a potential survey. Within the length of 1 ft from the north end of Girder 2, potential readings were in the range of - 0.13 to - 0.23 V CSE. Further from the end, at approximately 3 ft (0.91 m) potential readings became less negative, about -0.03 V CSE. Apparently, negative potential readings at the end of the girder reflected the corrosion activity in conventional steel bars, which were located close to the surface of the girder. Based on results of the study it was concluded the possibility of corrosion in the prestressing steel in a typical span of the bridge was minimal.

## **NUECES BAY CAUSEWAY**

### **Bridge Description**

The Nueces Bay Causeway is located on Highway 181 (figure 122). The causeway was built in 1962. The total length of the causeway is 9,637 ft (2940 m). The overall width of a typical span is 31.3 ft (7.95 m). The causeway consists of two separate bridges, the south bound steel span bridge and the north bound prestressed beam span bridge. A typical section of the causeway consists of a cast-in-place 7.25-in (184.2 mm) deck slab, cast-in-place end diaphragms flush with beam ends, and a total of 4 precast pretensioned girders supported by a cast-in-place cap beam resting on precast prestressed piles (figure 123). Details of the reinforcement of a typical girder are shown in figure 124.

### **Visual Examination**

No corrosion-related deterioration of concrete was noted in prestressed elements except for some cracking of concrete cover in piles at the south end of the bridge. To determine the presence of the corrosive environment, special attention was paid to conventionally reinforced elements in areas of expansion joints. Since concrete in conventionally reinforced members is more permeable than in precast prestressed beams, it is reasonable to expect that corrosion of steel would occur first in pier caps and in diaphragms. Also, reinforced concrete in these areas is exposed not only to chloride-laden water vapor but also to chloride-laden moisture from the deck surface coming through leaking expansion joints. In addition, the presence of mildew and algae suggest that moisture content in the concrete in these locations was higher than in the rest of the bridge. Nevertheless, no signs of corrosion were observed in prestressed or in conventionally reinforced structures adjacent to expansion/contraction joints.

This observation suggests the atmosphere surrounding the bridge is not corrosive enough to cause corrosion of the reinforcing steel. This may be due to lack of a sufficient amount of chlorides, or moisture, or a combination of both.

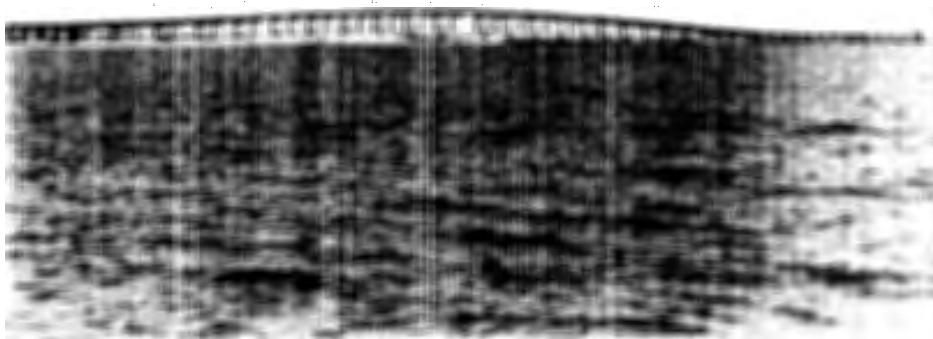
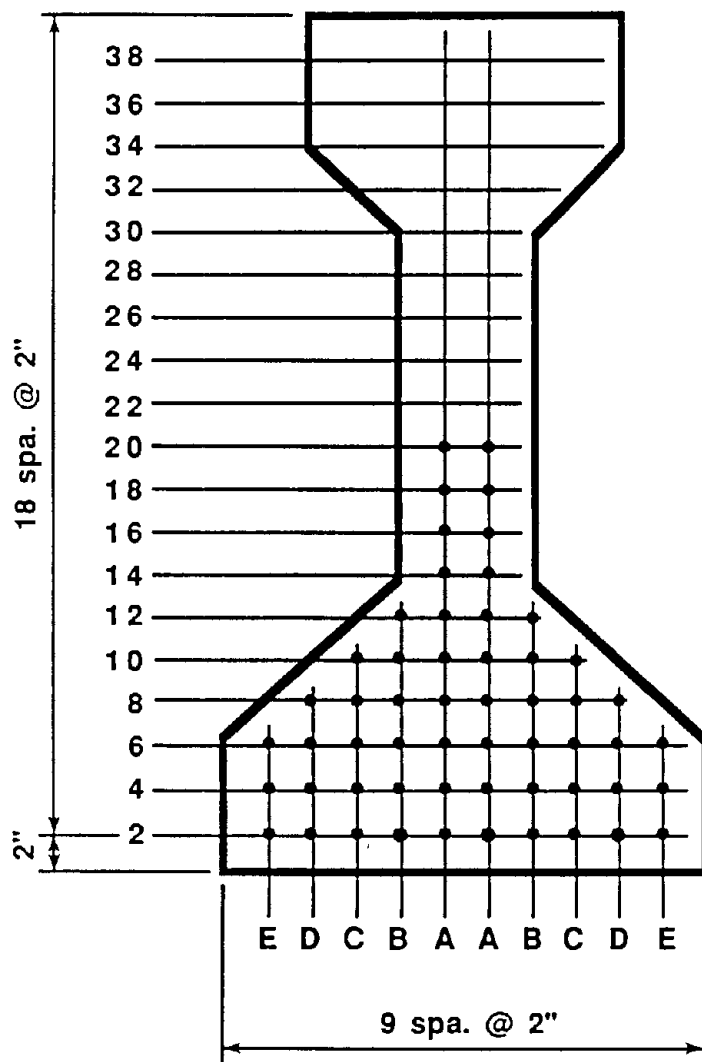


Figure 122. The Nueces Bay Causeway.



Figure 123. Typical prestressed girder span.





Q Section  
60 - 3/8"  $\varnothing$  Strands

Number of Strands	Position of Strands
10	A2 to E2
12	add E4
14	" D4
16	" C4
18	" B4
20	" A4
22	" A6
24	" E6
26	" D6
28	" C6
30	" B6
32	" A8
34	" D8
36	" C8
38	" B8
40	" A10
42	" C10
44	" B10
46	" A12
48	" B12
50	" A14
52	" A16
54	" A18
56	" A20
58	" A22
60	" A24

Figure 124. Strand patterns for prestressed concrete beams.

Much corrosion was noted in steel beams and cast iron piles of the south bound steel span bridge. The City of Corpus Christi has a permanent maintenance crew on the steel bridge, yet it still is difficult to keep it in good condition. Because of the high maintenance cost, the City is reportedly planning to demolish this bridge as soon as the prestressed concrete bridge is expanded.

### **Summary**

- The three bridges studied in Corpus Christi were:  
Intracoastal Canal Bridge, Ship Channel Bridge, and Nueces Bay Causeway.
- No cracks were noticed in beams of the Intracoastal bridge except for beam ends adjacent to expansion/contraction joints at transition bents separating pre-tensioned spans from segmental box spans.
- No concrete deterioration was observed in prestressed planks between pre-tensioned beams.
- Severe cracking was observed inside segmental boxes over top prestressing tendons, apparently caused by excessive tensile stresses developed in concrete during prestressing operations.
- The advantage of the drain system design used in the Intracoastal bridge is the lack of standing water on the surface of the deck, and especially in areas of expansion/contraction joints. The disadvantage of this drain system is that the storm water is allowed to run along the sides of adjacent beams.
- Cracks in the deck slab of the Intracoastal bridge propagated through the cast-in-place deck slab only, without affecting precast, prestressed planks.

- All joints over bents were found in good condition except for joints at transition bents. The sealer in these joints became loose and later was removed. This was the only location where concrete cracking due to corrosion of prestressing strands had occurred.
- No signs of moisture penetrating through joints in the segmental box unit were noted. There was good bond between the epoxy compound and concrete in areas of joints without any visible signs of distress.
- No corrosion was observed on the surface of the exposed strands neither in pretensioned girders nor in post-tensioned segmental boxes of Intracoastal bridge.
- Neither prestressed nor post-tensioned girders exhibited any signs of delamination of concrete over prestressing steel.
- Concrete in prestressed structures of the Intracoastal bridge is of good quality and relatively low permeability, without any evidence of progressive deterioration.
- In general, the concentration of chlorides in pretensioned and post-tensioned girders of the Intracoastal bridge was low.
- Permeability of concrete to chloride ions in the Intracoastal bridge varied from low to moderate.
- Concrete cover in pretensioned girders of Intracoastal bridge was slightly in excess of the specified value. Because of the lack of access, concrete cover in post-tensioned box girders was not determined.

- Based on results of the potential survey it is concluded that there is greater than 90 percent probability that no corrosion activity had occurred in girders of Intra-coastal bridge.
- No evidence of corrosion of the prestressing steel was noted in prestressed girders of the Ship Channel Bridge. The concentration of chloride ions at the level of prestressing tendons was generally low.
- Based on results of the study, it was concluded the possibility of corrosion in the prestressing steel in a typical span of the Ship Channel Bridge was minimal.
- No corrosion-related deterioration of concrete was noted in prestressed elements of the Nueces Bay Causeway except for some cracking of concrete cover in piles at the south end of the bridge.
- In general, neither corrosion of the prestressing steel nor corrosion related deterioration of concrete were detected in the bridges in Corpus Christi except for minor cracking in pretensioned girders in the Intracoastal bridge.

## **METHODS FOR DETECTING CORROSIVE ENVIRONMENTS AND ACTIVE CORROSION OF PRESTRESSING STEEL**

The following approaches were used to identify and quantify corrosive environments and extent of active corrosion in prestressed concrete bridges:

- Visual examination.
- Delamination survey.
- Chloride analysis.
- Potential survey.

Since delamination was found to be not a common type of corrosion related deterioration of concrete in prestressed bridge components it will not be discussed further.

### **Visual Examination**

Visual examination is the most common method for detecting steel corrosion in prestressed concrete structures. Normally structures are examined for the following signs of the steel corrosion:

- Longitudinal cracks along prestressing tendons.
- Cracks in concrete or mortar cover protecting anchorage steel plates.
- Rust stains on the surface of concrete along tendons.
- Spalling of concrete cover over the prestressing steel.

Cracking can be observed along prestressing tendons, especially in areas of leaking joints and in concrete or mortar cover over anchorage steel plates. Longitudinal cracks over tendons are a strong indication of rather severe corrosion of the steel.

In severe cases, cracking is accompanied by spalling. The type of spalling depends on the type of prestressing reinforcement used: shallow and wide over seven wire strands and deep and narrow over post-tensioned tendons. Both cracking and spalling are highly undesirable because they reduce the protective power of concrete

cover.

Rust staining was not common in prestressed bridges, and was observed only in one girder in the Gandy Bridge and in one repaired girder of the O'Hare Airport Leads Bridge. Since rust staining was observed along with cracking it was difficult to say which occurred first, rust staining or cracking.

Failure in prestressing tendons in the Sixth South Street Viaduct occurred without any visible signs of corrosion. On the other hand, cracks in mortar over anchorage steel plates in affected girders and severe corrosion of these plates gave sufficient warning that chloride-laden water may penetrate into tendons and cause corrosion of the prestressing rods. It is important not only to inspect a structure for visible signs of corrosion but also to determine if a corrosive environment exists in the vicinity of the prestressing steel. This can be done by inspecting the structure for leaking joints and drains, wet spots, white deposits, and in some areas, algae. Since concrete in conventionally reinforced bridge components is more susceptible to corrosion related damage, the inspection of these components may also give a good indication of the corrosive environment.

One way to delineate zones of a corrosive environment is to follow the route of chloride-laden water. In a deicer environment chloride-laden water normally originates on top of a bridge deck and penetrates to the prestressing steel through cracks in the deck slab, leaking joints, and malfunctioning drains. In a marine environment the most damaging forms of chloride-laden water are sea water sprays reaching bridge components. After examining these routes and analyzing the danger of corrosion of the prestressing steel measures should be taken to prevent chloride-laden water from contacting the prestressing steel.

## **Chloride Analysis**

Measurements of chloride ion concentration were made following the testing procedure outlined in ASTM C 114-85. Results are expressed as a percent of acid-soluble chloride ions by weight of concrete. Samples were obtained at various depths between 0.5 in (12.7 mm) from the surface of a prestressed member and the level of the prestressing steel, in areas representing various extents of corrosion-related deterioration of concrete. Sampling was accomplished using a rotary hammer. To determine the baseline concentration of chloride ions, several samples were obtained from depths of about 4 to 4.5 in (102 to 114 mm) in areas where intrusion of chloride salts was unlikely. Samples were also obtained from mortar protecting elements of a prestressing system and from areas with potential readings in the range of -0.20 to -0.35 V CSE, i.e. representing uncertainty of corrosion activity of the reinforcing steel.

The maximum surface level concentration of chloride ions in a deicer environment was in the range of 0.610 to 0.742 percent as compared to 0.316 to 0.417 percent in a marine environment. The maximum concentration of chloride ions at the 1.5-2 in (38-51 mm) level of the reinforcement was higher in a deicer than in a marine environment, 0.516 to 0.550 and 0.319 percent, respectively.

Concentration of chloride ions in mortar cover over anchorage steel plates was higher than that in concrete cover, other conditions being similar.

The highest concentration of chloride ions was observed in areas exposed to direct contact with chloride-laden water. In areas adjacent to leaking joints but not exposed to direct contact with chloride-laden water, concentration of chloride was as low as in any area remote from these joints.

Concentration of chlorides in areas of severe corrosion of reinforcement and corrosion deteriorated concrete was in the range of 0.319-0.550 percent.

Concentration of chloride ions was always lower at the level of the prestressing steel than near the surface. The ratio between concentrations at these locations varied from 0.29 to 0.89 in wet areas, to 0.007 to 0.029 in areas exposed only to atmospheric moisture conditions.

Baseline concentration of chloride ions in deicer environments was in the range of 0.005 to 0.053 percent. Based on results of measurements of the baseline chloride content it can be concluded that chloride ions in prestressed bridge members do not penetrate deeper than 3.5-4 in (89-102 mm).

No corrosion activity was noted in prestressing steel at a concentration of acid-soluble chloride ions up to 0.092 percent under normal atmospheric conditions.

Concentration of chlorides in prestressed girders in a marine environment, where the only source of chlorides was the surrounding atmosphere, was in general low. Chloride induced corrosion was responsible for the failure of the prestressing steel in the O'Hare Airport Leads Bridge and in the Route Seven Viaduct. There is a greater than 90 percent certainty that chloride induced corrosion was also the cause of failure of the reinforcing steel in the Sixth South Street Viaduct and in the Gandy Bridge.

### **Potential Survey**

Application of the potential survey technique to detect corrosion in bridge members was first reported in 1968. Later it was adopted by ASTM as Standard Test Method C876-77. This technique involves the measurement of the electrical potential of uncoated steel using a copper-copper sulfate half cell and a high impedance voltmeter.

Test data may be presented in the form of a series of contours plotted through the points of equal or interpolated equal potential readings, or as a cumulative frequency distribution, or a combination of both. The first method of data presentation is more suitable for bridge decks where steel bars are equally spaced and where the moisture content of concrete cover is relatively uniform. In the case of prestressed girders it is more convenient to present test data by plotting the frequency and the cumulative frequency diagram, as shown in figures 23 and 24. These diagrams provide an indication of the magnitude of the affected area of the concrete member by showing the range of most common readings, and the percent of readings less and more negative than - 0.20 V CSE.



It is well known that potential readings are largely affected by the moisture content of concrete cover over prestressing steel. A concrete surface that has dried to the extent it has become dielectric will not provide a path for an electrical circuit. Prewetting the overhead concrete surface prior to taking measurements may not be sufficient to obtain condition when the measured value of the half-cell potential does not change or fluctuate with time (ASTM C876- 87, condition b). At the Sixth South Street Viaduct and at the Ship Channel Bridge, where concrete cover was found to be exceptionally dry, potential readings appeared to reflect the condition of conventional stirrups, not the prestressing steel.

This technique is also not applicable when concrete and/or steel surfaces are protected against corrosion with a dielectric material, such as epoxy coatings, plastic sheathing, grease, etc.

Of all the inspected bridges the most reliable test data were obtained on prestressed girders reinforced with uncoated seven wire strands. In the case of post-tensioned girders it was not clear if potential measurements reflected conditions of the steel duct or the steel rod, or a combination of both.

In bridges where reliable data were obtained there was a good correlation between results of the potential survey and other tests. Test results were in agreement with the findings of other investigators and with the criteria given in ASTM C 876-87. Potentials more negative than -0.50 V CSE were measured in areas of deterioration of concrete and exposed prestressing steel. Positive readings were obtained in areas of low moisture in the concrete.

It appears that while the potential measuring technique is a promising approach to locating areas of corrosion of prestressing steel, further research is needed to establish the effects of concrete cover moisture content, electrical resistance of concrete surrounding the prestressing steel, and concentration of chloride ions on potential measurements.

## **SUMMARY, CONCLUSIONS AND RECOMMENDATIONS**

Seven pre- and post-tensioned bridges built between 1959 and 1979 were selectively sampled and data analyzed to determine if active corrosion of the prestressing steel was occurring. The following bridges were examined:

- O'Hare Airport Bridge, Des Plaines, Illinois.
- The Route Seven Viaduct, Chicago Ridge, Illinois.
- The Sixth South Street Viaduct, Salt Lake City, Utah.
- The Gandy Bridge, Tampa, Florida.
- Intracoastal Canal Bridge, Corpus Christi, Texas.
- Ship Channel Bridge, Corpus Christi, Texas.
- Nueces Bay Causeway, Corpus Christi, Texas.

Bridges in the Chicago area and in Salt Lake City were representative of prestressed bridges exposed to a deicer environment. The rest represented bridges exposed to the marine environment.

Corrosion-related distress was observed most often in bridge elements adjacent to leaking joints and faulty drains. Distress occurred due to corrosion of prestressing strands, steel anchor plates, and conventional reinforcement. Distress was far more pronounced in a deicer than in a marine environment.

In prestressed bridge members exposed to direct action of sea water, corrosion related deterioration can occur in any area within the reach of water spray.

Severe noncorrosion related cracking may occur inside segmental boxes over top prestressing tendons due to excessive tensile stresses developed in concrete during prestressing operations. This type of cracking impairs the protective power of concrete

cover and under unfavorable conditions may become the major cause of steel corrosion.

Most common sources of chlorides in concrete were water running from bridge decks and sprays of sea water.

Water from decks reached the prestressing steel through cracks in the deck overlay, leaking joints, through concrete cover, and through mortar end plugs. In post-tensioned unbonded tendons deck water enters ducts through anchorage zones. The primary path for spray of sea water is through concrete cover.

Poor condition of deck slab joints was largely responsible for corrosion-related deterioration of concrete in members of prestressed bridges.

Among the most common joint defects were: deteriorated sealer, lack of sealer, and cracking of concrete around joints on the top surface of a deck overlay.

Routine inspection and proper maintenance are extremely important in eliminating major deck-to-steel water routes in prestressed concrete bridges.

Protection to anchorages provided by mortar filling girder end recesses was not satisfactory.

None of the examined bridges had a drainage system that would provide an effective removal of storm water from a bridge deck without letting it be in contact with adjacent substructure elements.

Important elements of a good drainage system are: sufficient size of intake, (not less than 8 by 8 in (200 by 200 mm), removable intake grids, sufficient pipe diameter (not less than 6 in (152 mm), and a pipe slope not less than 60 deg. It is important for

drain intakes not to be located close to expansion/contraction joints in a deck slab. It is also important to inspect and to clean drain intakes on a routine basis.

Epoxy based mortar if properly applied may be an effective temporary remedy.

External tendons observed in the Sixth South Street Viaduct in Salt Lake City were detailed such that even when located next to leaking joints the danger of penetration of moisture into tendons was unlikely.

Fiberglass jackets applied to bridge piles did not provide sufficient protection to the prestressing strands against chloride induced corrosion.

Delamination of concrete cover over prestressing steel in examined bridges was not common, though it may occur to some extent on the bottom side of pretensioned box girders.

Delamination surveys should not be considered an important element of an overall condition survey of prestressed bridge members.

Concrete in prestressed girders of examined bridges was generally of good quality with low to moderate permeability and did not exhibit major signs of distress. Concrete in deicer environments was air-entrained and had a rather low water-cement ratio, with the exception of the viaduct in Salt Lake City.

None of the examined bridges exhibited corrosion related distress that was attributed to poor quality of concrete.

Concentration of chlorides in concrete varied from significant in bridges exposed to a deicer environment, to rather high in bridges exposed to direct action of sea water, and to low in bridges exposed to sea water vapor.

The highest concentration of chlorides in concrete was found in girders where most corrosion-related deteriorations took place, i.e. in areas adjacent to leaking joints.

Rapid chloride permeability of concrete in the examined bridges varied from very low to moderate. Care should be taken in interpretation of rapid chloride permeability results on old bridges, as permeabilities may have been significantly higher earlier in the life of the bridge.

Insufficient concrete cover over prestressing steel was found in two of five bridges. This was due to faulty design and/or due to poor construction practices.

Specified values of concrete cover were found to be adequate in I-shaped pretensioned girders and rather low in pretensioned box girders. Cover was also low in girders reinforced with post-tensioned grouted tendons and in prestressed piles.

A pachometer did not appear to be directly applicable to post-tensioned elements, and must be calibrated on the items of interest just prior to use.

Potential readings were affected by moisture condition of concrete to such an extent that in some bridges no readings were obtained because of low moisture contents.

The most essential information to characterize the extent of corrosion activity in members other than post-tensioned are the average potentials and the percent of readings more negative than -0.35 V CSE.

Correlations may be necessary between the moisture content of concrete and potential readings in the evaluation of results of a potential survey.

Of three prestressing steel samples two failed by a ductile overload, primarily due to reduction in the effective cross section caused by corrosion.

Because of extensive rusting and oxidation which occurred on the fractured surface of the bar sample obtained from the Gandy bridge, the cause of failure was difficult to classify. The failure appeared to be more brittle in nature than a ductile overload failure and may have resulted from an impact or sudden application of a load.

The fracture in prestressing rods of the Sixth South Street Viaduct may have occurred due to hydrogen embrittlement, with the cathodic surface of a corrosion galvanic cell being a source of atomic hydrogen.

Corrosion of prestressing steel in examined bridges was related to an aggressive environment and occurred due to one or a combination of several of the following causes:

- Water permeable deck overlay.
- Leaking expansion/contraction joints.
- Malfunctioning drains.
- Inadequate concrete cover over prestressing steel.
- Improper protection of the anchorage systems.
- Access of water into sheathing through anchorages.
- Poor corrosion protection of portland cement mortar. Lack of grease in unbonded tendons.
- Exposure to direct action of sea water.
- Relatively high ratio of steel to concrete surface area.
- High permeability of concrete to chloride ions.
- Poor grouting.
- Poor protection of shotcrete mortar.

No evidence of corrosion was observed that could be related to the presence of dissimilar metals, manufacturing defects, or poor transporting and handling.

It is important not only to inspect a structure for visible signs of corrosion but also to determine if a corrosive environment exists in the vicinity of the prestressing steel.

Chloride induced corrosion was responsible for the failure of the prestressing steel in the O'Hare Airport Leads Bridge and in the Route Seven Viaduct. There is a greater than 90 percent certainty that chloride induced corrosion was also the cause of failure of the reinforcing steel in the Sixth South Street Viaduct and in the Gandy Bridge.

It appears that while the potential measuring technique is a promising approach to locating areas of corrosion of prestressing steel, further research is needed to establish the effects of concrete cover, moisture content, electrical resistance of concrete surrounding the prestressing steel, and concentration of chloride ions on potential measurements.

## REFERENCES

- (1) Schwier, F., "Wires and Bars for Prestressed Concrete," Proceedings, World Conference on Prestressed Concrete, San Francisco, California, July 1957, pp. 443-464.
- (2) Bate S. C., "The properties, Testing and Specification of Steel for Prestressed Concrete," World Conference on Prestressed Concrete, Proceedings, San Francisco, California, July 1957, pp. 443-464.
- (3) Buhrer, R., "Reinforced-Concrete Construction Wires and Bars, Seen from the View-Point of Users and Designers," World Conference on Prestressed Concrete, Proceedings, San Francisco, California, July 1957, pp. 525-545.
- (4) "Standard Specification for Steel Strand, Uncoated Seven-Wire Stress-Relieved Strand for Prestressed Concrete," (ASTM A416- 87a), 1988 Book of ASTM Standards, Volume 01.04, American Society for Testing and Materials, Philadelphia, pp. 248-250.
- (5) "Standard Specification for Uncoated Stress-Relieved Wire for Prestressed Concrete," (ASTM A421-80), 1988 Book of ASTM Standards, Volume 01.04, American Society for Testing and Materials, Philadelphia, pp. 252-254.
- (6) "Standard Specification for Uncoated High-Strength Steel Bar for Prestressing Concrete," (ASTM A 722-86), 1988 Book of ASTM Standards, American Society for Testing and Materials, Philadelphia, pp. 487-490.
- (7) Podolny, W., "Understanding the Steel in Prestressing," PCI Journal, October, 1967, pp. 55-66.



- (8) Shupack, Morris, "A Survey of the Durability Performance of Post-Tensioning Tendons," ACI Journal, October 1978, American Concrete Institute, Detroit, pp. 501-510.
- (9) Shupack, M., Suarez, M., "Some Recent Corrosion Embrittlement Failures of Prestressing Systems in the United States," PCI Journal, March-April 1982, pp. 38-55.
- (10) Van Loenen, J. H., and Etienne, C. F., "Wire Failure in Prestressing Steel Caused by Hydrogen Embrittlement." Paper presented at FIP Symposium on Steel for Prestressing, Madrid, 1968.
- (11) Etienne, C. F., "Wire Failure in Prestressing Steel Caused by Hydrogen Embrittlement," Proceedings, Symposium on Stress Corrosion of Prestressing Steel, Oosterbeek, The Netherlands, Sept. 1971, Part 1, p.148.
- (12) Moore, D. G., Klodt, D.T., and Hensen, R. J., "Protection of Steel in Prestressed Concrete Bridges," NCHRP Report 90. HRB, Washington, 1970.
- (13) Bender, M. E., "Prestressed Concrete Bridges for the Illinois Toll Highway," Proceedings, World Conference on Prestressed Concrete, San Francisco, California, July 1957, PP. A11.1 - A11.8.
- (14) Gustafarro, A., Hillier, M. A., Janney, J. R., "Performance of Prestressed Concrete on the Illinois Tollway After 25 Years of Service," PCI Journal, January-February 1983, pp. 51-67.
- (15) Kluge, F. W., Sawyer, H. A., "Interacting Pretensioned Concrete Form Panels for Bridge Decks," PCI Journal/May-June 1975, pp. 34-61.

- (16) Jones, H. L. and Furr, H. L., Research Report No. 145-1: Study of In-Service Bridges Constructed With Prestressed Panel Sub-Decks, PCI Journal/May-June 1975, pp. 63.
- (17) Barker, J. M., "Research, Application, and Experience with Precast Prestressed Bridge Deck Panels," PCI Journal, November-December 1975, pp. 66-85.
- (18) Roshore, E. C., "Durability and Behavior of Prestressed Concrete Beams; Pre-tensioned Concrete Investigation, Progress to July 1960." Technical Report No. 6-570, Report 1, U.S. Army Waterways Experiment Station, Vicksburg, 1961, 52 pp.
- (19) Roshore, E. C., "Durability of Prestressed Concrete Beams," PCI Journal, October 1965, pp. 49-59.
- (20) Roshore, Edwin C., "Durability and Behavior of Prestressed Concrete Beams; Report 2, Post-Tensioned Concrete Investigation Progress to July 1966," Technical Report No. 6- 570, U. S. Army Waterways Experiment Station, Vicksburg, 1967, 38 pp.
- (21) Roshore, C. E., "Field Exposure Tests of Reinforced Concrete Beams," ACI Journal/May 1967, pp. 253-258.
- (22) Roshore, E. C., "Durability and Behavior of Prestressed Concrete Beams; Report 3, Laboratory Tests of Weathered Pretensioned Beams." Technical Report No. 6-570, U.S. Army Waterways Experiment Station, Vicksburg, 1971, 39 pp.
- (23) O'Neil, Edward T., "Durability and Behavior of Prestressed Concrete Beams; Report 4, Posttensioned Concrete Beam Investigation with Laboratory Tests from

June 1961 to September 1975," Technical Report No. 6-570, U.S. Army Waterways Experiment Station, Vicksburg, 1977, 172 pp.

- (24) O'Neil, E. F., "Durability and Behavior of Prestressed Concrete Beams; Report 5, Laboratory Tests of Weathered Pretensioned Beams." Technical Report No. 6-570, U.S. Army Waterways Experiment Station, Vicksburg, 1976, 37 pp.
- (25) O'Neil, E. F., "Study of Reinforced Concrete Beams Exposed to Marine Environment," Performance of Concrete in Marine Environment, ACI Publication SP 65-8, ACI, Detroit, Michigan 1980, pp. 113-132.
- (26) Schupack, M., "Behavior of 20 Post-Tensioning Test Beams Subject to up to 2200 Cycles of Freezing and Thawing in the Tidal Zone at Treat Island, Maine," Performance of Concrete in Marine Environment, ACI Publication SP 65-9, ACI, Detroit, Michigan, 1980, pp. 133-152.
- (27) Monfore, G. E., Verbeck G. J., "Corrosion of Prestressed Wire in Concrete," Journal of the American Concrete Institute, November, 1960, No. 5, V.32, Proceedings V. 57, pp. 491-515.
- (28) Dickinson, W. E., Ratliff, G. D., Unz, M., Wakeman, C. M., "Corrosion of Prestressed Wire in Concrete," Journal of The American Concrete Institute, V. 32, No. 12, June 1961 (Proceedings V.57), pp. 1639-1648.
- (29) Legget, R. F., "Failure of Prestressed Concrete Pipe at Regina, Saskatchewan," Proceedings of the Institution of Civil Engineers, Vol. 22, May 1962, pp. 11-20.
- (30) "Cases of damage due to corrosion of prestressing steel," CUR Report No. 49, Netherlands Committee for Concrete Research on Reinforcing and Prestressing Steel, Zoetermeer, 1971.

- (31) Kozak, J. J., Bezouska, T. J., "Twenty Five Years of Progress in Prestressed Concrete Bridges," PCI Journal, September- October 1976, pp. 90-111.
- (32) Uhlig, H. H., Corrosion and Corrosion Control, 2nd Edition, John Wiley & Sons, New York, 1971, 419 pp.
- (33) Verbeck, G., "Mechanisms of Corrosion of Steel in Concrete," Corrosion of Metals in Concrete, SP-49, American Concrete Institute, Detroit, 1975, pp. 21-38.
- (34) Woods, H., "Durability of Concrete Construction." ACI Monograph No.4, ACI, Detroit, Michigan, 1968.
- (35) Locke C. E., "Corrosion Effect of Stray Currents and the Techniques for Evaluating Corrosion of Rebars in Concrete," Corrosion of Steel in Portland Cement Concrete: Fundamental Studies, ASTM STR 906, A symposium sponsored by ASTM Committee G- 1 on Corrosion of Metals, Williamsburg, VA, Nov. 1984, pp. 5-13.
- (36) Roberts, M. H., "Effect of Calcium Chloride on the Durability of Pre-Tensioned Wire in Prestressed Concrete," Magazine of Concrete Research: Vol. 14, No. 42: November 1962, pp. 143- 154.
- (37) Killick, H. S., and Bannister, J. L., "Characteristics of Prestressing Tendons," Proceedings, World Conference on Prestressed Concrete, San Francisco, California, July 1957, pp. 443-464.
- (38) Lobry de Bruyn, C. A., "Corrosion Problems with Prestressed Concrete," Report of the RILEM-FIP-IABSE Committee, Proceedings of the Fifth Congress of the FIP, Paris, 1966. London, Cement and Concrete Association, 1967. pp. 81-86.

- (39) Szilard, R., "Corrosion and Corrosion Protection of Tendons in Prestressed Concrete Bridges," ACI Journal, January 1969, Title No. 66-5, pp. 42-59.
- (40) West J. M., Basic Corrosion and Oxidation. John Wiley & Sons, New York, 1986, pp. 160-164.
- (41) Naumann, F. K., and Baumel, A., "Rupture of Prestressing Wires Due to Hydrogen-Embrittlement in Concrete Made of High Alumina Cements," Archiv fur das Eisenhüttenwesen, V. 32, No. 2, Feb. 1961, pp. 65-69.
- (42) Rehm, G., "Damage of Prestressed Concrete Elements Cast with High Alumina Cement," Betonstein Zeitung, V. 29, No.12, Dec. 1963, pp. 651-661.
- (43) Bergsma, F., Boon, J., and Etienne, C. F., "Endurance Tests for Determining the Susceptibility of Prestressing Steel to Hydrogen Embrittlement," Heron, Vol. 22, No. 1, 1977, Delft, The Netherlands, pp. 47-76.
- (44) Pollard, R. E., "Stress Corrosion Cracking," Report for an ASTM Symposium. New York, 437 pp.
- (45) Everling, W. O., "Stress Corrosion in High-Tensile Wire," Yearbook of the American Iron and Steel Institute, 1954, pp. 185-202.
- (46) Bukowiecki, A., "Corrosion Problems with Prestressed Concrete," Report of the RILEM-FIP-IABSE Committee, Proceedings of the Fifth Congress of the FIP, Paris, 1966. London, Cement and Concrete Association, 1967. pp. 81-86.
- (47) Kusenberger, F. N., Barton, J. R., "Detection of Flaws in Reinforcing Steel in Prestressed Concrete Bridge Members," FHWA/RD-81/087 (Washington, DC: Federal Highway Administration, 1979), 197 pp.

- (48) Kusenberger, F. N., Birkelbach, R. S., "Signal Enhancement and Interpretation for the Detection of Flaws in Reinforcing Steel in Prestressed Concrete Bridge Members," FHWA/RD-83/081 (Washington, DC: Federal Highway Administration, 1982), 124 pp.
- (49) PCI Committee on Segmental Construction, "Recommended Practice for Segmental Construction in Prestressed Concrete," PCI Journal, March-April 1975, pp. 23-41.
- (50) Muller, J., "Ten Years of Experience in Precast Segmental Construction, PCI Journal, January-February 1975, pp. 29-61.
- (51) ACI Committee 224, "Control of Cracking in Concrete Structures," (ACI 224R-80), ACI Manual of Concrete Practice, 1988. American Concrete Institute, Detroit, pp. 43.
- (52) Gergely, P., "Anchorage Systems in Prestressed Concrete Pressure Vessels; Anchorage Zone Problems," ORNL-TM-2378, Oak Ridge National Laboratory, U.S. Atomic Energy Commission, Oak Ridge, Tenn., 1969, pp. 1-49.
- (53) Zielinski, J. L., and Rowe, R. E., "An Investigation of the Stress Distribution in the Anchorage Zones of Post-Tensioned Concrete Members," Technical Report No. 9, Cement and Concrete Association, London, Sept. 1960, 32 pp.